Vol. 67 • No. 9

September 2024

Microwave Journal

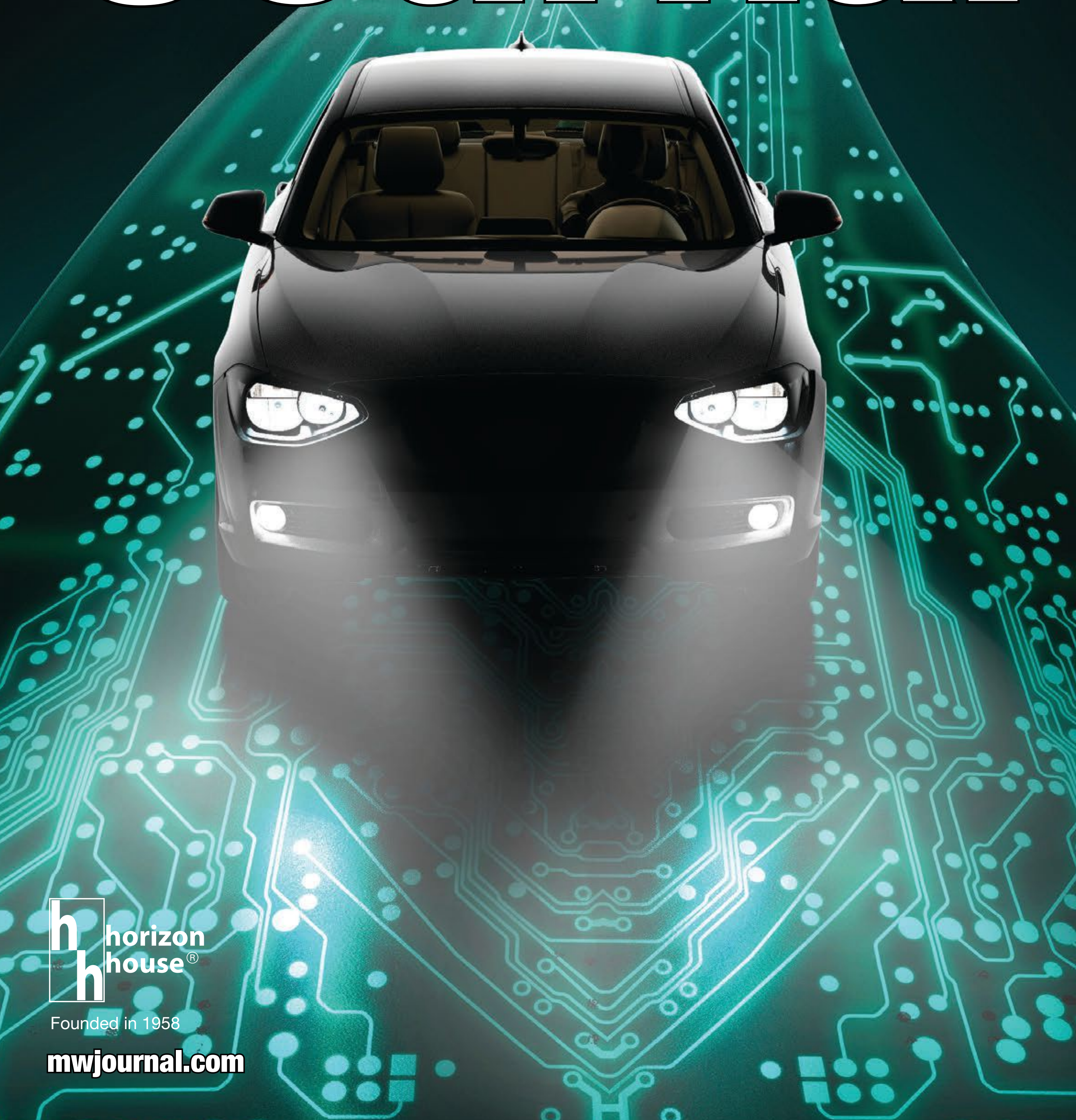

horizon house®

Founded in 1958

mwjournal.com

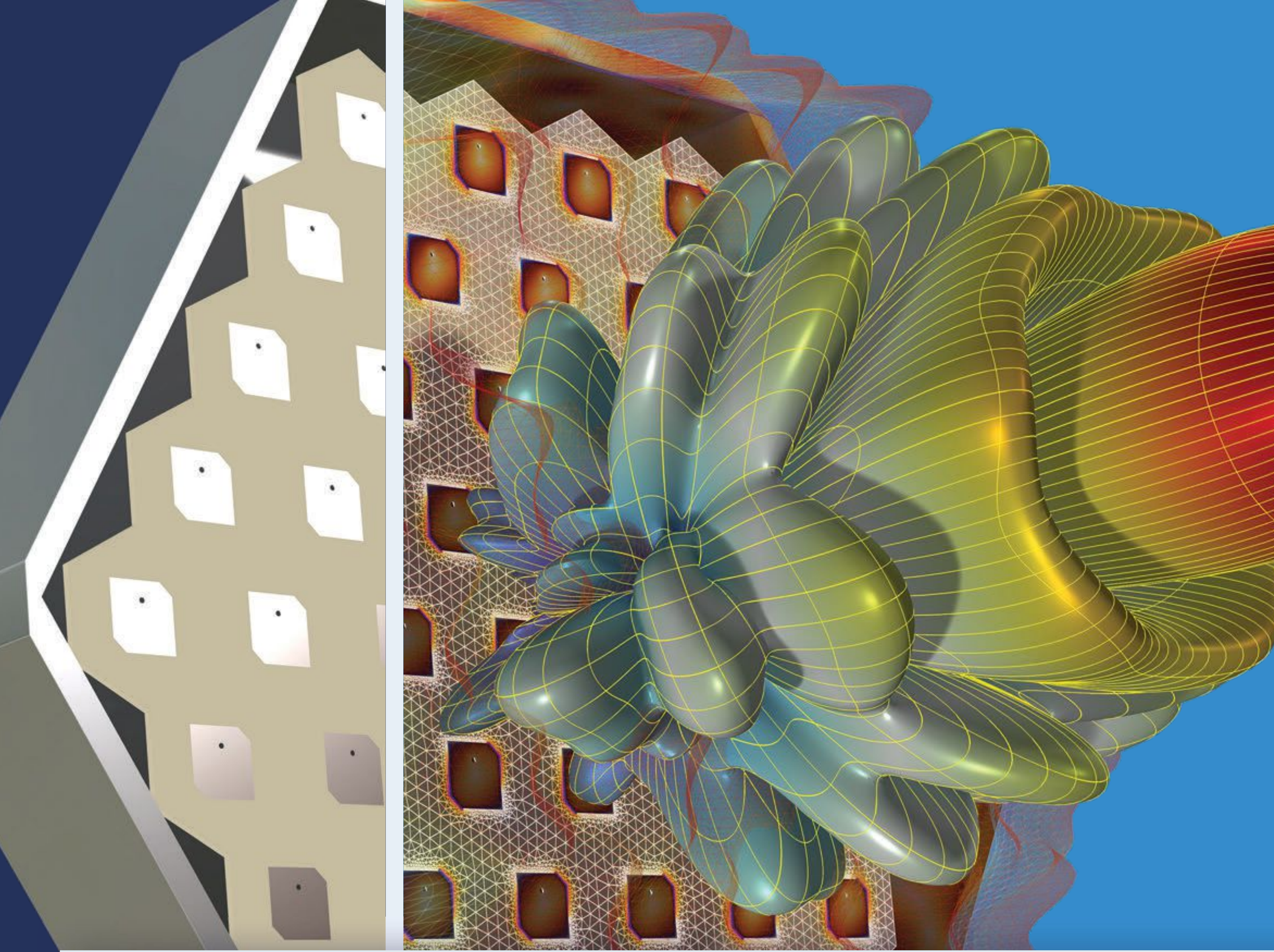

UP TO 110 GHz

High-Frequency Solutions

Amplifiers & Modules for mmWave Applications

WAVEGUIDE AMPLIFIERS

- Bandwidths from 40 to 110 GHz
- Low noise, high gain & medium power options
- WR10, WR12, WR15 & WR15 interfaces
- Ideal for TRP & TIS over-the-air testing

CONNECTORIZED AMPLIFIERS

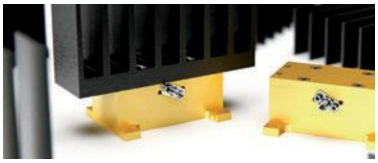

- Bandwidths from 50 kHz to 95 GHz
- 2.92, 2.4, 1.85 & 1.0mm connector options
- Gain up to 45 dB
- NF as low as 1.7 dB
- Power up to 1W

VARIABLE GAIN AMPLIFIERS


- Bandwidths from 18 to 54 GHz
- Gain up to 50 dB
- Calibrated 17 dB attenuation with analog or TTL control
- PSAT up to +1W
- Interactive GUI with telemetry

More High-Frequency Modules

BIAS TEES

- 10 to 54 GHz
- DC current up to 250mA
- RF power up to +30 dBm
- >30 dB isolation
- Low insertion loss

DIGITAL STEP ATTENUATORS

- 100 MHz to 50 GHz
- 0 to 31.5 dB attenuation
- 0.5 dB step size
- 6-bit parallel control
- +50 dBm IIP3

FREQUENCY MIXERS

- LO/RF from 5 to 65 GHz
- IF from DC to 20 GHz
- Double-balanced and I/Q designs
- +15 dBm LO power
- Excellent L-R isolation

FREQUENCY MULTIPLIERS

- Output from 10 to 40 GHz
- Wide input power range spanning +11 to +22 dBm
- Low conversion loss
- Excellent harmonic suppression

POWER DETECTORS

- 0.1 to 43.5 GHz
- -35 to +15 dBm
- Single supply voltage
- CW & RMS models

SWITCHES

- 10 MHz to 67 GHz
- 45 dB isolation
- Supports bi-directional use
- All-off state available
- Convenient digital snap-fit connector

Mini-Circuits®


RF-LAMBDA
THE LEADER OF RF BROADBAND SOLUTIONS
BROADBAND SSPA / EMC BENCHTOP
SOLID STATE POWER AMPLIFIER
0.1-22GHZ
ULTRA BROADBAND SSPA
RFLUPA01M22GA
4W 0.1-22GHZ
RFLUPA0218GB
20W 1-19GHZ
300W 6-18GHZ SOLID STATE BROADBAND
400W 8-11GHZ
SOLID STATE BROADBAND
0.1-6GHZ VHZ,
UHF, L, S, C BAND
RFLUPA02G06GC
100W 2-6GHZ
RFLUPA0706GD
30W 0.7-6GHZ
MADE IN USA
6-18GHZ C, X, KU BAND
RFLUPA08G11GA
50W 8-11GHZ
RFLUPA0618GD
60W 6-18GHZ
RFLUPA06G12GB
25W 6-12GHZ
18-50GHZ K, KA, V BAND
RFLUPA18G47GC
2W 18-47GHZ
RFLUPA27G34GB
15W 27-34GHZ
RFLUPA47G53GA2
10W 47-53GHZ
RFLUPA27G34GB
30W 18-40GHZ
BENCHTOP RF MICROWAVE SYSTEM POWER AMPLIFIER
RAMP00G06GA- 30W 0.01-6GHZ
RAMP39G48GA- 4W 39-48GHZ
RAMP01G22GA- 8W 1-22GHZ
RAMP27G34GA- 8W 27-34GHZ
www.rflambda.com
sales@rflambda.com
1-888-976-8880
1-972-767-5998
San Diego, CA, US
Carrollton, TX, US
Ottawa, ONT, Canada
Frankfurt, Germany

RF MINIATURIZATION

Breaking Through Size & Performance Barriers

New miniaturized high-Q RF filter family

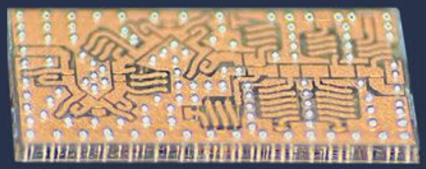

2.6 mm

5.4 mm

10X Smaller than filters with comparable performance

4X Better out-of-band rejection than high dielectric ceramic filters

High performance antialiasing filters for lowpass, highpass, bandpass, and diplexer applications.
Surface-mount, BGA devices from 500 MHz to 10 GHz using wafer-scale manufacturing on glass substrates

SpectrumControl.com/highq-smt

Complete RF front end with integrated digital control in a BGA package.

Top View

Bottom View

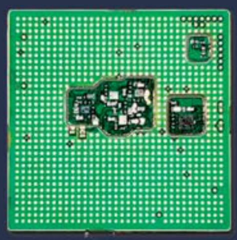

30 mm

30 mm

6X Density improvement

86% Reduction in lifecycle costs

With superior wideband performance, compact footprint, and volume-ready design, this new RF+ SiP platform addresses an urgent defense industry need for high performance, cost-effective, miniaturized RF solutions. It delivers the capabilities of an integrated microwave assembly (IMA) in a 30 mm^2, surface mount package.

SpectrumControl.com/sip-ima

SPECTRUM CONTROL ™

spectrumcontrol.com

Relax
We've got you covered
Your supplier of high performance, precise equipment for AWGN
NOISEWAVE
The new wave in NOISE
Ph. (973) 386-1119 • Fax (973) 386-1131 • info@noisewave.com • www.noisewave.com

Microwave Journal

CONTENTS

September 2024
Vol. 67 • No. 9
Automotive & Connected Vehicles
mwjournal.com

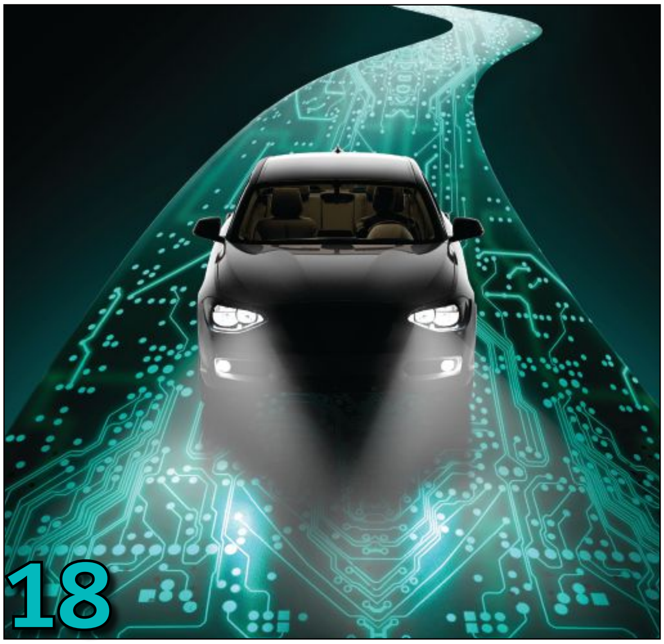

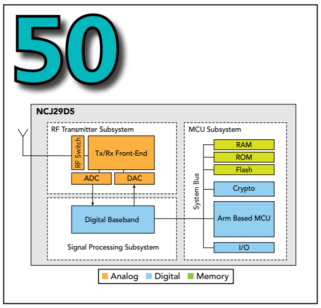

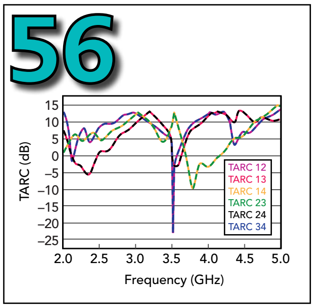

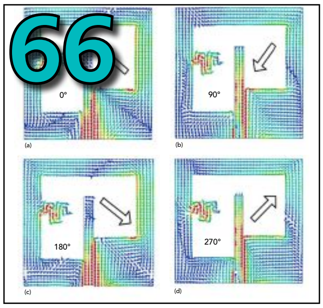

ACCESS NOW!
digital.microwavejournal.com

eXclusive Digital Content ›››

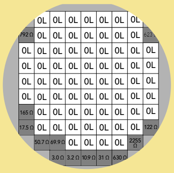

67 YEARS OF PUBLISHING EXCELLENCE

Microwave Journal

CONTENTS

mwjournal.com

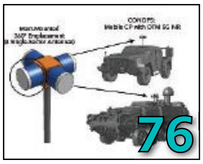

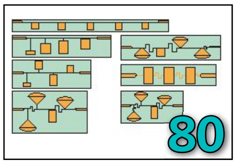

Product Features

Tech Briefs

Departments

Microwave Journal (USPS 396-250) (ISSN 0192-6225) is published monthly by Horizon House Publications Inc., 685 Canton St., Norwood, MA 02062. Periodicals postage paid at Norwood, MA 02062 and additional mailing offices.

POSTMASTER: Send address corrections to Microwave Journal, PO Box 1028, Lowell, MA 01853 or e-mail mwj@e-circ.net.com. Subscription information: (978) 671-0446. This journal is issued without charge upon written request to qualified persons working in the RF & microwave industry. Other subscriptions are: domestic, $130.00 per year, two-year subscriptions, $200.00; foreign, $225.00 per year, two-year subscriptions, $400.00; back issues (if available) and single copies, $20.00 domestic and $30.00 foreign. Claims for missing issues must be filed within 90 days of date of issue for complimentary replacement.

STAFF

Group Director: Carl Sheffres
Associate Publisher: Michael Hallman
Media Director: Patrick Hindle
Brand & Content Director: Jennifer DiMarco
Technical Editor: Eric Higham
Associate Technical Editor: Cliff Drubin
Editorial & Media Specialist: Kelley Roche
Associate Editor: Kaitlyn Joyner
Multimedia Staff Editor: Barbara Walsh
Electronic Marketing Manager: Chris Stanfa
Senior Digital Content Specialist: Lauren Tully
Digital Content Specialist: Vincent Carrabino
Director of Production & Distribution: Edward Kiessling
Art Director: Janice Levenson
Graphic Designer: Ann Pierce

EUROPE
Office Manager: Nina Plesu

CORPORATE STAFF
CEO: William M. Bazzy
President: Ivar Bazzy
Vice President: Jared Bazzy

EXECUTIVE EDITORIAL OFFICE
685 Canton Street, Norwood, MA 02062
Tel: (781) 769-9750
FAX: (781) 769-5037
e-mail: mwj@mwjournal.com

EUROPEAN EDITORIAL OFFICE
16 Sussex Street, London SW1V 4RW, England
Tel: Editorial: +44 207 596 8730 Sales: +44 207 596 8740
FAX: +44 207 596 8749

SUBSCRIPTION SERVICES
Send subscription inquiries and address changes to:
Tel: (978) 671-0446
e-mail: mwj@e-circ.net

www.mwjournal.com

Printed in the USA

Microwave Journal ONLINE .COM

E LEARNING CENTER

PolyStrata® Delivers High-Performance QFN Package Alternative
Sponsored by: RFMW and Nuvotronics 9/5

Digital Twin for Multi-physics Systems
Sponsored by: Altair 9/24

AS940 Calibration Performance and How to Use It
Sponsored by: Teledyne e2v 9/26

Executive Interview

Jr-Tai (Ted) Chen, Founder and CEO of **SweGaN**, discusses his background, what led him to found SweGaN, the recent growth and development of the company and the future direction of SweGaN.

Catch *Frequency Matters*, the industry update from *Microwave Journal*,
microwavejournal.com/FrequencyMatters

WHITE PAPERS

COPPER MOUNTAIN TECHNOLOGIES — VNA Time Domain Processing

FORTIFY — Antenna Lenses for Commercial Applications: Repeatability and Scalability of Luneburg Lens Production

JFW — Supercharging your VNA with an RF Matrix Switch (VNA Port Extension)

REMCOM — Technical Report: Simulation of Plasma Materials in XFdtd

pSemi A Murata Company — RF Switch FET Low Frequency Power De-Rating: Design Challenges and Trade-offs

SKYWORKS — Empowering Next-Generation Data Center Switches with the Skyworks® Si5360/61/62/63 Family

TELEDYNE e2v Everywhereyoulook — TELEDYNE e2v's EV10AS940 "SILVER BULLET" RF/Microwave ADC

Join Us Online

Follow us
@Pathindle
@MWJEric
@MWJEditor

Join us at the RF and Microwave Community

Become a fan at facebook.com/microwavejournal

Visit us @ mwjournal.com

PROPRIETARY TECHNOLOGIES

LTCC Filter Innovations

The Industry's Widest Selection

LEARN MORE

Ultra-High Rejection

- Rejection floor down to 100+ dB
- Excellent selectivity
- Built-in shielding
- 1812 package style
- Patent pending

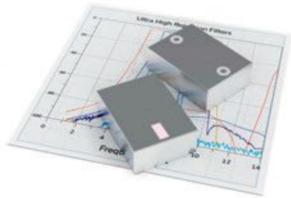

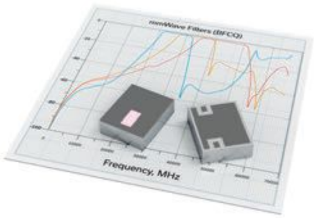

mmWave Passbands

- Passbands to 50+ GHz
- The industry's widest selection of LTCC filters optimized for 5G FR2 bands
- Growing selection of models for Ku- and Ka-band Satcom downlink
- 1812 & 1008 package styles

Substrate Integrated Waveguide

- First commercially available SIW LTCC filter in the industry
- Narrow bandwidth (~5%) and good selectivity
- Internally shielded to prevent detuning
- 1210 package style

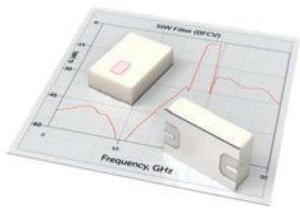

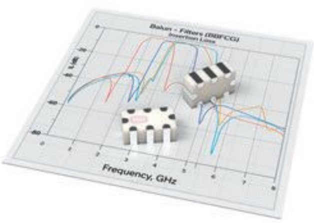

Integrated Balun-Bandpass Filters

- Combine balun transformer and bandpass filter in a single device
- Saves space and simplifies board layouts in ADCs, DACs and other circuits
- 1210, 1008 & 0805 package styles

Mini-Circuits

STAY CONNECTED TO COMING EVENTS

MARK YOUR CALENDAR

SEPTEMBER

22-27
EuMW 2024
Paris, France
www.eumweek.com

23-27
IEEE HPEC 2024
Online
https://ieee-hpec.org

OCTOBER

2-4
COMSOL Conference
Burlington, Mass.
www.comsol.com/conference/boston

8-10
MWC Las Vegas
Las Vegas, Nev.
www.mwclasvegas.com

15-18
IEEE International Symposium on Phased Array Systems & Technology
Boston, Mass.
www.ieee-array.org

27-30
IEEE BCICTS
Fort Lauderdale, Fla.
https://bcicts.org

27-Nov. 1
AMTA
Cincinnati, Ohio
https://2024.amta.org

NOVEMBER

4-7
Global MilSatCom
London, U.K.
www.smgconferences.com/defence/uk/conference/global-milsatcom

12-15
electronica
Munich, Germany
https://electronica.de/en/

17-20
APMC 2024
Bali, Indonesia
https://apmc2024.org

DECEMBER

9-13
IEEE MAPCON
Hyderabad, India
https://ieeemapcon.org

ONLINE PANEL SERIES

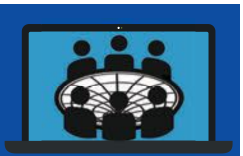

9/17
The Best 5G/6G Beamsteering Antenna Arrays and Repeaters for mmWave Deployments

Call for Papers Deadlines

9/15	WISEE 2024
10/4	IEEE Aerospace Conference
10/18	EuCAP 2025

FOR DETAILS VISIT MWJOURNAL.COM/EVENTS

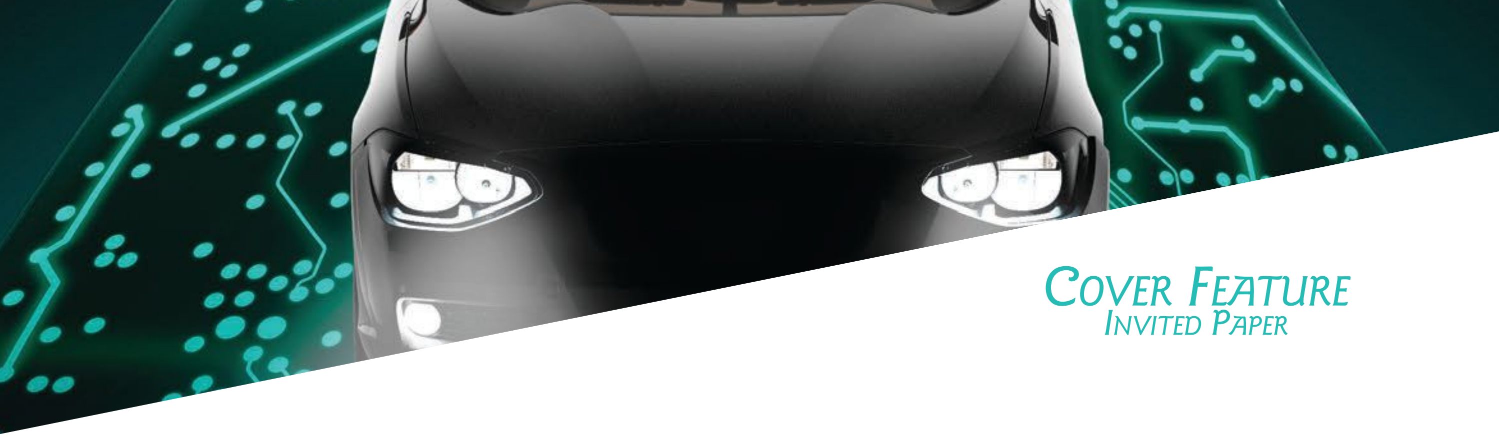

COVER FEATURE
INVITED PAPER

CISPR 25 Methodology Enhances In-Vehicle Infotainment Display EMC

Zong Si Wu and Jenq Shiou Leu

This article discusses mitigating the challenges related to radiation emission non-compliance while evaluating in-vehicle infotainment (IVI) displays per the guidelines set forth by CISPR 25 automotive electromagnetic (EM) compatibility standards. The research shows that IVI display systems infringe upon these standards, exhibiting radiation levels that exceed the permissible limits by 2.51 dB in the frequency band ranging from 555 to 960 MHz. In-depth analytical work pinpoints the root cause of this excessive radiation to be the printed circuit board assembly (PCBA) embedded within the IVI screens. To counteract this problematic scenario, the study described in this article finds that a fine-tuned adjustment of a conductive foam gasket solves the issue. The applied modifications substantially reduce radiative interference, allowing the system to comply with existing standards. The study reported in this article serves a dual purpose. First, it identifies the primary culprit behind the elevated radiation emission levels during CISPR 25 compliance assessments and second, it presents an effective remedial approach. The findings offer considerable practical implications for achieving regulatory compliance in the automotive electronics sector.

THE CHALLENGE

Addressing CISPR 25 Challenges in IVI Systems

The research described in this article advances the compliance of IVI displays with CISPR 25[1] automotive EM compatibility standards,[2] identifying the PCBA as the primary source of non-compliance. To ensure standards compliance, a novel adjustment using conductive foam gaskets was introduced to reduce radiative interference significantly. This approach offers a model for similar diagnostics, contributing to the automotive electronics field by improving EM interference understanding in IVI systems. The findings propose practical solutions for maintaining regulatory adherence, impacting automotive design and testing and supporting the evolution of more refined EMC policies and standards. This research, aimed at enhancing vehicle safety and performance, provides a strategic framework for addressing EM interference, marking a significant advancement in automotive electronics.

Automotive Electronics Regulations

Radiated emissions regulations for automotive electronics vary globally but share core testing and implementation principles. The FCC in the U.S., ECE Regulation No. 10 in the EU and CISPR 25 internationally set crucial standards for minimizing interference and ensuring EM compatibility. Japan's VCCI and China's CQC contribute to a worldwide regulatory framework, ensuring the safety, reliability and compatibility of automotive electronics across regions to support global trade and consumer safety.

Radiated Emissions in Automotive Electronic Products

Radiated emissions from automotive electronics pose risks to safety, performance, regulatory compliance, brand reputation and economic success. Emissions can lead to health issues for occupants, impair critical vehicle functions like braking and navigation and disrupt data exchanges in connected vehicles. Compliance with international emission standards is crucial to avoid penalties, product recalls or bans that can damage brand image and lead to financial challenges. Conversely, meeting these standards enhances market competitiveness, consumer trust and economic benefits, highlighting the importance of rigorous testing and control measures in automotive electronics development.


The only
QPL Certified
MECHANICAL
SWITCH
House!
Quick Turn
RF FILTER
Prototypes
are in our DNA!
Huge Library
of PASSIVES
with Best in Show
HIGH POWER
COUPLER
offering!
RLC ELECTRONICS
L-4241A
S/N 2206001
RUGGED & RELIABLE
AGILE & ADAPTIVE
HIGH POWER & VARIETY
RLC
RF MECHANICAL SWITCHES,
RF FILTERS & RF PASSIVES
AS9100 CERTIFIED, MADE IN USA
High Performance Precision Microwave Components
Serving the world-wide aerospace & defense community since 1959
Robust Catalog Portfolio - no hassle, quick turn, custom solutions our specialty
RLC Electronics | 83 Radio Circle, Mt. Kisco, NY 10549 | 914-241-1334 | sales@rlcelectronics.com | www.rlcelectronics.com

The Origin of CISPR 25

CISPR 25, established by the International Special Committee on Radio Interference under the International Electrotechnical Commission (IEC), is a key international standard for EMI testing in vehicles, ships and engines. Created to address RF interference issues identified since 1934, CISPR 25 focuses on automotive and maritime sectors, evolving to manage the complexities of EM interference with the growth of automotive electronics. It has gained worldwide recognition, being incorporated into the regulatory frameworks of many countries to ensure EMI compliance and the standard plays a crucial role in mitigating EMI issues globally.

TABLE 1

ANTENNA CHARACTERISTICS AND APPLICATIONS

	Rod	Biconical	Log-Periodic	Horn
Frequency	VHF-UHF	Broad	Broad	High
Directivity	Omni	Variable	Directional	Highly
Usage	Basic Comms	EMC Tests	Spectrum	Radar

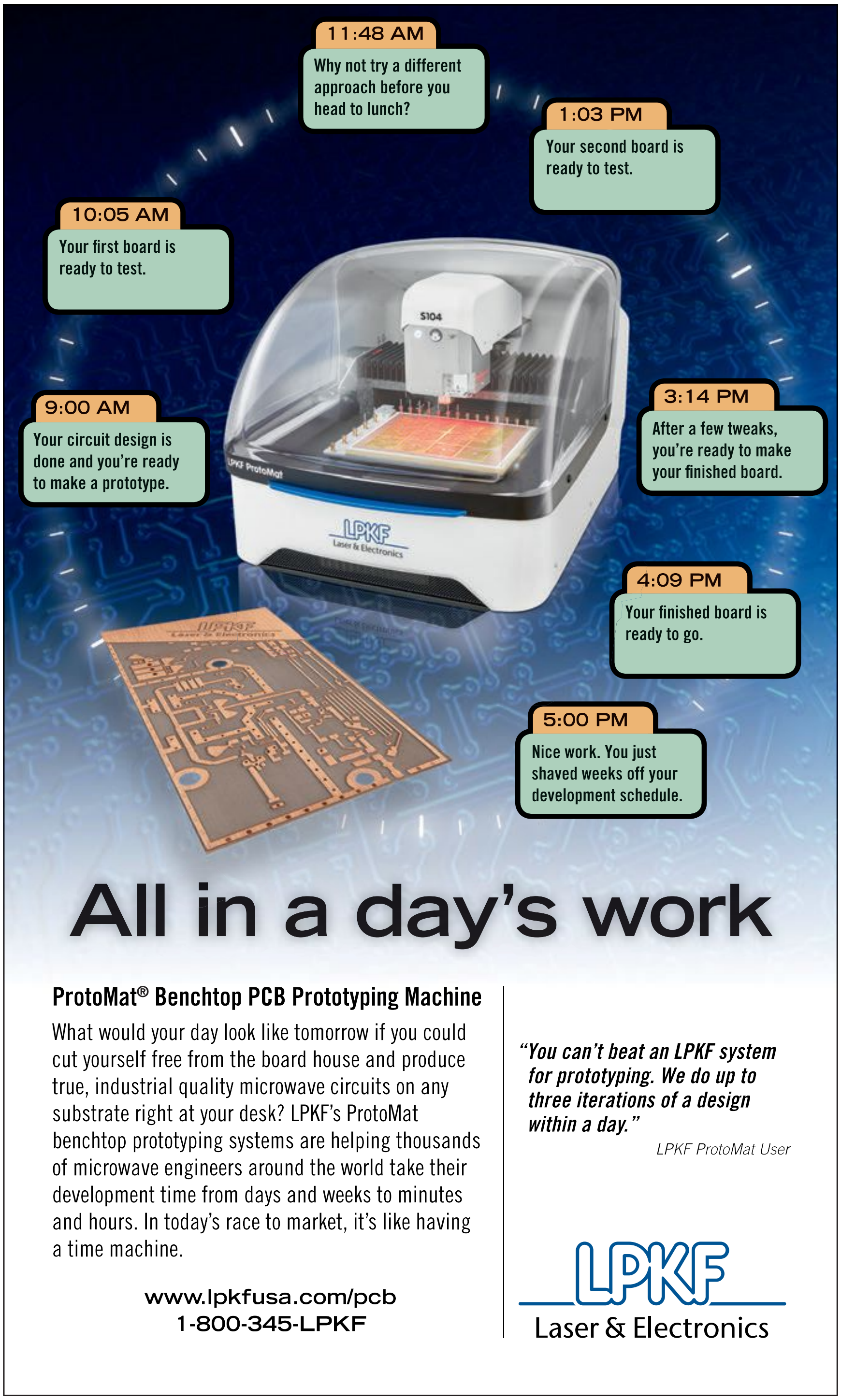

CISPR 25 Certification and Testing

CISPR 25, under the IEC, is essential for EMI testing in vehicles, ships and engines, focusing on integrity against EM disturbances. Globally recognized, it guides regulatory compliance, detailing procedures for conducted and radiated emission tests to ensure EM compatibility. The certification process involves preliminary review, testing in certified labs and result analysis, with ongoing updates reflecting new technology. CISPR 25 certification indicates EMC proficiency, enabling regulatory compliance and commercial success. This standard addresses the challenges of managing radiated emissions in automotive electronics, guiding manufacturers in adhering to EMC standards and solving issues.

RESEARCH BACKGROUND

Generating Radiated Emissions

Radiated emissions arise from electronic devices when current and voltage changes lead to EM wave propagation. This propagation is primarily due to rapid digital signal switching and clock oscillations. Power supplies, Wi-Fi, Bluetooth and mechanical components, like motors, also contribute to these emissions. Common-mode radiation, where current flows uniformly through conductors, is a significant emission source, amplified by antenna-like structures and resonant frequencies. Mitigating these emissions is vital for EM compatibility, ensuring products meet standards and maintain user safety and quality.

Mitigating Radiated Emissions

Mitigating radiated emissions during electronic device design and testing is crucial for regulatory compliance and product quality. The design phase involves minimizing high frequency component use, employing filters to limit unwanted fre-

quencies, separating sensitive components from high frequency components and implementing comprehensive ground and power planes to reduce emissions. Selecting low-emission components and incorporating impedance matching enhances EMI mitigation.

Shielding Principles

Shielding involves the use of conductive or magnetic materials to encase devices. It blocks or absorbs EM waves from external and internal sources. The material choice, considering conductivity, device proximity and EM wave frequency, significantly influences shielding effectiveness. Effective shielding strategies include ensuring material-to-ground connectivity and minimizing enclosure openings. In this study, conductive foam gaskets effectively reduced radiation emissions in the 555

Test No.	Frequency Band	Frequency	PK				QP				AV			
			Limit Class			BW	Limit Class			BW	Limit Class			BW
		(MHz)	3	4	5	(kHz)	3	4	5	(kHz)	3	4	5	(kHz)
			(dB(µV)/m)				(dB(µV)/m)				(dB(µV)/m)			
Mobile Services														
6	125 kHz	0.1 ... 0.15	61	51	**41**	9/10	-			-				
7	4 m/TETRA	84,015 ... 87,255	47	41	**35**	120	-			-	14	8	**2**	9/10
8	2 m/TETRA	146 ... 164	47	41	**35**	120	-			-	14	8	**2**	9/10
9	2 m/TETRA	167,56 ... 169,38	47	41	**35**	120	-			-	14	8	**2**	9/10
10	2 m/TETRA	172,16 ... 173,98	47	41	**35**	120	-			-	14	8	**2**	9/10
11	SRD	300 ... 330	46	40	**32**	120	-			-	26	20	**14**	9/10
12	SRD	420 ... 450	46	40	**32**	120	-			-	26	20	**14**	9/10
13	2-5G	555 ... 960	61	55	**49**	1000	-			-	41	35	**29**	1000

Fig. 1 Examples of limits for radiated disturbances–ALSE method.

to 960 MHz frequency range from PCBAs. This demonstrates the role shielding plays in mitigating EM radiation, which is crucial for automotive electronics with high frequency applications.

Shielding acts as a barrier to block EM field transmission, reducing product emission and preventing external radiation interference. Shielding efficiency, measured in dB, is the ratio of unshielded to shielded wave amplitude. This ratio includes absorption losses, surface reflection losses due to impedance discontinuities and internal reflection losses. A high shielding efficiency value reflects a method that reduces radiated energy propagation. Clayton R. Paul[3-5] has proposed examples of such methodologies, where gaskets are modified to prevent emission leaks.

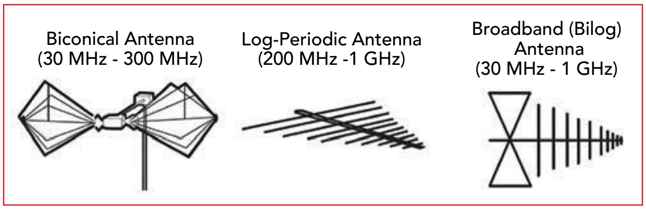

Fig. 2 **Log-periodic antenna.**[8]

Fig. 3 **Radiation measurement setup showing log-periodic antenna.**

EXPERIMENTAL DESIGN

Testing to verify radiated emissions involves EMC simulations and lab tests to identify and address excessive radiation, using shielding, filtering and grounding techniques to ensure compliance with standards like FCC, CE or CISPR.

TABLE 2

ANTENNA SELECTION FOR EMI TESTING

Frequency Range	Recommended Antenna	Polarization
150 KHz to 30 MHz	Monopole	Vertical
30 MHz to 300 MHz	Biconical	Horizontal & Vertical
200 MHz to 1 GHz	Log-Periodic	Horizontal & Vertical
30 MHz to 1 GHz	Broadband	Horizontal & Vertical
1 GHz to 2.5 GHz	Horn	Horizontal & Vertical


qorvo QPA0017
qorvo QPA0812
qorvo QPA0001

TABLE 3

EMI CHAMBER EQUIPMENT LIST

Equipment Name	Manufacturer	Model
EMI test receiver	Keysight	N9038A
EMI test receiver	R&S	ESR 7
Pre-amplifier	EMEC	EM330
Pre-amplifier	EMCI	EMC051845SE
Coaxial cable	Huber+Suhner	SUCIFLEX
Coaxial cable	Huber+Suhner	SUCIFLEX
Monopole antenna	SCHWARZBECK	VAMP9243B
Biconical antenna	SCHWARZBECK	VHB9124/BBA9106
Log-periodic antenna	SCHWARZBECK	VULP9118A
Horn antenna	SCHWARZBECK	BBHA9120J
LISN	FCC	FCC-LISN models
LISN	FCC	FCC-LISN models
Loop antenna	SCHWARZBECK	FMZB 1513-60
Software	EZ-EMC5A2	NA

Testing Radiated Emission Frequency Bands

Radiated emissions testing for automotive electronics mandates simulating real-world vehicle conditions, documenting operational parameters, like load and voltage and specifying device orientation in the test plan. Measurements need vertical polarization for frequencies up to 30 MHz and require both polarizations up to 2500 MHz, per CISPR 25:2016. Recommended antennas include the rod for VHF/UHF frequencies, biconical for wideband use, log-periodic for its broad range and directionality and horn for high gain in microwave bands. This structured approach ensures consistent, safety-compliant testing across the automotive industry. ***Table 1*** shows some characteristics and applications of these antennas.

Radiated Interference Limitations – ALSE Method

According to the CISPR 25 standard, the absorber-lined shielded enclosure (ALSE)[6,7] method for measuring radiated interference includes five distinct classes of limitations. Each class has its specific radiated interference limits, which are clearly outlined in the respective tables:

- Class 1 is the most lenient category, suitable for scenarios less sensitive to radiated interference
- Class 2 imposes stricter limitations than Class 1 and is commonly used for general vehicle components and modules
- Class 3, a medium-level restriction, is often considered the minimum acceptable standard by most vehicle manufacturers
- Class 4 includes more stringent limitations for applications that are particularly sensitive to radiated interference
- Class 5, the most rigorous category, is reserved for special applications with extreme sensitivity to radiated interference.

These classification levels enable vehicle manufacturers and suppliers to choose suitable restrictions for their needs, ensuring radio system stability across different environments. ***Figure 1*** shows the ALSE radiated disturbance limits for various mobile service applications.

Most end users require passing at least a Class 3 level of performance. The study reflected in this article confirms that the 555 to 960 MHz frequency band meets CISPR 25 standards, emphasizing the importance of these classes in maintaining compliance and system reliability. The 555 to 960 MHz frequency range, part of the broader 200 MHz to 1 GHz spectrum, requires a log-periodic antenna, like the example in ***Figure 2***, for EM interference testing.

When measuring specific frequency bands, the measurement environment[9] has been designed and the antenna has been chosen in accordance with the CISPR 25 regulations. ***Figure 3*** illustrates the setup concept for the measurement environment. ***Table 2*** shows the frequency response and polarization capabilities of various antenna types. In this case, the measurement frequency band is 555 to 960 MHz and the log-periodic antenna is the best solution.

The antenna setup involves meticulous positioning and orienting the antenna to maximize testing accuracy. The setup process specifies the distance between the antenna and the equipment under test and details the frequency range the log-periodic antenna covers. Additionally, the usage scenarios for vertical and horizontal polarization are outlined, which may vary depending on the testing frequency range. Representative examples of all necessary measuring instruments, like spectrum analyzers and cables, are listed in ***Table 3*** with guidance on their connections.

The test environment may also be described with specific requirements, such as anechoic or low-re-

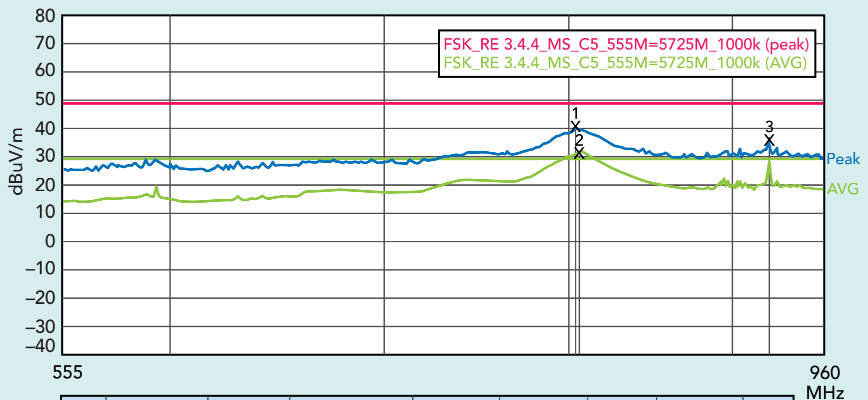

No.	Frequency (MHz)	Reading (dBuV)	Correction Factor (dB/m)	Result (dBuV/m)	Limit (dBuV/m)	Margin (dB)	Detector	P/F
1	804.500	47.59	–7.37	40.22	49.00	–8.78	Peak	P
2	806.500	38.85	–7.34	31.51	29.00	2.51	AVG	F
3	924.000	43.35	–5.83	37.52	49.00	–11.48	Peak	P
4	924.000	35.52	–5.83	29.69	29.00	0.69	AVG	F

Fig. 4 Radiation emissions results.

flection chambers, to ensure consistent and comparable test results across different testing sites and conditions. It is important to note that this is a generalized explanation and the specifics can vary with different editions or revisions of the CISPR 25 standard. The setup outlined provides a reference standard for experimenters to ensure reliable testing outcomes.

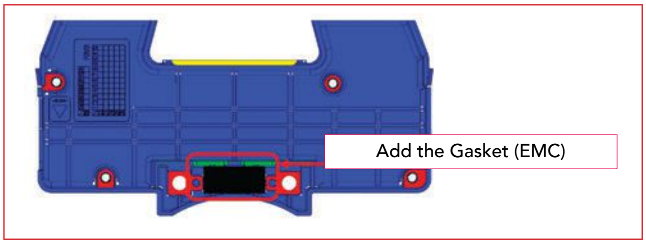

Fig. 5 **Identifying the problem area.**

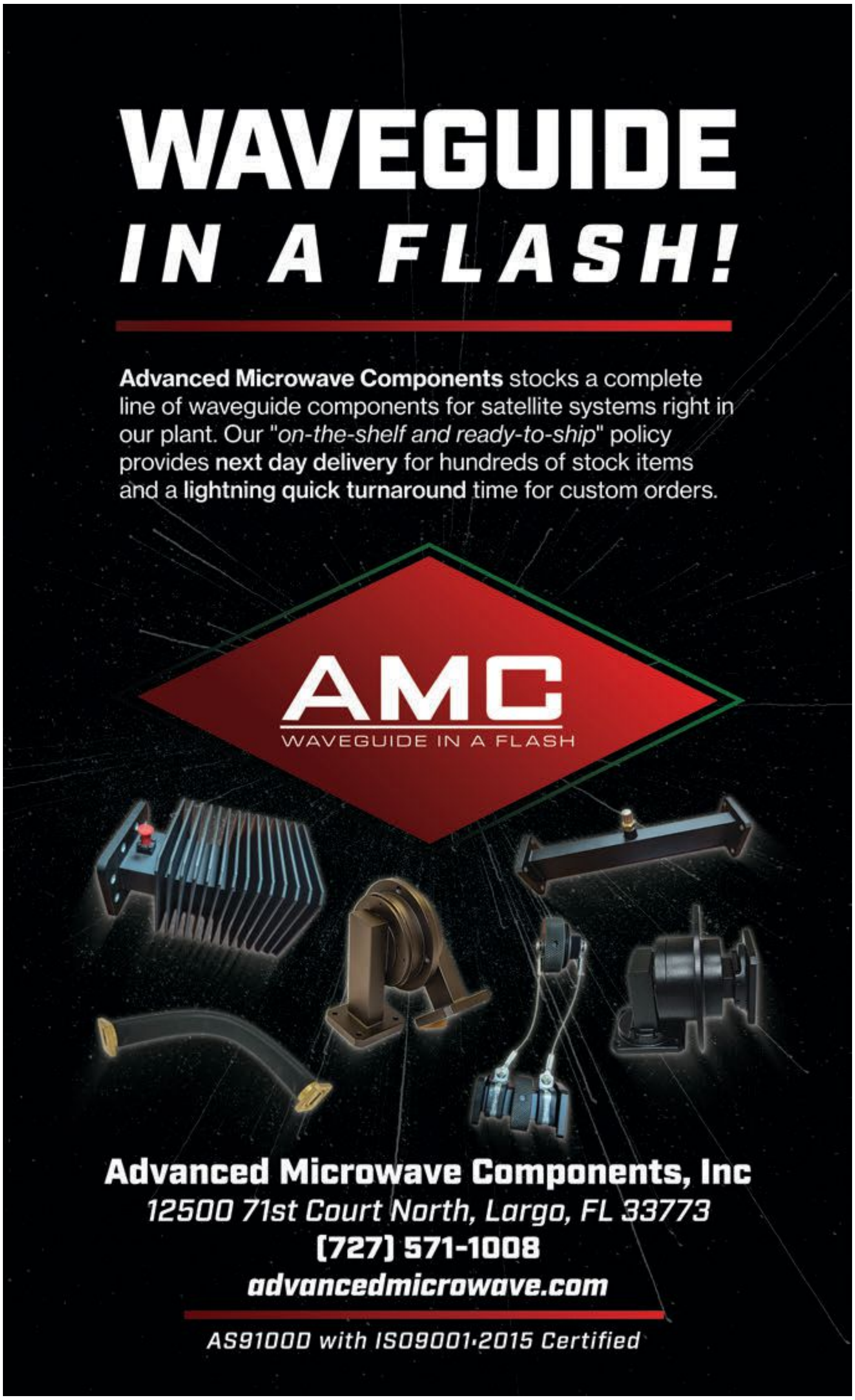

EXPERIMENTAL RESULTS

In the radiation emission tests, spanning the frequency range of 555 to 960 MHz, values exceeding the limits were identified, particularly at specific frequencies. Notably, the average radiation levels at the 806.5 MHz frequency exceeded the prescribed limit by 2.51 dB and the measured result at 924 MHz was 0.69 dB higher than the standard. The graph of the results and tabulated data is shown in ***Figure 4***.

A particular focus has been placed on the 806.5 MHz frequency to address these non-compliance issues, where the deviation was most significant. Drawing from the stringent criteria outlined in Class 5, as outlined in Figure 1, both peak and average emission limits are defined at 49 dBμV/m and 29 dBμV/m, respectively. Any frequency exceeding these thresholds is considered a failure that necessitates remedial actions. Figure 1 delineates more lenient criteria under Class 3 and Class 4, with peak limits of 61 dB/m and 55 dB/m and average limits of 41 dB/m and 35 dB/m, respectively. The test details reveal that for average emissions, the 806.5 MHz frequency showed a reading of 31.51 dB/m, surpassing the limit by 2.51 dB and the 924 MHz frequency registered 29.69 dB/m, exceeding the limit by 0.69 dB. For peak emissions, the 804.5 MHz and 924 MHz frequencies measured 40.22 dB/m and 37.52 dB/m, respectively, well within the Class 5 peak limit, thereby not exceeding the stringent 49 dBμV/m limit.

Testing circuit boards used in automotive electronic screens with a near-field probe detected excessive EM interference that could potentially affect screen function. The result showed notable spikes at specific frequencies, suggesting circuit instability. Despite recording peak values, the measurement equipment only indicated high noise levels without providing detailed insights, hinting at issues such as unstable power, inadequate grounding or component failure. Additional tests are needed to pinpoint the noise source and address it effectively.

Implementing the Conductive Foam Solution

The region indicated in ***Figure 5***

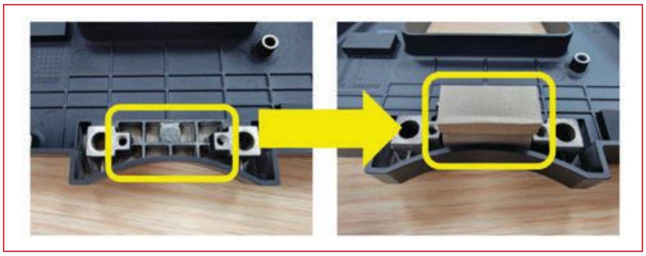

Fig. 6 **Implementing the conductive foam.**

was identified as the cause of the oscillations that pushed the measured results past the limits highlighted in Figure 4. This effect occurred after mounting the PCBA within the chassis. Before the assembly of the chassis, this specific area did not exhibit high noise levels. The conjecture is that the noise increase in this area could be due to the assembly of the chassis, which contains metal components.

To address this issue, foam encased in a conductive fabric was used to encapsulate the metal area. After this modification shown in ***Figure 6***, subsequent measurements with a near-field probe showed an 8 dB reduction in noise. This demonstrates the effectiveness of employing conductive foam in reducing noise in areas prone to oscillation.

Initially, radiation at the 806.5 MHz frequency exceeded limits by 2.51 dB. Retesting after the foam was installed revealed an 8 dB improvement at the 790 MHz, significantly better than the original levels and confirming the foam's effectiveness across multiple frequencies, including the initially problematic 806.5 MHz and 924 MHz. Despite all intervals passing upon retest, caution is advised due to values nearing failure thresholds. Notably, retests at 806.5 MHz and 924 MHz showed compliance with CISPR 25 standards, which prescribe limits for various types of EMI measurements to ensure the operational integrity of automotive components and that the components do not cause and will not suffer from interference. The retest results are shown in ***Figure 7***.

CONCLUSION

This study identifies an issue with radiation exceeding the CISPR 25 standard limits in automotive electronic vehicle information system screens. The study pinpointed the PCBA used in the screens as the primary radiation source. A significant improvement was achieved by modifying a gasket with conductive foam, effectively reducing the radiation levels. The excess radiation presents a compliance threat that could prevent the product from legally entering the market, affecting both the development cycle and costs. The identification of the PCBA as the primary radiation source underscores the necessity for design improvements focused on this area.

However, the scope of the study is limited to the 555 to 960 MHz frequency range. It is specific to a particular model of automotive electronic screens, which may not be universally applicable across other models or brands. Future research should encompass a broader frequency range and investigate why the PCBA is a significant radiation source, considering more comprehensive improvement strategies. Additionally, evaluating other radiation reduction technologies or materials beyond conductive gasket foam and conducting experiments on a larger scale across various automotive electronic devices would expand the applicability of this study. This research lays the groundwork for addressing specific radiation issues, proposing using conductive gasket materials to shield against radiated emissions. While conductive foam installation offers an effective way to mitigate the issue, the exact source of emissions is unknown, suggesting further investigation is needed to ensure compliance with regulations. ■

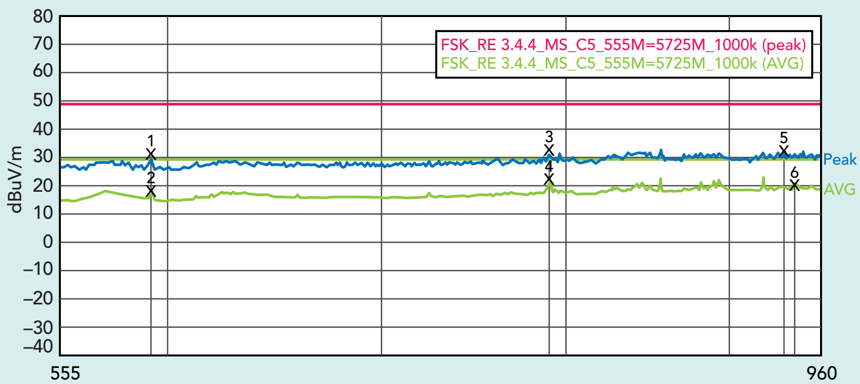

No.	Frequency (MHz)	Reading (dBuV)	Correction Factor (dB/m)	Result (dBuV/m)	Limit (dBuV/m)	Margin (dB)	Detector	P/F
1	592.500	40.86	–9.98	30.88	49.00	–18.12	Peak	P
2	592.500	28.15	–9.98	18.17	29.00	–10.83	AVG	P
3	790.000	39.55	–7.51	32.04	49.00	–16.96	Peak	P
4	790.000	29.88	–7.51	22.37	29.00	–6.63	AVG	P
5	936.000	38.66	–5.83	32.83	49.00	–16.17	Peak	P
6	943.000	26.30	–5.74	20.56	29.00	–8.44	AVG	P

Fig. 7 **Radiation emissions results with the conductive foam.**

References

1. IEC, International Special Committee on Radio Interference (CISPR) *Guidance for Users of the CISPR Standards*, February 2015.
2. UNECE, "Uniform Provisions Concerning the Approval of Vehicles with Regard to EM Compatibility," *Regulation No. 10*.
3. C. R. Paul, Introduction to EM Compatibility, 1st Ed. *John Wiley Sons*, 1992.
4. M. P. Robinson, T. M. Benson, C. Christopoulos, J. F. Dawson, M. Ganley, A. C. Marvin, S. J. Porter and D. W. P. Thomas, "Analytical Formulation for the Shielding Effectiveness of Enclosures with Apertures," *IEEE Trans. Electromagn. Compat.*, Vol. 40, August 1998, pp. 240–248.
5. M. P. Robinson, J. D. Turner, D. W. P. Thomas, J. F. Dawson, M. D. Ganley, A. C. Marvin, S. J. Porter, T. M. Benson and C. Christopoulos, "Shielding Effectiveness of a Rectangular Enclosure with a Rectangular Aperture," *Electronics Letters*, Vol. 32, August 1996, pp. 1559–1560.
6. C. F. M. Carobbi and D. Izzo," Evaluation and Improvement of the Reproducibility of CISPR 25 ALSE Test Method," *IEEE Transactions on EM Compatibility*, Vol. 60, No. 4, August 2018, pp. 1069-1077.
7. C. Carobbi and D. Izzo," Reproducibility of CISPR 25 ALSE Test Method," *IEEE International Symposium on EM Compatibility Signal/Power Integrity (EMCSI)*, 2017, pp. 57–62.
8. T. Hegarty, "An Overview of Conducted EMI specifications for Power Supplies," *Texas Instruments, Tech. Rep.*, June 2018.
9. CISPR, "Vehicles, Boats and Internal Combustion Engines–Radio Disturbance Characteristics–Limits and Methods of Measurement for the Protection of On-board Receivers," *CISPR, Tech. Rep.*, October 27, 2016.

RF-LAMBDA

MADE IN USA

THE LEADER OF RF BROADBAND SOLUTIONS

EMC Broadband RF Power Amplifier

High Power Solid State

HUNDREDS IN STOCK

FAST SHIPPING

FREQUENCY UP TO 90GHZ

POWER UP TO 2KW CW

REMC06G18GG

6-18GHZ 300W

- AUTOMATIC BUILT IN SELF CALIBRATION AND BIAS ADJUSTMENT.
- OVER TEMPERATURE, CURRENT, INPUT POWER PROTECTION.
- VSWR MEASUREMENT AND OPEN CIRCUIT PROTECTION.
- USER FRIENDLY CONTROL INTERFACE.
- REMOTE ETHERNET CONTROL AND FIRMWARE UPDATE.
- HIGH POWER EFFICIENCY AND LIGHTWEIGHT.

RAMP42G47GA 42-47GHZ 8W

RAMP18G40GB-U 18-40G 20W

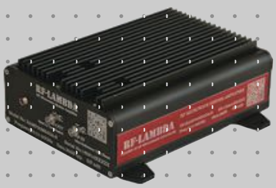

RAMP05M80GC 0.5-80GHZ

REMC02G06GE 2-6GHZ 500W

REMC08G11GE 8-11GHZ 400W

INVITED PAPER

Flat Panel Antennas: Why We Need Industry Collaboration to Foster Innovation

Joakim Espeland
QuadSAT, Odense N, Denmark

I was recently involved in the Satcoms Innovation Group (SIG) and Global Satellite Operators Association (GSOA) roundtable at Satellite 2024 and subsequent webinar. The two groups are working together to spearhead an initiative aimed at enabling innovation around flat panel antennas (FPAs) without risking the all-important quality of services. FPAs bring a number of crucial benefits that will be key to enabling the next generation of satcoms. Their lightweight nature, coupled with the ability to allow instantaneous beam steering, makes them ideal for comms-on-the-move, where the position is constantly changing. At the same time, the high reliability and low latency afforded by these antennas will be important both for low Earth orbit (LEO) and multi-orbit environments. However, a number of challenges currently stifling innovation need to be addressed. One thing that is clear is that the industry simply cannot get there without collaboration and QuadSAT looks forward to being an integral part of this joint project.

CURRENT MARKET DYNAMICS

While the satellite industry remains largely focused on parabolic antennas, the number of FPAs have been growing significantly. In a recent webinar, it was stated that there are 196 FPA manufacturers around the globe. This is backed up by a recent report by NSR,[1] which states that the FPA market is due to grow significantly over the coming years. While mobility, government and military are the major revenue growth areas, low-cost terminals for broadband have the potential to see a substantial increase in revenues.

Of course, we are already seeing widescale adoption of these systems in operation. There are thousands already in service, especially on airlines and boats, for example. These environments need multiple links to multiple satellites and FPAs are the only way to achieve that, making them not only ideal but, in fact, a necessity.

Despite this, the quality varies greatly between manufacturers and as we see more and more coming into operation. When this challenge is coupled with the staggering growth of satellites in orbit, with some public estimates claiming that 65,000 satellites will be in orbit by the end of this decade, the problem will only grow. At the same time, manufacturers have huge cost pressures on them, with customers expecting low-cost systems. While most manufacturers are ultimately striving to provide the most reliable, lowest cost of ownership system, this can be complex to achieve and even harder to prove due to the lack of regulatory requirements.

At the same time, many non-GEO satellite operators have been making their FPAs, meeting their own very specific requirements. Meanwhile, antenna manufacturers need to design their antennas according to multiple requirements from different operators, none of which are particularly clear right now. This is further complicated by the varied use cases these antennas are being deployed for, each with very different requirements and expectations. As applications increase, this will become more complex.

THE COMPLEX NATURE OF TESTING AND QUALIFYING FPAS

As mentioned above, FPAs are low profile with high reliability, thanks to a lack of mechanical parts, with much lower latency than parabolic antennas. All of this, plus the ability to create multiple beams, is a must for LEO and multi-orbit environments. They do have some disadvantages, the main one being that they are typically less efficient, as there is a more lossy RF distribution network. Some of this can be mitigated by having individual elements addressable and the electronics built into the back of them. They also introduce a number of technical challenges that make the operation more complex and complicate testing. For example, as you sweep the antenna pattern off its normal axis, the gain decreases by about cosine of the scan angle. This means that you can lose upwards of 15 dB in gain, as well as increase the beam width, which can cause interference.

These challenges make testing more important than ever. However, this is not as easy as it seems for several key reasons listed below.

Existing Test Methods Do Not Translate to FPAs

Current test facilities are built for dish antennas, with one beam and beam state. FPA is ushering in multibeam and a dynamic beam state. With FPAs, unlike parabolic antennas, the radiation pattern changes depending on the steering angle. Properly testing how they will perform requires testing of the entire radiation pattern, something that is both complex and time-consuming using traditional testing methods.

With established test facilities, it is often not possible to change the test setup once established, which does not allow the flexibility that is often needed for testing different types of antennas with different specifications. Often, a simulator is used instead. However, it relies on an assumption rather than being able to see the real behavior of the antenna under test. This is a problem, especially when you consider that errors could be easily introduced on specific antennas during the manufacturing process.

Testing Mistakes Produce False Data

Satellite operators and manufacturers alike need to be able to rely on the test data being provided. Without a dedicated testing procedure, it is very difficult to provide the correct performance information to cover every type of application. If the data cannot be trusted, it will simply be ignored. Testing FPAs, therefore, requires a new approach and proof that the performance data is reliable.

There is No Standardized Approach

One of the main things the SIG and GSOA projects aim to address is the need for a standardized approach. The previous Satellite Operators Minimum Antenna Performance (SOMAP) group established a common agreement on performance expectations and data requirements among the major satellite operators. However, it only applies to parabolic antennas. For FPAs, not only is there no agreed-upon common approach, but there are also no guidelines from individual satellite operators. The approach for parabolic antennas cannot simply be translated because of the challenges mentioned above.

Why We Need Standardized Testing

Standardization is extremely important because, without it, we are stifling innovation. Manufacturers need the guidelines because, without them, it is difficult to develop new systems that will be appropriate for the market. Without that innovation, it is harder to push boundaries without knowing the desired outcome. A lack of standards also increases the barrier to entry for newcomers, as it is challenging to understand how they can fit into the market and ensure compatibility. In a world where satcom is facing not only internal competition but also external competition from other technologies, the industry needs to ensure it is not left behind due to its lack of standards.

Due to the lack of guidelines, everyone is working in the dark. With no real guidance on what data needs to be provided, manufacturers often find themselves providing more than necessary. This is not ideal for either party, as the satellite operators have far too much data to trawl through to get the information they need to qualify an antenna. This is making the entire test and qualification process far less efficient than it should be for everyone involved.

How Do We Get There?

Getting to a point where there is a standardized approach for FPAs will require input from across the entire industry. It cannot be solved by one person, company or even group alone. We need to move forward, but once the industry has agreed, we should aim to have any guidelines and/or standards stamped and sealed by regulatory organizations.

That said, it will be a huge undertaking and one that will need to build into milestones with clearly defined roles. Antenna manufacturers, for example, have a role to play in suggesting and outlining performance metrics they believe should be provided, as well as highlighting what is and is not realistic to achieve. Testing solutions and service providers, such as QuadSAT, need to suggest new approaches to testing FPAs that better address their complex nature. QuadSAT has done a number of test scenarios using their drone technology that are better able to give a more holistic view of the antenna under test.

Of course, there may be other solutions. If we jointly suggest possible approaches, this can be encapsulated in the guidelines to ensure the right approach is used for the right type of antenna and application. Of course, satellite operators are an extremely important part of this puzzle, as they will ultimately need to define and approve any suggested procedures, approaches and performance metrics that will work for their networks. ■

References

1. B. Schneiderman, "Flat Panel Antennas Market," *Satellite Markets & Research*, April 5, 2024, Web: satellitemarkets.com/market-trends/flat-panel-antennas-market.

Cliff Drubin, Associate Technical Editor

Everyday Life, Improved by Light: GRYPHON's Photonic Discoveries

RF and microwave signals are integral carriers of information for technology that enriches our everyday life, such as cellular communication, automotive radar sensors and GPS navigation, among others. At the heart of each system is a single-frequency RF or microwave source, the stability and spectral purity of which is critical. While these sources are designed to generate a signal at a precise frequency, in practice the exact frequency is blurred by phase noise, arising from component imperfections and environmental sensitivity, that compromises ultimate system-level performance.

This reality drives undesirable tradeoffs between performance, environmental sensitivity and size that make the simultaneous achievement of stability, precision and agility in an ultra-compact form factor an elusive feat. However, DARPA's Generating RF with Photonic Oscillators for Low Noise (GRYPHON) program could change all of that, as performers recently demonstrated in the first phase of the program aimed at developing compact, ultra-low noise microwave frequency oscillators.

GRYPHON (Source: DARPA)

GRYPHON performers, using different light-based approaches, have made critical progress toward generating high-purity microwaves in significantly reduced form factors. By integrating low noise lasers with complex optical structures on low loss photonic platforms, along with high speed integrated circuits, researchers have established the viability of achieving ultra-low phase noise performance and shrinking these capabilities from conventional table-top sizes down to microchip-size form factors.

"The results and impact from Phase 1 of GRYPHON really show what is possible. For the first time, we are seeing how integrated photonics allows us to break from the traditional size vs. performance vs. capability trade space and operate in a regime with exquisite performance that is exponentially better than current state of the art," said Dr. Justin Cohen, GRYPHON program manager. "Better and faster communications, more accurate sensing, improved detection capabilities – this work could disrupt and advance countless applications."

The research findings of GRYPHON's performers were recently featured in Science and Nature journal articles, as well as via the National Institute of Standards and Technology, highlighting the work of contributing NIST researchers and their team. Now in Phase 2, GRYPHON researchers are seeking to further reduce phase noise in their already high performance sources while introducing tunability and compactifying to targeted form factors, all of which aim to provide systems with unprecedented utility and access to previously unattainable applications.

L3Harris Demonstrates EW Operations During Valiant Shield 2024 Exercise

L3Harris Technologies successfully demonstrated its new electronic warfare (EW) capability in the U.S. Indo Pacific Command's (USINDOPACOM) Valiant Shield 2024, a biennial field training exercise focused on integrating interoperability in a multi-domain environment. The company's new capability, Distributed Spectrum Collaboration and Operations (DiSCO™), is a cloud-connected electromagnetic spectrum operations architecture that will enable military forces to counter complex threats.

DiSCO (Source: L3Harris Technologies)

During the exercise, DiSCO successfully shared real-time RF signal data between Joint Base Pearl Harbor-Hickam, Hawaii, and multiple EW payloads operating in Hawaii and in San Diego, Calif. Small form factor payloads operated on two Seasats' autonomous surface vehicles along with satellite communications links at both locations. L3Harris operators also received real-time information from sensors through the cloud and initiated rapid reprogramming actions over-the-air from Hawaii and a remote company terminal in Clifton, N.J.

"DiSCO helps the warfighter to identify new threats through the use of artificial intelligence and machine learning tools to rapidly reprogram EW systems at the edge and make more informed, faster decisions across a network of distributed platforms," said Ed Zoiss, president, space and airborne systems, L3Harris. "Ultimately, our technology will ensure tactical forces have the tools they need for spectrum superiority."

This capability connects sensors and shooters to computer resources and cross-domain data sources through a combination of edge nodes and cloud applications, fusing and analyzing live mission data to enable rapid reprogramming, electromagnetic battle management and synchronization of non-kinetic effects across all domains.

For More Information Visit mwjournal.com for more defense news.

Wearable Secure Wireless Hub for Advanced Network and Edge Communications

Viasat, Inc. recently announced the introduction of the Secure Wireless Hub (SWH), a wearable tactical gateway solution for dismounted soldiers that is easy to carry and simple to use. The SWH solution was developed as part of a multiphase effort with U.S. Special Operations Command (USSOCOM) to identify and develop advanced tactical communications capabilities for mobile ground forces.

SWH (Source: Viasat, Inc.)

The SWH is the first wearable addition to Viasat's portfolio of tactical gateway solutions, providing a flexible, all-in-one design to enable faster set up for warfighters to improve user experience and support situational awareness within minutes. With a base of less than one kilogram, the SWH system offers significantly reduced size, weight and power to seamlessly integrate with body armor without adding unnecessary weight. In addition to reducing the physical load soldiers carry, the SWH provides an 85 percent reduction in cabling compared to other wearable hub systems, further simplifying ease of use for ground operators.

Viasat's SWH is designed to provide the capability of much larger systems to meet expanding requirements for tactical edge compute and networking in a small form factor for dismounted users. As a complete solution, the SWH will offer a body-worn tactical gateway that can provide a level of interoperability only previously seen in larger transit boxes that are too big for dismounted operations. Viasat's mobile software defined networking platform, NetAgility, will enable the SWH to use various tactical transports and advanced networking capabilities to improve situational awareness and data exchange. The edge compute capability will also offer a secure VPN, allowing the use of multiple transports and waveforms across a range of devices to provide resilient connectivity and safely share critical battlefield information.

Reactel, Inc.
Reacting First to All Your Filter Needs.
Let our Engineers show you what we can do in tight spaces!
High Performance, Rugged Packaging, Small Size and Weight
Great things can come in small packages. Reactel filters are ideally suited for the demanding environments that unmanned vehicles encounter.
Many manufacturers rely on Reactel to provide units which are:
High performance - Lightweight - Low profile
Contact a Reactel engineer with your filter or multiplexer requirements. We can create a unit which will be the perfect fit for your applications.
RF & Microwave Filters - Multiplexers - Multifunction Assemblies
REACTEL, INC.
REACTEL, INC.
REACTEL, INC.
Reactel is your source for RF & Microwave Filters, Multiplexers and Multifunction Assemblies covering DC – 67 GHz. Trust Reactel's highly skilled engineers to quickly develop and produce the most reliable products for your filter requirements.
8031 Cessna Avenue • Gaithersburg, Maryland 20879 • (301) 519-3660 • reactel@reactel.com • www.reactel.com
Intertek
RoHS Compliant
@reacteljim
MADE IN MD
Since 1979

DC TO 50 GHz

MMIC Amplifiers

300+ Models Designed in House

Options for Every Requirement

CATV (75Ω)

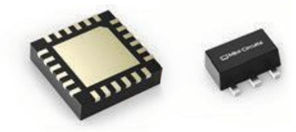

Supporting DOCSIS® 3.1 and 4.0 requirements

Dual Matched

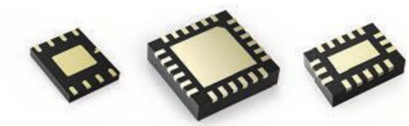

Save space in balanced and push-pull configurations

Hi-Rel

Rugged ceramic package meets MIL requirements for harsh operating conditions

High Linearity

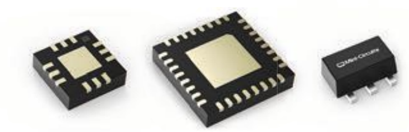

High dynamic range over wide bandwidths up to 45 GHz

Low Noise

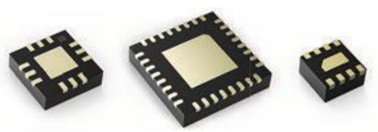

NF as low as 0.38 dB for sensitive receiver applications

Low Additive Phase Noise

As low as -173 dBc/Hz @ 10 kHz offset

RF Transistors

<1 dB NF with footprints as small as 1.18 x 1.42mm

Variable Gain

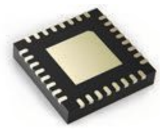

Up to 31.5 dB digital gain control

Wideband Gain Blocks

Flat gain for broadband and multi-band use

Mini-Circuits®

Satellite Network Operators to Launch 15,000 New Satellites Over Next 5 Years to Support IoT Growth

A new study from Juniper Research has found that the number of satellites in orbit that can be leveraged for IoT connectivity will grow 150 percent over the next five years.

The study predicts that these satellites will grow from 10,000 in 2024 to over 24,000 by 2029; owing to increased demand for connectivity in nomadic locations from IoT network users. It forecasts that 98 percent of satellites launched over the next five years will be low earth orbit (LEOs), due to the low cost of launches.

> Study urges substantial investment in multi-orbit satellite solutions.

To meet this growing demand for satellite IoT connectivity, the study urges substantial investment in multi-orbit satellite solutions. This model combines the low latency and high throughput from LEO satellites and the extensive geographical coverage of geostationary earth orbit (GEO) satellites over a single service. This will enable satellite IoT providers to cater for the wide spectrum of IoT use cases, including data-intensive and low power, wide area connections.

The study urges satellite network operators to form strategic partnerships that fill in coverage gaps between LEO and GEO capabilities. It identified construction and infrastructure, and logistics, as two key growth opportunities. It found that the wide range of connectivity requirements, such as nomadic operational areas and conditional monitoring, necessitate the use of both LEOs and GEOs for complete service provision. Partnerships that enable the use of LEOs and GEOs for IoT networks will be essential to attract enterprise users in these sectors.

NTN and Direct-to-Cellular Markets to Exceed US$17B by 2032, with Apple and Starlink Leading the Charge

The non-terrestrial network (NTN) market is entering a new mass adoption phase. During 2H 2024, iOS release 18 and Android 15 are set to introduce satellite messaging as a core feature, enabling millions of devices worldwide to tap into satellite connectivity. At the same time, SpaceX's new direct-to-cellular (D2C) Starlink network is expected to launch commercial services in 2H 2024, enabling millions of LTE devices using Android 15 to access satellite connectivity. According to a new report from ABI Research, the total connection revenue generated from the NTN and D2C markets will reach US$17 billion a year by 2032, representing a compound annual growth rate of 39.8 percent.

With the rapid deployment of non-geostationary orbit D2C networks like Starlink, AST Space Mobile, Lynk, alongside legacy Mobile Satellite Service (MSS) and NTN services available from GSO operators like Viasat (Inmarsat), EchoStar and China Aerospace Science and Technology Corporation, innovation in the satellite NTN and D2C segment is accelerating. Andrew Cavalier, satellite communications senior analyst at ABI Research, explained, "The market is now rapidly shifting from narrowband emergency services supported on specific devices by NTN IoT protocols to two-way messaging and data services over terrestrial LTE, MSS and NTN standards via satellite. While these services are taking distinct evolutionary tracks, this competition is reducing overall cost to these services while increasing accessibility to more users."

> Increased launch capacity has set the stage for a surge in satcom applications.

The increased launch capacity within the satellite industry has set the stage for a surge in satcom applications, heralding a new era of abundance in lower-cost satellite services. According to Cavalier, "NTN is primed to experience a surge in popularity, and ecosystems players such as chipset vendors alongside organizations like the Mobile Satellite Services Association are helping bridge the gap in technology, connectivity and collaboration." Companies like Starlink and Apple are poised to lead the satellite NTN marketplace with the widespread launch of commercial services in 2024. "We anticipate the seamless access of Starlink and Apple Satellite connectivity on devices will attract new and existing customers to leverage this technology when outside terrestrial coverage. Users will expect these services to be affordable if not completely bundled together in more premium service offerings," Cavalier pointed out.

5G Americas Examines Spectrum Challenges and Opportunities in New Briefing Paper

Recently, 5G Americas announced the publication of its briefing paper, "Spectrum Sharing: Challenges and Opportunities," providing an in-depth exploration of the various spectrum sharing models, their technical, regulatory and economic complexities and the potential benefits they offer to the wireless industry.

For More Information Visit mwjournal.com for more commercial market news.

Along with standardized same and multi-technology spectrum sharing techniques, the briefing paper discusses implementation of evolved spectrum access systems and dynamic spectrum sharing (DSS) technology, as the demand for wireless services continues to surge. The paper highlights the differences in industry specifications and regulatory perceptions in relation to DSS, as well as identifying the challenges of spectrum sharing. It highlights the significance of the 3.1 to 3.45 GHz band, emphasizing its potential for commercial services and the advancements needed in sensing technologies to ensure effective spectrum management.

Chris Pearson, president, 5G Americas said, "Dedicated exclusive use radio spectrum is a critical resource affecting the U.S. wireless industry, economy and technology leadership. Yet, effective spectrum sharing could be a part of some solutions but will require innovative technologies and collaborative regulatory frameworks to ensure that both legacy users and new entrants can coexist without compromising performance."

The white paper provides an in-depth examination of various spectrum management models including licensed, unlicensed and shared spectrum approaches along with complexities of DSS. Key sections of the 5G Americas briefing paper include:

- An overview of existing spectrum management models, detailing the licensed, unlicensed and shared spectrum mechanisms
- Definitions and techniques of DSS, exploring its various interpretations by leading industry bodies such as 3GPP and 5G Americas
- A review of current commercial experiences in the U.S., focusing on the Citizens Broadband Radio Service and Automated Frequency Coordination in the 6 GHz band
- An exploration of potential spectrum sharing approaches in the 3.1 to 3.45 GHz band
- An analysis of the technical, regulatory and economic challenges associated with spectrum sharing.

"The ability to share spectrum efficiently is not just a technical challenge but a strategic opportunity. We must develop policies that incentivize cooperation and ensure fair access to this critical resource," said work group co-leader Karri Kuoppamaki, SVP, advanced and emerging technologies, T-Mobile, USA, Inc.

"Exclusive spectrum use is vital for societal, economic and national security benefits, but when dedicated spectrum for commercial services is not possible, spectrum sharing offers a possible solution," stated Brian Daly, AVP Wireless Technology Strategy & Standards, AT&T. "Spectrum sharing, using advanced radar sensing methods, could provide part of the solution to meet the additional spectrum needs of wireless services, if preferred commercially licensed spectrum is not available."

Around the **Circuit**

Barbara Walsh, Multimedia Staff Editor

MERGERS & ACQUISITIONS

AMCAD Engineering announced that it has been acquired by **Dassault Systèmes**, joining its **SIMULIA** brand, dedicated to delivering science-based multi-scale, multiphysics modeling and simulation solutions that enable companies to accelerate the development of safe, reliable and sustainable products. This move aligns with the mission of AMCAD Engineering to streamline design processes and lower prototyping expenses by making measurement, modeling and simulation more accessible to RF and microwave circuit-system designers throughout the development process. AMCAD Engineering's software products, including IVCAD, VISION IQSTAR and Whiteboard, are now part of the SIMULIA brand.

L Squared Capital Partners and **CogneSense** announced that they have completed the acquisition of **L&J Technologies**. L&J is the first acquisition made by CogneSense since its founding by L Squared in late 2023. CogneSense, led by Paul Dhillon, is pursuing a buy and build strategy with a focus on combining long-standing, trusted and leading environmental sensing, measurement, monitoring and control businesses with younger companies that add additional technological innovation and capabilities. The focus of this strategy is the highly fragmented environmental, health and safety end-markets within the broader sensing and IoT market. They will operationally integrate these companies and add resources that will accelerate their go-to-market and R&D capabilities while driving increased operational efficiency at substantially larger scale.

COLLABORATIONS

EMITE's state-of-the-art over-the-air chambers can now be combined with the latest sophisticated testing features of the R&S CMX500 one-box signaling tester from **Rohde & Schwarz**. The radio communication tester offers a wide range of device testing capabilities, supporting cellular technologies such as LTE, 5G NR frequency range 1 (FR1) up to 8 GHz and FR2 mmWave frequency range up to 50 GHz, including the latest 5G RedCap technology. It also supports non-cellular technologies, including the latest Wi-Fi 7, all in a single instrument. As a consequence of this collaboration, EMITE's customers obtain a comprehensive environment for accurately assessing the performance of Wi-Fi 7 as well as 5G RedCap devices.

Texas Metering & Device Company (TMD), a provider of advanced metering infrastructure (AMI) and services for electric, water and gas utilities, and **The Antenna Company**, a pioneer in the design of high performance antennas and provider of industry-proven RF coupler/external antenna isolator solutions, announced a robust solution for improved wireless connectivity of off-network smart meters for electric utilities. This collaboration combines TMD's AMI expertise and industry knowledge with The Antenna Company's innovative high-efficiency LTE antennas (AC94541-01) and RF Coupler solution (AC20424-01) to solve the connectivity problem of off-network utility smart meters. TMD will serve as a U.S. distributor for The Antenna Company's products included in the smart meter retrofit kit.

Viavi Solutions Inc. and the **Telecom Infra Project (TIP)** announced a strategic collaboration aimed at expanding the testing capabilities of the VIAVI Automated Lab-as-a-Service for Open RAN (VALOR™). VALOR, made possible by a $21.7 million grant from the U.S. National Telecommunications and Information Administration Public Wireless Supply Chain Innovation Fund, provides fully automated, open and impartial testing and integration for Open RAN. VALOR provides a pathway to certification in the U.S. for new entrants, startups and academia and ensures the interoperability, performance and security of Open RAN components. TIP, a global consortium dedicated to advancing and adopting open and disaggregated networks, thrives on the collective contributions of its member companies.

Tech Soft 3D and **Spatial**, a **Dassault Systèmes** subsidiary, have strengthened their strategic alliance with the goal of driving the engineering industry forward. This enhanced partnership aims to deliver best-in-class technology, fostering rapid application development and solving real-world engineering challenges more effectively. For more than two decades, Spatial and Tech Soft 3D have shared a vision of empowering engineers with cutting-edge visualization technology. This collaboration underscores their commitment to innovation and excellence in the engineering software market. Most recently, Spatial has chosen to add Tech Soft 3D's HOOPS Communicator graphics engine for web visualization to its portfolio of components.

NEW STARTS

ISE Labs Inc., a leading provider of semiconductor engineering services, announced it is broadening customer access to its world-class capabilities with the opening of a second U.S. facility, located in San Jose, Calif. Together, the Fremont and San Jose sites will double ISE's available R&D lab and business space, reinforcing the company's commitment to Silicon Valley while expanding its North American footprint and helping to strengthen the U.S. semiconductor supply chain.

ACHIEVEMENTS

Keysight Technologies Inc. gained validations for the industry's first 5G NR FR1 1024-QAM demodulation test cases based on the 3GPP TS 38.521-4 test specification. The validated test cases, which are for use with Keysight's 5G network emulation conformance test platform (TP168), were secured at the Conformance Agreement

For More Information — For up-to-date news briefs, visit mwjournal.com

Group #79 meeting of the Global Certification Forum in July. Developed by 3GPP, 5G NR radio access technology delivers the performance needed to support enhanced Mobile Broadband (eMBB), which provides end users with better multimedia experiences through higher data rates, increased bandwidth, improved reliability and lower latency.

NXP® Semiconductors announced that its single-chip NFC and embedded secure element solution, the SN220, has been certified by the **Car Connectivity Consortium®** (CCC) under its CCC Digital Key™ Certification Program, launched in December 2023. This marks NXP as the first digital car key solution provider to receive a certification for its NFC chips. This is a part of NXP's complete system solutions encompassing the full digital car key ecosystem across ultra-wideband, NFC chips and Bluetooth® Low Energy for both mobile device manufacturers and car OEMs. The SN220 is a convergence solution, combining an NFC controller with an embedded secure element in a single chip and is part of an overall digital key system solution.

As part of the Investing in America tour, the **Biden-Harris Administration** announced that the **U.S. Department of Commerce** along with **GlobalWafers America LLC** and **MEMC LLC**, subsidiaries of **GlobalWafers Co. Ltd.**, have signed a non-binding preliminary memorandum of terms to provide up to $400 million in proposed direct funding under the CHIPS and Science Act to help onshore critical semiconductor wafer production and advance U.S. technology leadership. President Biden signed the bipartisan CHIPS and Science Act, a key component of his Investing in America agenda, to usher in a new era of semiconductor manufacturing in the U.S., bringing with it a revitalized domestic supply chain, good-paying jobs and investments in the industries of the future.

Raytheon, an **RTX** business, was awarded two strategic Mentor Protégé Agreement initiatives from the **Department of the Navy Office of Small Business Programs** to support the development of operational AI for Department of Defense (DOD) platforms and programs. Through joint sponsorship from **NAVAIR** and the **Office of Naval Research**, Raytheon will mentor Anacapa Micro Products, Inc. and Nara Logics, Inc. Under two individual three-year contracts, Raytheon will provide mentorship for operational AI on system design, software architecture, systems integration, IT security constraints and authority-to-operate requirements in a collaborative environment.

Anywaves announced the delivery of its 1,000th product, marking a major milestone in its journey as a pure manufacturer of space antennas. This 1,000th delivery not only confirms Anywaves' position as an indispensable leader in its sector but also the seriousness and reliability of its products. Since its inception in 2017, the company has consistently stood out for its commitment to excellence and customer satisfaction, designing, manufacturing and delivering off-the-shelf and custom antennas worldwide. Today, major players in the global space industry such as Maxar, Airbus Constellation Satellites, Magellan, The Exploration Company, Hera Systems and many others turn to Anywaves for their antenna needs.

CONTRACTS

CACI International Inc. announced that it was awarded a ten-year expertise contract valued at up to $450 million to support the **Joint Navigation Warfare Center (JNWC)**, an operational center of **U.S. Space Forces – Space** and the **DOD's** center of excellence for navigation warfare (NAVWAR). CACI will provide 24/7 operations support, joint and operational planning, adversary positioning, navigation and timing capability and order of battle assessment and other tasks that inform and enhance joint force, DOD combatant commander, interagency and allied NAVWAR requirements.

Sensor specialist **HENSOLDT** is further expanding its position as a national technology champion for air defence sensors. **Rheinmetall Air Defence** has awarded HENSOLDT a contract to supply SPEXER air defence radars for use in the new Skyranger 30 anti-aircraft gun tank (FlakPz). The order is worth almost 100 million euros. With the Skyranger 30, Rheinmetall Air Defence is providing the successor to the Gepard FlakPz in the Bundeswehr's newly established air defence force. With the SPEXER 2000, this will be equipped with a radar whose high detection performance will enable the effectors of the new FlakPz to develop their full potential.

SES Space & Defense, a wholly owned subsidiary of **SES**, has been awarded a multi-year contract worth USD 46.8 million by the **U.S. Air Force (USAF) Air Combat Command (ACC)** to provide geostationary (GEO) Ku-Band satellite services in support of the ACC remotely piloted aircraft (RPA) training and testing program. SES Space & Defense will use SES's GEO high-throughput satellite fleet to provide ground-to-air and air-to-ground transmissions coverage over the continental U.S., Hawaii, Alaska and the Pacific Ocean for airborne operations. In addition, SES Space & Defense's Global Network Operations Center will provide network management and monitoring support.

Barnes Aerospace announced a long-term agreement extension with **MTU Aero Engines AG**, through which it will provide a package of precision fabricated components valued at $33 million. Leveraging its existing manufacturing capabilities, Barnes Aerospace–Singapore OEM will produce mission-critical aero-engine components to be used in Pratt and Whitney's A320neo/A220 and Gulfstream G500/G600 engines. These applications require high-precision technologies in high volume. This agreement aligns with the company's growth strategy to scale Barnes Aerospace through deepening customer relationships and providing diverse capabilities with differentiated service offerings.

The Office of the Undersecretary of Defense for Research & Engineering's Trusted & Assured Microelectronics program through Naval Surface Warfare Center Crane Division's Strategic & Spectrum Missions

Advanced Resilient Trusted Systems (S2MARTS) other transaction agreement vehicle has awarded **BAE Systems'** FAST Labs™ and Development organization a $22 million contract. The contract will support the Strategic Transition of Microelectronics to Accelerate Modernization by Prototyping and Innovating in the Packaging Ecosystem (STEAM PIPE) project and will be managed by National Security Technology Accelerator. Microelectronics play a critical role in furthering the DOD's warfighting capabilities.

PEOPLE

▲ *Rick Stuby*

The Antenna Company announced it has appointed **Rick Stuby** as vice president of product management and marketing. In this role, Stuby will define and launch innovative solutions to the market, with an emphasis on IoT and 5G market segments. Stuby brings extensive industry experience and product leadership in the antenna market. Prior to joining The Antenna Company, Stuby served in the same VP role for Linx Technologies, where he defined their antenna product roadmap, spearheaded process changes and achieved substantial growth in business prior to their acquisition by TE Connectivity.

Sivers Semiconductors AB announced the appointment of **Vickram Vathulya** as its new president and CEO, succeeding Anders Storm, effective August 19, 2024. Dr. Vathulya brings over 25 years of experience in the semiconductor industry with a proven track record in building strategically sound businesses backed by strong organizational talent while navigating complex market dynamics to lead Sivers through its next phase of growth. As CEO, Vathulya leverages his senior leadership experience, extensive network and deep understanding of the semiconductor industry to drive Sivers' strategic initiatives worldwide.

REP APPOINTMENTS

Spirit Electronics announced franchised distribution for **Q-Tech Corporation**, offering crystal oscillators for the aerospace and defense supply chain. Q-Tech produces high-reliability crystal oscillators for space, military, avionics and extreme environment applications. The Q-Tech product portfolio adds to Spirit's curated domestic space and defense product lines alongside supply chain services including MIL-STD-883 testing, circuit card assembly and ASIC programs Q-Tech pioneered hybrid crystal oscillator technology as the first manufacturer to appear on the MIL-PRF-55310 qualified products list in 1972. Since then, Q-Tech oscillators have supported government and commercial space programs, both in the U.S. and internationally, as an award-winning manufacturer.

INVITED PAPER

UWB's Increasing Role in Automotive Applications

Kevin Mak and Asif Anwar
TechInsights, Milton Keynes, U.K.

Ultra-wideband (UWB) technology is increasingly being deployed in the automotive sector for a variety of reasons. One common application is to use the technology to surmount the vulnerabilities of RFID-enabled key fobs, which can easily be hacked and allow vehicles to be stolen. It is also being considered as a radar technology to ensure children are not left behind in the back seat.

AUTOMOTIVE ENTRY SYSTEMS

The 1982 Renault Fuego was the first model to use a remote key fob to unlock the car doors. Although the growth of this approach was initially slow, it accelerated in the 1990s. By 1995, around a third of vehicles made that year had the feature, with the penetration rate exceeding 50 percent in 2000.

In 1993, the Chevrolet Corvette was the first to use a passive entry system. In this system, an enabled fob would send out low frequency (LF) signals to unlock the car doors when it was near the vehicle. By 2014, penetration of passive entry systems reached 20 percent and this has now grown to 50 percent in 2024, with essentially all vehicles now being fitted with either remote or passive entry systems. ***Figure 1*** shows data from TechInsights on the market share of remote and passive keyless entry systems.

Early passive entry systems were proprietary systems based on the ISM band before being replaced by the Bluetooth standard. The 2017 Tesla Model 3 was the first model to feature a Bluetooth Low Energy (BLE)-based entry system. The fob in this system used a Texas Instruments TMS37F128 controller chip. Replacing the earlier LF solution, BLE has become the communication standard for passive entry systems. Another technology being deployed in automotive entry systems includes near-field communication (NFC). The first model fitted with an NFC entry system was the 2016 Mercedes-Benz E-Class. Here, an enabled key card or smartphone handset is placed over an NFC reader on the vehicle to unlock the doors. Tesla models also come with NFC cards for use in valet parking.

Digital Key

Both NFC and BLE have now become the standard communication protocols for the Car Connectivity Consortium (CCC). These protocols were defined in its second and third digital key releases in April 2020 and July 2021, respectively. The purpose of the CCC is to develop and standardize entry systems for vehicles to add convenience to families and fleets sharing identical vehicles and enable new services. Members of the CCC include many original equipment manufacturers (OEMs), automotive Tier 1 integrators, mobile OEMs and semiconductor suppliers, including Infineon, NXP and STMicroelectronics.

These new services include car-sharing and remote delivery, among others. Enabling the new services is the digital key. The digital key dispenses with the need for mechanical blade keys that have been the cornerstone of the automotive sector since the 1950s, when they were first used to start engines. With such virtual "keys," the same vehicle can be used by different drivers without the costly need for service centers to hold different keys. This technology can provide many benefits. Cars-for-hire companies stand to gain with lower operating costs and a delivery can be made to a vehicle instead of a customer who could be away from home. These digital keys can be exchanged via an app on a smartphone.

Standardization enables interoperability between different suppliers and OEMs in the automotive and mobile sectors. It also ensures the security of the resulting systems. In addition, it raises competition between suppliers to make the digital key concept affordable and bring about widespread adoption.

UWB

Hackers can intercept the LF BLE and/or NFC transmission and gain

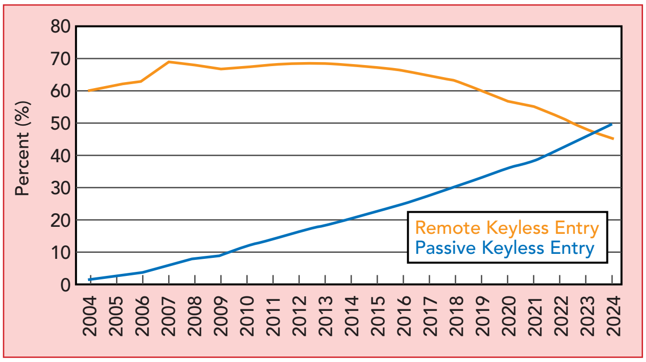

Fig. 1 **Demand for remote and passive keyless entry systems.** ***Source:*** **TechInsights.**

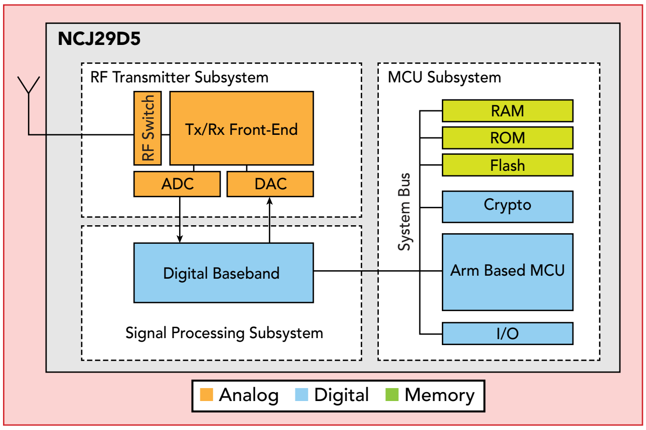

Fig. 2 **NXP Trimension NCJ29D5 functional block diagram.** ***Source:*** **NXP.**

access to the unlocking codes from the fob. This allows a thief to steal a vehicle without needing to be in close proximity. This is where UWB provides an advantage. UWB has the resolution to accurately determine the position of the enabled device and ensure that the actual owner of the vehicle is approaching the vehicle. Jaguar-Land Rover was the first OEM to implement UWB technology when they put it on the 2018 Jaguar I-Pace electric crossover and the Range Rover SUV. Other OEMs that have now adopted UWB-based keyless entry systems include BMW, Hyundai, Mercedes-Benz, NIO, Tesla and Volkswagen.

NXP supplied the IC that was installed in these first vehicles and the enabling fob. That IC carries the IP developed by a Dublin, Ireland-based start-up called Decawave, which Qorvo acquired in February 2020. NXP has since become a major chip supplier of UWB solutions in the automotive sector, supplying the Trimension NCJ29D5 IC to BMW vehicles and the SR100T IC to smartphone handsets. ***Figure 2*** shows a block diagram of the NXP Trimension NCJ29D5 IC.

For mobile applications, Apple and Qualcomm are the leading vendors of UWB-enabling chips. These chips are often integrated into system-on-chip (SoC) packages. Infineon is another key player. In October 2023, Infineon acquired 3dB Access, a start-up based in Zurich, Switzerland. 3dB Access brought its design capabilities for incorporating integrated SoCs into UWB systems. Infineon has leveraged this capability to become a major supplier, which includes supporting Volkswagen for both the vehicle and enabling fobs.

3dB Access has brought some valuable capabilities to Infineon. Where the CCC Release 3.0 standard calls for the high-rate pulse (HRP) version of UWB, 3dB offers a solution that encompasses both HRP and low-rate pulse (LRP) methods. The IEEE sets out these methods in its 802.15.4z standard. The 3dB dual-mode solution has an LRP method that has a lower frequency of pulses at a higher energy, resulting in lower power consumption. This dual-mode solution proved ideal for battery-operated devices such as key fobs. The HRP part of 3dB's solution reduces current consumption in both the transmitter and receiver yet remains compliant with the standards.

The new IEEE 802.15.4z standard, released in 2020, optimizes UWB signaling to exploit best the energy stipulated in the two rules regulating the use of the UWB frequency spectrum. The first rule limits the maximum mean power spectral density (PSD), which is the radiated power within a given bandwidth when averaged over 1 ms, to -41.3 dBm/MHz or 74 nW per MHz. The second rule addresses the strength of a single pulse that can be transmitted. It limits the power of the UWB signal to a maximum of 0 dBm when passing it through a filter with a bandwidth of 50 MHz. This is 10 percent of the energy of the original 500 MHz wide signal. This second rule prevents solutions involving just one large pulse. The IEEE is currently working on IEEE 802.15.4ab, an enhanced version of the UWB standard. This version aims to include various new features such as narrowband (NB)-assisted UWB, lower power consumption, higher data rates, security and more.

Chinese automakers are also keen to offer this feature to their customers, particularly start-up electric vehicle makers. A group of Chinese semiconductor vendors is offering UWB solutions to the market. These vendors include Chi Xin Semiconductor, Ultraeption, Yuducomm and UniSoC, whose SoCs embed UWB capability. However, it is interesting to note that these vendors are not members of the CCC.

CHILD PRESENCE DETECTION

UWB is also being considered for use in sensing cabin occupants. Impulse radio UWB (IR-UWB) is already a well-established method for radar sensing and UWB radar has the resolution necessary to detect small movements. This capability allows for motion detection, presence sensing and vital sign detection for "sleeping" consumer electronics devices. This can save power or detect intruders in surveillance systems.

Automotive radars are increasingly being developed for child presence detection (CPD) systems. Such sensors have the resolution to detect movements from heartbeats or breathing. CPD alerts drivers of any children who could be left behind in the rear seats and suffer injuries from hot conditions in the vehicle. In 2023, 29 children reportedly died in the U.S. from heat stroke while left in vehicles. Also, in 2023, CPD was included in the European New Car Assessment Program (Euro-NCAP) five-star safety award criteria. In 2016, 20 automakers made an agreement with National Highway Traffic Safety Administration (NHTSA)

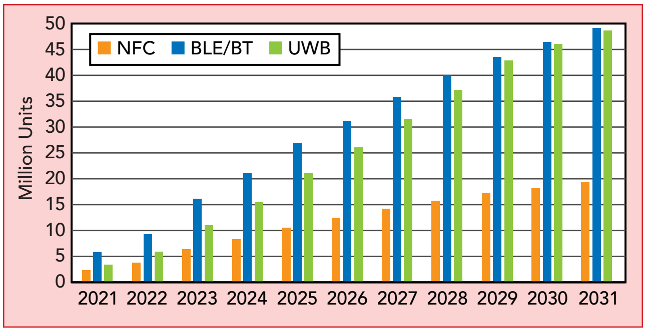

Fig. 3 Demand for NFC, BLE/BT and UWB in passive keyless entry systems. *Source:* TechInsights.

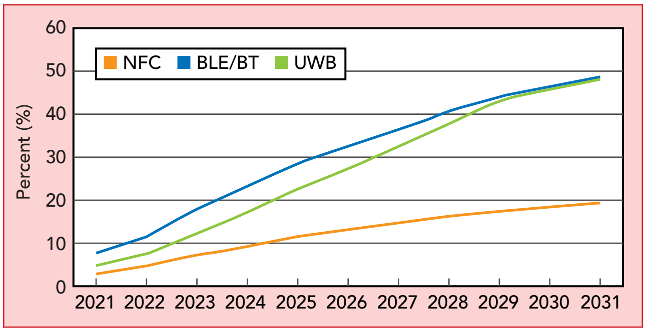

Fig. 4 Penetration of NFC, BLE/BT and UWB in passive keyless entry systems. *Source:* TechInsights.

and Insurance Institute for Highway Safety (IIHS) to fit rear seat alert systems as part of CPD by Model Year 2025. Because of the Hot Cars Act of 2021 (HR 3164), the 2021 Build Back Better Act also required NHTSA to consider the mandated fitment of CPD as early as 2027.

In the above applications, the same UWB chipset can be used not only for ranging in applications like entry systems but also for sensing. The sensing application typically requires a different software configuration that comes with a higher feature set. This gives UWB radar a cost advantage over conventional 60 GHz frequency-modulated continuous wave (FMCW) radars that require a dedicated electronic control unit (ECU) and chip to implement the sensing functions.

OEMs can also reduce the system bill of materials by repurposing chip devices already in use. For example, a CPD radar can be used for intrusion detection in a security system, to "sleep" display screens or to turn off interior lights. Another use case for these devices is a kick-sensing application where a UWB device operating in radar mode is used to detect a kick gesture from a user to open the trunk. Presently, there are no standards for UWB radar, but the IEEE 802.15.4ab standards team is working on standardizing UWB as a radar for mono- and multi-static sensing.

MARKET DEMAND

The cost of implementing digital key systems will mean that penetration of digital key-enabling passive entry systems (with NFC and BLE) will be highest in North America, South Korea and Western Europe, as well as among the premium brands. China will also see a high level of demand, primarily from the technology-leading electric vehicle start-ups, but not at the same level of penetration. Additional demand will also come from Eastern Europe and Japan. TechInsights forecasts that global demand for BLE and Bluetooth (BT)-enabled systems will increase from 16 million units in 2023 to 40 million in 2028 at a cumulative annual average growth rate (CAAGR) of 20 percent and reach nearly 50 million in 2031. In addition:

- Mature market regions like North America, South Korea and Western Europe will see penetration rates increase from around 26 percent in 2023 to around 65 percent in 2031
- Eastern Europe and Japan will see penetration rates increase from 13 to 14 percent in 2023 to around 50 percent in 2031
- China will see slower growth in the adoption rate, increasing from 15 percent in 2023 to 40 percent in 2031
- Thailand will see penetration rates increase from 9 percent in 2023 to 37 percent in 2031
- India and Brazil will see penetration rates increase from 5 percent in 2023 to around 30 percent in 2031.

Within the demand for these passive entry systems, BLE will see more rapid growth than NFC because of the added convenience to the user and the challenging requirement to integrate NFC-reading antennas into the vehicle.

- NFC will be deployed in lower volumes to support car-sharing services and to provide valet parking for premium brands. It is assumed that NFC will be deployed in around 40 percent of digital key-enabling passive entry systems.
- UWB will also see rapid growth among passive entry systems because of the added security it brings to BLE-based passive entry systems. It is assumed that all digital key-enabling passive entry systems will deploy BLE, with UWB seeing penetration rising steadily from 58 percent of digital key-enabling passive entry systems in 2021 to 99 percent by 2031.

Figure 3 shows the latest TechInsights forecast for the volume of passive keyless entry systems in automotive applications from 2021 to 2031. It shows the expected volumes for NFC-, BLE/BT- and UWB-enabled systems. ***Figure 4*** shows the expected market share for the three different technologies over the forecast period.

At this early stage in its development, internal radar demand is estimated to be very low. However, deployments and interest are growing. The Acconeer 60 GHz pulsed coherent sensor, manufactured by Alps-Alpine, is deployed on the 2022 Volvo EX90 electric SUV, 2023 Lotus Eletre and Polestar 3. The pulse-coherent sensor uses time-of-flight measurements from a sequence of pulses that are pulsed in picosecond intervals. The technique is an alternative to FMCW, which has a higher power consumption.

CONCLUSION

The convenience of remote keyless entry and passive entry systems is resulting in faster adoption of these technologies by the automotive industry. The CCC is leading efforts to standardize and enhance security as the automotive sector embraces the digital key concept, with consumers embracing the added convenience. Some of the other benefits of this approach are a reduction in operating costs for fleets and car-for-hire operators and the growth of new mobility services such as car-sharing. Efforts to enhance security will drive UWB demand. This demand will see steady growth as solution providers leverage the resolution UWB offers to accurately determine the position of the enabled device and ensure that the actual owner of the vehicle is approaching. Furthermore, the technology offers dual-use capabilities and could provide an alternative occupant detection requirement currently being pursued through the adoption of 60 GHz radar solutions. ■

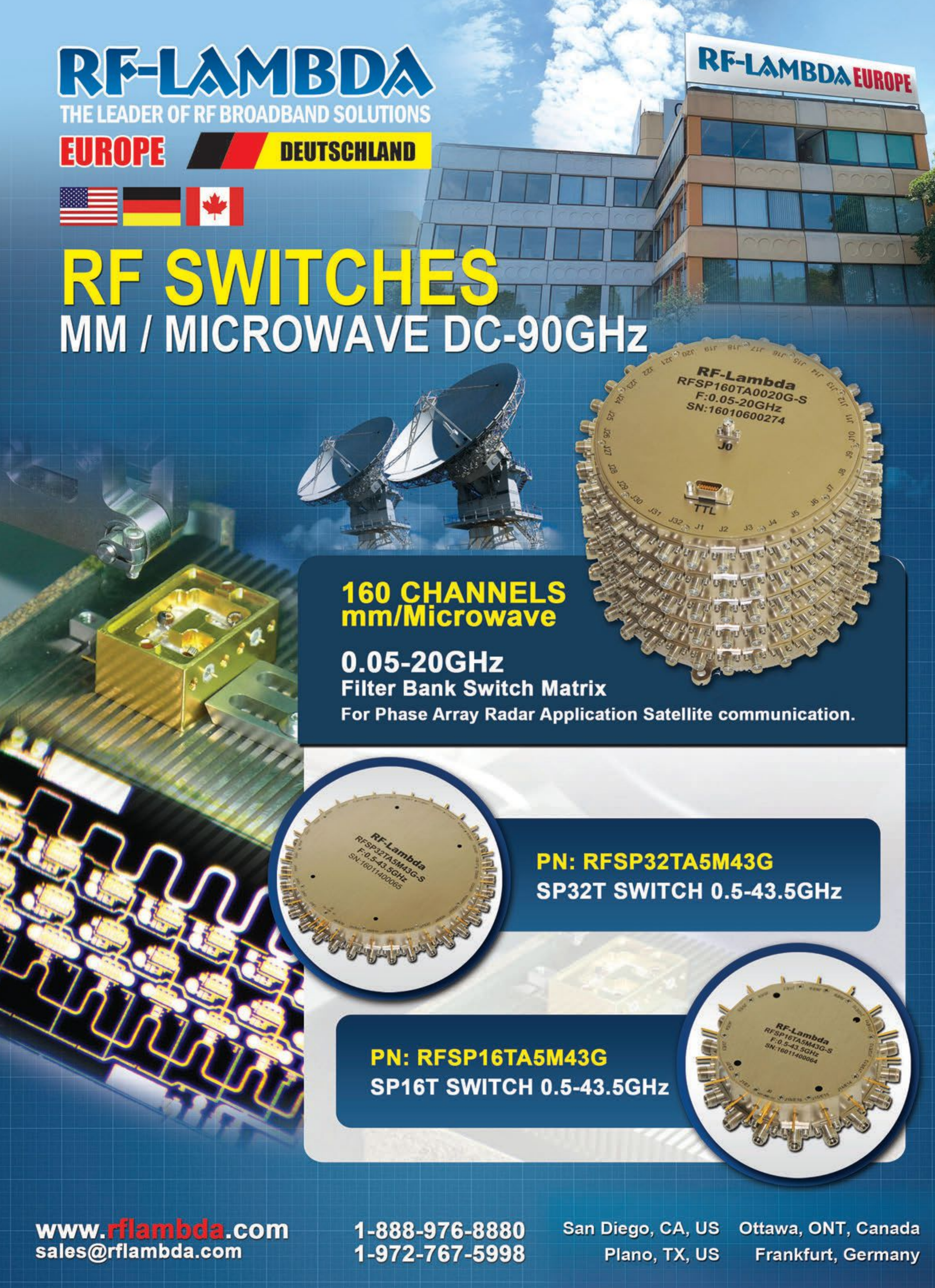
RF-LAMBDA
THE LEADER OF RF BROADBAND SOLUTIONS
EUROPE
DEUTSCHLAND
RF-LAMBDA EUROPE
RF SWITCHES
MM / MICROWAVE DC-90GHz
RF-Lambda
RFSP160TA0020G-S
F:0.05-20GHz
SN:16010600274
160 CHANNELS
mm/Microwave
0.05-20GHz
Filter Bank Switch Matrix
For Phase Array Radar Application Satellite communication.
PN: RFSP32TA5M43G
SP32T SWITCH 0.5-43.5GHz
PN: RFSP16TA5M43G
SP16T SWITCH 0.5-43.5GHz
www.rflambda.com
sales@rflambda.com
1-888-976-8880
1-972-767-5998
San Diego, CA, US
Plano, TX, US
Ottawa, ONT, Canada
Frankfurt, Germany

Low-Profile Slotted Notch MIMO Antenna with Low Envelope Correlation Coefficient

R. Rathna and M. A. Bhagyaveni
Anna University, Chennai, India

S. S. Shamina
Vellore Institute of Technology, Vellore, India

P. Latha
St. Joseph's College of Engineering and Technology, Chennai, India

A low-profile single frequency multiple-input multiple-output (MIMO) microstrip patch antenna with elements that include dual U-shaped slots and notches is proposed for use in several applications, including vehicle-to-vehicle communication, WiMax and sub-6 GHz networks. The chief motivation, however, is the design of a vehicular antenna with minimal envelope correlation coefficient (ECC) for independent performance of the MIMO antenna elements. The elements are fabricated on an FR-4 substrate and the antenna exhibits a 150 MHz bandwidth at 3.5 GHz. The design, analyzed and simulated using CST software, is evaluated in terms of port separation, ECC, mean effective gain (MEG) and channel capacity loss (CCL). Measured results are in strong agreement with the simulations. The design successfully achieves the desired ECC value of less than 0.001 with a gain of greater than or equal to 5 dBi, which is extremely low when compared to ECC values reported in previous research.

5G automotive communications is a core concept of the intelligent transportation system. This system involves communication between vehicles and vehicle communication with roadside infrastructure, and it is a rapidly expanding sector. Real-time communication between infrastructure and automobiles is now possible because of advancements in wireless communications. These advancements result in applications to improve car safety and passenger communication with the internet.

Within the broader vehicle-to-everything (V2X) communications umbrella, the desire for vehicle-to-vehicle (V2V) communications has grown recently, driven by efforts to improve automobile vehicle safety. Various design choices, including the size and type of antenna, influence the performance of a V2V system. Some classic designs include monopole,[1] slot[2] and patch antennas.[3]

These antennas provide low profiles and simple structures but with narrow bandwidths and low coverage efficiencies. To enhance the bandwidth and enable the antenna to operate in two bands, a microstrip monopolar patch system[4] may be used. However, the substrate's excessive thickness results in increased size and it complicates the design process.

Ozpinar et al.[5] developed a mmWave antenna to achieve broad bandwidth, high gain, high coverage and high radiation efficiency in a compact, low-profile structure. Although it has several advantages, the antenna is severely affected by high transmission, penetration and atmospheric propagation losses. Most importantly, it requires high gain radiation beams.

To overcome these issues, systems on modern vehicles employ MIMO techniques. A MIMO system uses multiple antennas for both transmission and reception. This architecture enables the MIMO system to enhance bandwidth, data rate and throughput without altering transmit power or the frequency band of operation.

MIMO systems also have the advantages of high dependability and low latency in an environment with strong electromagnetic scattering. They support operation in LTE/5G sub-6 GHz, WLAN and V2X over 5G sub-6 GHz bands with a small design.[6] Using precoding techniques, many input channels are used to transmit various types of information while the receiver combines and processes the various pieces of received information. System capacity is wasted if these channels broadcast the same information. This limitation is known as correlation and the ECC can be used to quantify this quantity. A MIMO antenna should have low correlation between elements with high overall antenna efficiency.[7]

Different methods for creating compact MIMO structures with low ECC and high diversity gain have been developed. Dkiouak et

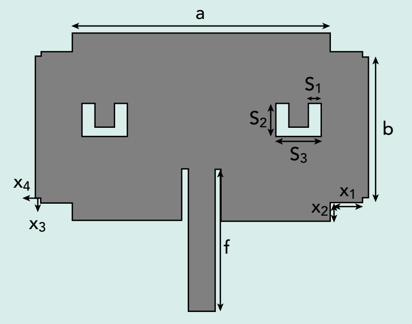

Fig. 1 **Single patch antenna element.**

TABLE 1

MIMO ANTENNA ELEMENT DESIGN PARAMETERS

Parameter	Value (mm)
a	20
b	15
s_1	0.5
s_2	5
s_3	2
x_1	3
x_2	2
x_3	0.5
x_4	0.5
f	12

al.[8] proposed a structure consisting of two parallel identical monopoles. A low-profile, compact-sized monopole antenna element was developed for a four-port UWB MIMO/diversity array with orthogonally placed resonating elements to achieve less than 0.004 ECC.[9] However, the phased array design and placement were expensive.

A 2 × 1 orthogonal, circularly-polarized MIMO antenna was introduced for 5G applications at 3.3 to 4.2 GHz and 5.9 GHz V2X applications. This antenna incorporates a Γ-shaped stripline to the ground and an asymmetric ground structure[10] to achieve an ECC lower than 0.02. To widen the impedance bandwidth, uniform and stepped U-shaped slot antennas were designed and implemented by Hu et al.[11]

In this work, a wideband microstrip patch element with U-shaped slots and notches is designed for incorporation into 2 × 2 and 4 × 4 element MIMO antenna systems. The slotted notch (SN) MIMO antenna performs in the band required for V2V communications as well as WiMAX.

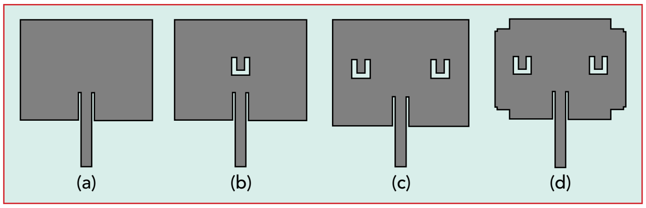

Fig. 2 **SN MIMO antenna element design evolution: Antenna 1 (a), Antenna 2 (b), Antenna 3 (c) and Antenna 4 (d).**

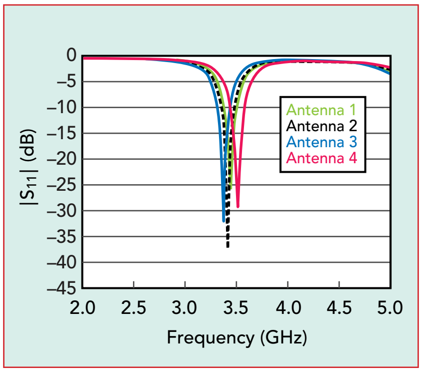

Fig. 3 **SN MIMO antenna element $|S_{11}|$ comparison.**

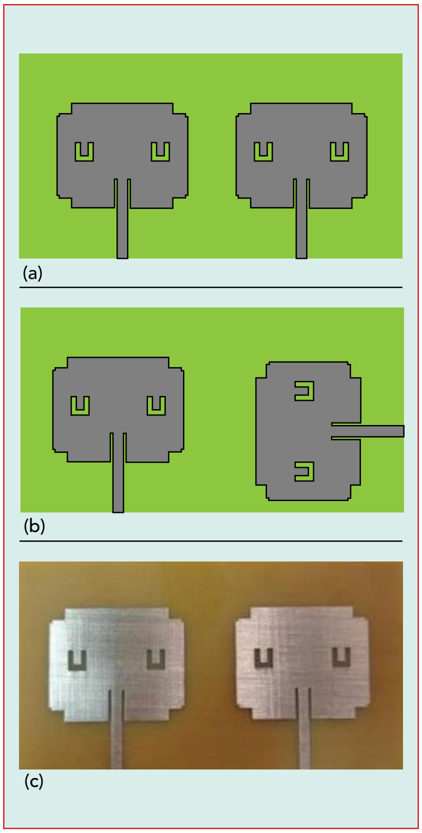

Fig. 4 **(a) Side-by-side 2 x 2 antenna configuration. (b) Orthogonal 2 x 2 antenna configuration. (c) Prototype side-by-side 2 x 2 antenna.**

SINGLE PATCH CONFIGURATION AND DESIGN PROCESS

Figure 1 shows the antenna element's configuration and related parameters are listed in ***Table 1***. The SN MIMO antenna resonates at 3.5 GHz and comprises a rectangular patch with two U-shaped slots to achieve circular polarization. Notches are introduced by etching out edge surfaces for low ECC at the desired frequency. The FR4 substrate is 1.6 mm thick, with a dielectric constant of ε_r=4.4 and tanδ= 0.02.

Figure 2a shows the beginning of the design evolution. In this circuit, a conventional rectangular patch antenna measuring 26 mm × 20 mm with an inset feed is designed. A single U-shaped slot is introduced, as shown in ***Figure 2b***, and then a second slot is added in ***Figure 2c***. These improve the element's match to 50 Ω. Subsequently, the first notches (χ_1, χ_2) and the second notches (χ_3, χ_4) are introduced in ***Figure 2d*** to achieve the desired frequency of 3.5 GHz.

Figure 3 shows the simulated $|S_{11}|$ of the four antennas. $|S_{11}|$ of the inset feed antenna, shown in Figure 2a, is -25.93 dB at 3.44 GHz. $|S_{11}|$ of the single U-shaped design of Figure 2b is -32.08 dB at 3.37 GHz. When two U-shaped slots are introduced in Figure 2c, the frequency shifts to 3.413 GHz with an $|S_{11}|$ of -34.05 dB. With the notches introduced in Figure 2d, the frequency shifts to 3.5 GHz with a fractional impedance bandwidth of 3.8 percent.

MIMO CONFIGURATION

2 × 2 SN MIMO Array

Figure 4a and ***Figure 4b*** illustrate two candidate configurations of the 2 × 2 SN MIMO microstrip patch antenna array, each with dimensions of 36 mm × 60 mm. The spacing between the two antennas is 10 mm. One of the key performance metrics is the ECC, which is remarkably low, measuring less than 0.02. ***Figure 4c*** shows a prototype of the side-by-side configuration of Figure 4a.

Figure 5a compares the $|S_{11}|$ performance of the two candidate configurations and ***Figure 5b*** compares the $|S_{12}|$ performance of the two candidate configurations. The graphical results show that the side-by-side orientation outperforms the orthogonal configuration in terms of both reflection coefficient and isolation. Additionally, this is achieved without the need for additional structures or complex modifications. Therefore, the side-by-side orientation is chosen for the 4 × 4 antenna design.

4 x 4 MIMO Array

Building upon the 2 × 2 SN MIMO results, a 4 × 4 SN MIMO antenna is designed with the circuit configuration shown in ***Figure 6***. Its dimensions are 68 mm × 68 mm with an inter-element spacing of 10 mm to provide good signal reception in a multipath environment. Simulated current distributions at 3.5 GHz are shown in ***Figure 7***. The current is primarily focused around each patch, substantiating the antenna's radiation in a specific frequency band. The current is also confined within each element without dissipation to other ports, supporting the observation of a high level of port-to-port isolation.

Figure 8a compares measured and simulated reflected S-parameters and ***Figure 8b*** compares measured and simulated transmitted S-parameters for the 4 × 4 SN MIMO antenna. The measured 10 dB impedance bandwidth of 4.25 percent and Port 1 isolation agree closely with the simulation. In the case of the measured data, both $|S_{12}|$ and $|S_{13}|$ exhibit values below -20 dB, while $|S_{14}|$ is lower than -40 dB.

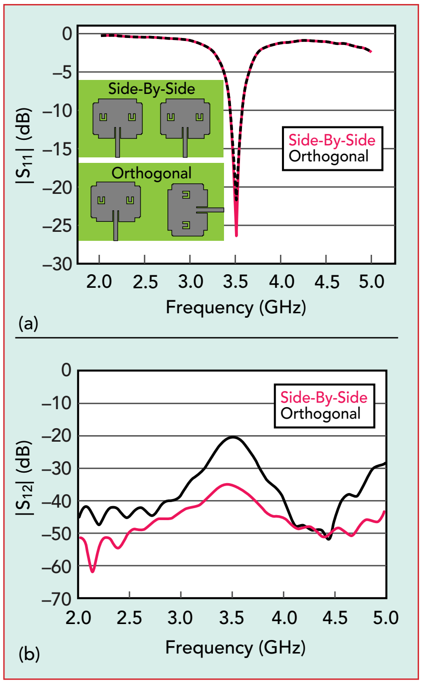

Fig. 5 **(a) $|S_{11}|$ for antenna element orientations. (b) $|S_{12}|$ for antenna element orientations.**

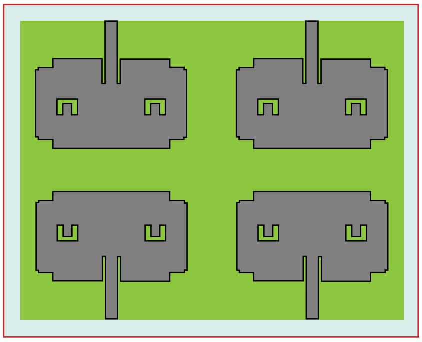

Fig. 6 **4 x 4 MIMO antenna.**

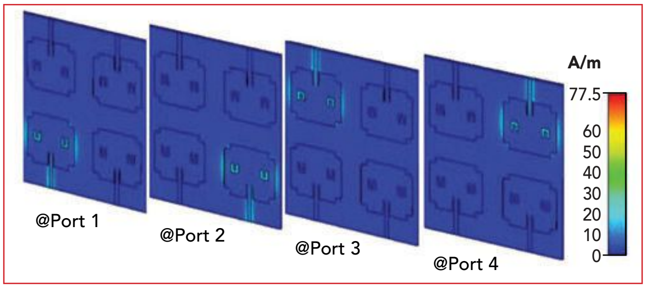

Fig. 7 **Current distribution of 4 x 4 SN MIMO antenna at 3.5 GHz with each port separately driven.**

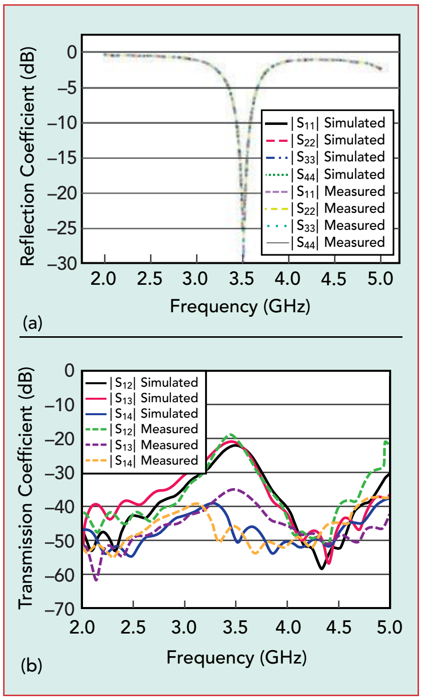

Fig. 8 **(a) 4 x 4 SN MIMO antenna measured and simulated reflection coefficients. (b) 4 x 4 SN MIMO antenna measured and simulated transmission coefficients.**

SN MIMO ANTENNA DIVERSITY ANALYSIS AND PERFORMANCE

The practicality of a MIMO antenna system relies on its ability to provide effective diversity performance. To assess this, ECC is used as a measure; a low ECC implies a significant degree of isolation between antennas. Far-field antenna characteristics are used to determine the ECC using ***Equation 1***.[12]

$$\rho e = \frac{\left| \iint_{4\pi} [s_i(\Theta,\Phi)] * [s_i(\Theta,\Phi)] d\Omega \right|}{\iint_{4\pi} |s_i(\Theta,\Phi)|^2 d\Omega \iint_{4\pi} |s_i(\Theta,\Phi)|^2 d\Omega} \quad (1)$$

Notably, when applied to outdoor scenarios, the SN MIMO antenna simulated and measured ECC value consistently falls below 0.001, as shown in ***Figure 9***. This value indicates minimal mutual coupling between antenna elements.

In MIMO, CCL is a measure of the channel capacity loss experienced by the four-port MIMO antenna array due to correlation effects when used in vehicles. The quantification of CCL is based on ***Equation 2***:[12]

$$C_{loss} = -\log_2 \det(\Psi^R) \quad (2)$$

Where:

ΨR is the receiving antenna's correlation matrix and it is expressed as ***Equations 3*** to ***7***:

$$(\Psi^R) = \begin{bmatrix} \Psi_{ii} & \Psi_{ij} \\ \Psi_{ji} & \Psi_{jj} \end{bmatrix} \quad (3)$$

Where:

$$\Psi_{ii} = 1 - (|S_{ii}|^2 + |S_{ij}|^2) \quad (4)$$

$$\Psi_{ij} = -(S_{ii} * S_{ij} + S_{ji} * S_{jj}) \quad (5)$$

$$\Psi_{ij} = -(S_{jj} * S_{ji} + S_{ij} * S_{ii}) \quad (6)$$

$$\Psi_{jj} = 1 - (|S_{jj}|^2 + |S_{ji}|^2) \quad (7)$$

In industrial and vehicular communication contexts, a CCL below 0.4 b/s/Hz is considered good. This antenna's CCL is shown in ***Figure 10***. These results indicate minimal correlation impact and a high data transfer rate.

The total active reflection coefficient (TARC) provides insight into signal quality and reflection, helping to optimize antenna design, mitigate interference and ultimately contribute to reliable and high performance MIMO communication. It is determined with S-parameters using **Equation 8**.[12]

$$TARC = \frac{\sqrt{\sum_{i=1}^{N}\left|S_{i1} + \sum_{n=2}^{N} S_{in}\, e^{j\Theta_{n-1}}\right|^{2}}}{\sqrt{N}} \qquad (8)$$

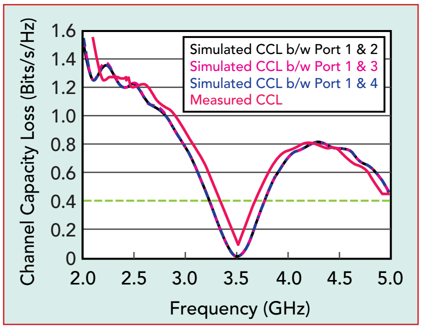

Fig. 10 Simulated and measured 4 x 4 SN MIMO antenna CCL.

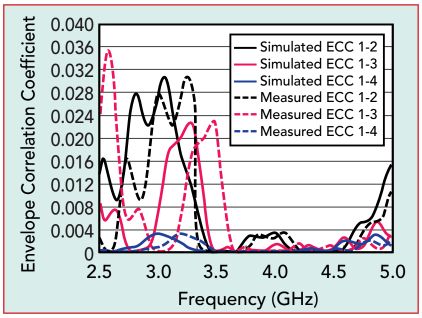

Fig. 9 Simulated and measured 4 x 4 SN MIMO antenna ECC.

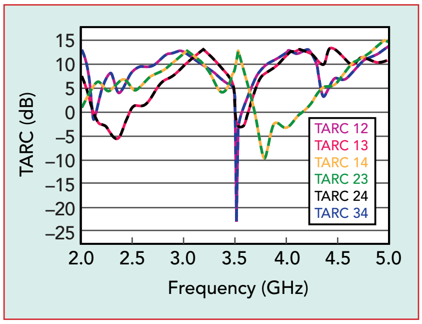

Fig. 11 4 x 4 SN MIMO antenna TARC.

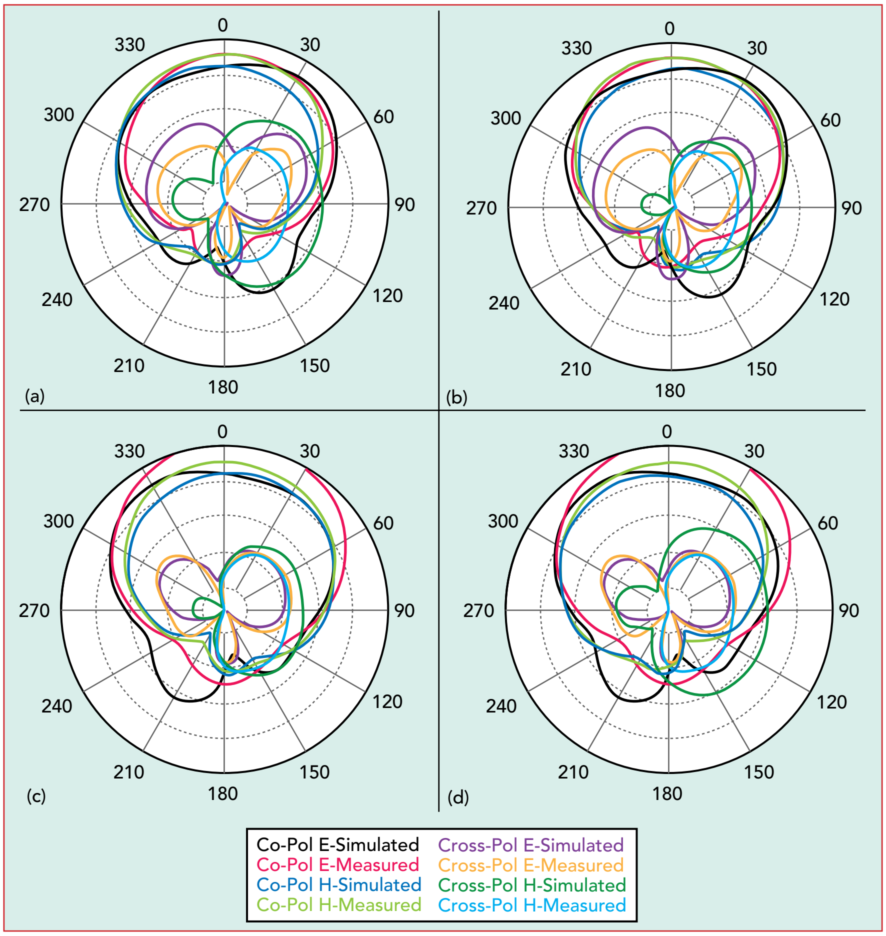

Fig. 12 (a) 4 x 4 SN MIMO Antenna 1 simulated and measured radiation patterns at 3.5 GHz. (b) 4 x 4 SN MIMO Antenna 2 simulated and measured radiation patterns at 3.5 GHz. (c) 4 x 4 SN MIMO Antenna 3 simulated and measured radiation patterns at 3.5 GHz. (d) 4 x 4 SN MIMO Antenna 4 simulated and measured radiation patterns at 3.5 GHz.

ALTUM RF

E-Band Power Amplifiers

- 1.8 W OUTPUT PA MMICS
- LOW- & HIGH-BAND OPTIONS

NEW!

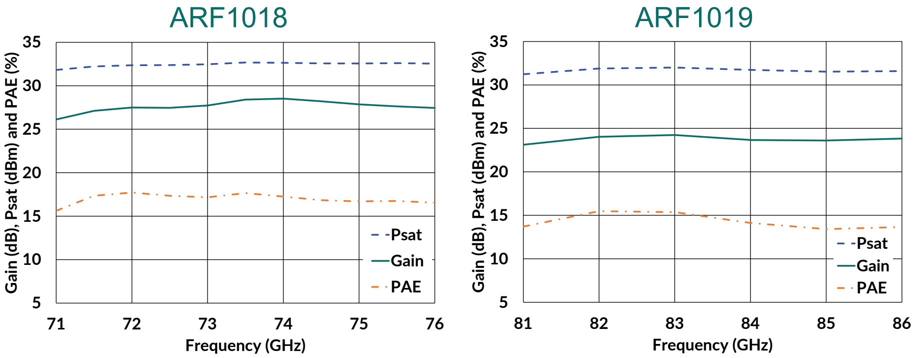

1.8 W Psat E-Band Power Amplifier GaAs MMICs

Altum RF's new E-band PA GaAs MMICs support today's demanding mmWave telecom and SATCOM applications by offering high output power and gain for longer-range links. The ARF1018 covers 71–76 GHz with 1.8 W Psat (including bonding transitions from die) and 27 dB small-signal gain. The ARF1019 covers 81–86 GHz with 1.6 W Psat (including bonding transitions from die) and 24 dB small-signal gain. Both bare die MMICs measure a compact 3.5 x 4.1 x 0.05 mm^3 and include an on-chip integrated power detector.

Part Number	Frequency Range (GHz)	Gain (dB)	Psat (dBm)	PAE (%)	OIP3 (dBm)	Vdd/Idq (V/A)
ARF1018	71–76	27	32.5	18	39	4.0/2.0
ARF1019	81–86	24	32.0	15	38	4.0/2.0

LEARN MORE AT BOOTH 815B AT EuMW 2024 & ALTUMRF.COM

INFO@ALTUMRF.COM | +31 (0) 40 2390 888 | TWINNING CENTER, DE ZAALE 11, 5612 AJ EINDHOVEN, THE NETHERLANDS

800.348.5580 / 630.208.2200 RELLPOWER@RELL.COM RELLPOWER.COM

Richardson Electronics
POWER & MICROWAVE TECHNOLOGIES

Visit Richardson Electronics, Ltd. at Booth 715B at EuMW 2024

40W267 Keslinger Road / P.O. Box 393
LaFox, IL 60147-0393

TABLE 2
COMPARISON WITH OTHER WORKS

Reference	Frequency (GHz)	Bandwidth	Dimensions (mm)	Gain (dBi)	ECC	TARC (dB)	CCL (b/s/Hz)
7	2.4 3.8	NG	110 × 55 × 9	NG	0.27	NG	NG
8	3.1 to 14.9	11.8 GHz	36 × 36 × 1.6	NG	<0.01	NG	NG
9	3.14 to 12.24	9.1 GHz	50 × 50 × 0.76 (4 × 4)	5.1	<0.004	<-14.41	NG
10	3.15 to 6.32	3.17 GHz	68.33 × 32 × 0.1 (2 × 1)	>3.5	<0.02	<-20	0.4
12	6	3.67 GHz	53 × 54 (4 × 4)	>3	<0.01	<-25	<0.4
13	2.45	120 MHz	50 × 50 × 6	5.09	NG	NG	NG
This Work	3.5	150 MHz	68 × 68 × 1.6 (4 × 4)	≥ 5	<0.001	<-20	<0.4

S_{in} denotes the reflection coefficients between distinct antenna ports. ***Figure 11*** shows TARC curves depicting different phase combinations. For the efficient performance of MIMO systems in V2V, it is important that TARC values consistently remain below -10 dB within the specified frequency range.

Figure 12a to ***Figure 12d*** show the 2D radiation patterns at 3.5 GHz for Antenna 1 to Antenna 4, respectively. The E-plane patterns are similar between Antennas 1 and 2 and Antennas 3 and 4. Likewise, in the H-plane, the patterns between Antennas 1 and 4 and Antennas 2 and 3 are similar. This ensures there are no interference issues during reception and demonstrates good radiation patterns in both planes.

Table 2 compares this work with similar works. It highlights this antenna's ECC bandwidth, spanning the 5G vehicular communication and sub-6 GHz bands, as well as its compact structure. Additionally, it demonstrates exceptional values for CCL and TARC.

CONCLUSION

A low-profile MIMO microstrip patch antenna featuring dual slots and notches is introduced and optimized for 5G V2V communication. The proposed design, operating at 3.5 GHz, exhibits a bandwidth of 150 MHz, an important requirement for intelligent transportation systems. A gain greater than or equal to 5 dBi is realized within the frequency band. Through simulation and measurement, the antenna's performance metrics, including ECC, CCL, TARC, MEG, radiation patterns and efficiency are analyzed. The ECC is below 0.001, surpassing previous research benchmarks. Its compact form factor, good radiation char-

acteristics and low ECC make this design suitable for vehicular communication, WiMAX and sub-6 GHz applications. ■

References

1. R. Praveena, T. R. Ganesh Babu, G. Sudha, N. Mahesh, J. Ganasoundharam and M. Birunda, "Design of Tilted E-Shaped Monopole Antenna for Vehicular Communication," *8th International Conference on Smart Structures and Systems*, April 2022.
2. R. S. Chen, L. Zhu, S.W. Wong, X. Z. Yu, Y. Li, L. Zhang and Y. He, "Low-Sidelobe Cavity-Backed Slot Antenna Array with Simplified Feeding Structure for Vehicular Communications," *IEEE Transactions on Vehicular Technology*, Vol. 70, No. 4, April 2021, pp. 3652–3660.
3. T. Sasikala, R. Arunchandar, M. A. Bhagyaveni and M. Shanmuga Priya, "Design of Dual- Band Antenna for 2.45 and 5.8 GHz ISM Band," *National Academy Science Letters*, Vol. 42, No.3, June 2019, pp. 221–226.
4. S. Gao, L. Ge, D. Zhang and W. Qin, "Low-Profile Dual-Band Stacked Microstrip Monopolar Patch Antenna for WLAN and Car-to-Car Communications," *IEEE Access*, Vol. 6, October 2018, pp. 69575–69581.
5. H. Ozpinar, S. Aksimsek and N. T. Tokan, "A Novel Compact, Broadband, High Gain Millimeter-Wave Antenna for 5G Beam Steering Applications," *IEEE Transactions on Vehicular Technology*, Vol. 69, No. 3, March 2020, pp. 2389–2397.
6. J. Malik, D. Nagpal and M. V. Kartikeyan, "MIMO Antenna with Omnidirectional Pattern Diversity," *Electronics Letters*, Vol. 52, No. 2, January 2016, pp. 102–104.
7. G. Srinivas, D. Jabin and A. K. Singh, "Multiband MIMO Antenna with Reduction in Mutual Coupling and ECC," *Students Conference on Engineering and Systems*, May 2014.
8. A. Dkiouak, A. Zakriti, M. El ouahabi, H. Elftouh and A. Mchbal, "Design of CPW-Fed MIMO Antenna for Ultra-Wideband Communications," *Procedia Manufacturing*, Vol. 46, May 2020, pp. 782–787.
9. S. Arumugam, S. Manoharan, S. K. Palaniswamy and S. Kumar, "Design and Performance Analysis of a Compact Quad-Element UWB MIMO Antenna for Automotive Communications," *Electronics*, Vol. 10, No. 18, pp. 2184, September 2021.
10. S. Virothu and M. S. Anuradha, "Conformal MIMO Circular Polarization Diversity Antenna for V2X Applications," *International Journal of RF and Microwave Computer-Aided Engineering*, Vol. 32, No. 4, December 2021.
11. H. -T. Hu, F. -C. Chen and Q. -X. Chu, "A Wideband U-Shaped Slot Antenna and its Application in MIMO Terminals," *IEEE Antennas and Wireless Propagation Letters*, Vol. 15, July 2016, pp. 508–511.
12. B. M. Yousef, A. M. Ameen, A. Desai, H. -T. Hsu, V. Dhasarathan and A. A. Ibrahim, "Defected Ground Structure-Based Wideband Circularly Polarized 4-port MIMO Antenna for Future Wi-Fi 6E Applications," *AEU - International Journal of Electronics and Communications*, Vol. 170, No. 2, July 2023.
13. C.E. Guan and T. Fujimoto, "Design of a Wideband L-Shape Fed Microstrip Patch Antenna Backed by Conductor Plane for Medical Body Area Network," *Electronics*, Vol. 9, No. 1, 2020.

Bandwidth-Enhanced Circularly Polarized Slot Coplanar Waveguide-Fed Antenna with Embedded Meander Line

Lianwu Yang and Ying Li
Yichun University, Yichun, China

A novel CPW-fed broadband circularly polarized (CP) slot antenna provides enhanced bandwidth. Its ground plane is a stepped stairs shape where CP is introduced. To enhance the bandwidth, a meander line branch is embedded in the side perpendicular to the feed line introducing a wideband orthogonal mode. The measured –10 dB impedance bandwidth is 103.2 percent (from 2.12 to 6.64 GHz) and the ARBW is 72.0 percent (from 2.82 to 5.99 GHz), which agrees well with simulations.

CP antennas can receive arbitrarily polarized electromagnetic waves, and electromagnetic waves radiated by CP antennas can be received by antennas of any polarization.[1] Further, the CP antenna can suppress interference from inclement weather and alleviate the effects of multipath reflections.[2]

The way to generate a circularly polarized wave is to excite two orthogonal modes with an equal amplitude and a phase difference of 90 degrees.[3-5] Various types of CP antennas have been proposed with broad impedance and axial ratio (AR) bandwidths. In addition, the demand for antenna miniaturization in modern communication systems has increased recently.[4]

Most CP antenna designs are asymmetric[5] and fed by L-shaped feed lines.[6] To produce CP, improve performance and widen the bandwidth, many methods are employed, such as the introduction of slots[7,8] and the embedding of various types of stubs.[9-11] However, achieving performance in all areas, simultaneously, is challenging. For example, an antenna with a novel chifre-shaped feed line demonstrates a wide bandwidth of 72 percent and a low profile, but with an insufficient CP characteristic.[12]

Metamaterials with unique physical characteristics have been used in CP antenna design. For example, Marouf and Ziani[13] demonstrated a 3×3 array of circular patches with the circular patch antenna at the center of the array fed by a modified CPW slot. Dual CP radiation was achieved, but bandwidth was no greater than 20 percent.

Weng et al.[14] described a dual-band, CP slot antenna with broadband characteristics in both AR and impedance, while Hoang et al. demonstrated ARBW improvement of a CP printed monopole antenna using a lumped capacitor.[15]

A high gain and broadband planar CP antenna was designed by Guthi and Damera with a single-layer substrate.[16-18] To realize a broadband antenna initially, a circular patch antenna was fed by a slot with a coplanar feed line in the ground plane. A metasurface was created with a 3×3 array of circle patches with the circular patch antenna at the center of the array. Moreover, the slot was also modified into an L-shape to generate circular polarization. In addition, stubs were introduced in the slot to improve the impedance bandwidth. Other technologies, such as artificial magnetic conductor reflectors,[19] asymmetrical dipoles with via holes[20] and multilayer structures[21] have also been used to widen the antenna bandwidth.

The above designs are large and non-conformal, and their bandwidths are relatively narrow. A monopole antenna with an asymmetrical ground was described by Bao and Ammann.[22] Its impedance bandwidth was 96.5 percent with an ARBW of 63.3 percent, while it was more compact than most CP antennas, its peak gain was just 3.5 dBic, which is extremely low relative to its size.

The CPW slot-feed has been shown to have potential for wide-

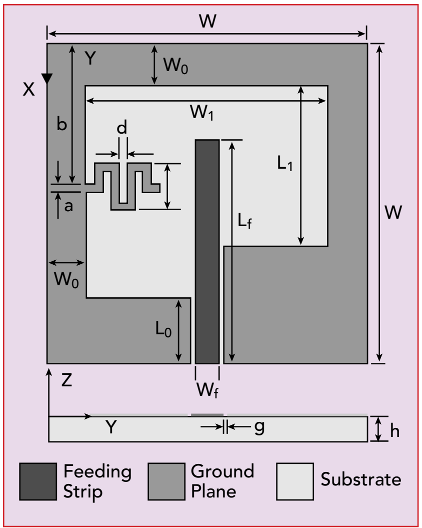

Fig. 1 **Antenna structure.**

band CP antennas,[23-27] but most are linearly polarized. In this work, a CPW-fed slot antenna with an asymmetrical ground is described. With an asymmetrical ground, a wide ARBW is achieved, then a meander line is etched on the ground to further improve its bandwidth and enhance CP performance.

ANTENNA CONFIGURATION

The antenna geometry shown schematically in ***Figure 1*** is based on the traditional design of a CPW-fed slot antenna. Its dimensions, determined through parametric analysis, are listed in ***Table 1.*** A rectangular metallic section of the ground plane on the left of the feed line is removed to produce a CP wave. Further, a meander line protruding off the ground plane is etched to the left of the feed line to improve CP performance. The dielectric substrate of the single-layer antenna is an FR4 composite with a dielectric constant of 4.4. The antenna is fed from a coaxial line with a standard SMA connector.

The design evolution is shown in ***Figure 2***. It starts with a conventional symmetrical CPW-fed slot antenna (see ***Figure 2a***). The slot is then enlarged on one side to produce an asymmetrical surface current, introducing CP (see ***Figure 2b***). To further enhance the CP bandwidth and improve impedance, an embedded slender meander line is positioned perpendicular to the feed line (see ***Figure 2c***) introducing wideband orthogonal modes.

The simulated –10 dB impedance bandwidth and ARBW are shown in ***Figure 3***. Compared with previous structures, which have achieved a broad band or dual-band circular polarization by loading with complex structures (such as spiral or branched microstrip), this antenna is designed based on a traditional CPW-fed slot antenna, so it has the advantages of a low profile and ease of fabrication.

To illustrate the effect of introducing the CP mode, the current distributions of Antennas 1 and 2 at 5 GHz are simulated (see ***Figure 4***). The current distribution vectors of Antenna 1 are mainly vertical and more dominant at the base of the feed, indicating that Antenna 1 radiates only linearly polarized waves (see ***Figure 4a***). With the ground plane shape of Antenna 2, horizontal currents are enhanced in the top branch of the ground plane. Two currents distributed perpendicularly are obtained, introducing the capability for CP. To further improve CP as well as impedance bandwidth, a meander line is placed perpendicular to the feed, introducing wideband orthogonal modes.

To demonstrate the CP mode introduced by Antenna 3, the time-varying current on the metal surface at phases of 0, 90, 180 and 270 degrees at 5 GHz is shown in ***Figure 5***. The dominant surface current flows counterclockwise. Consequently, it radiates a right-hand CP (RHCP)

TABLE 1

ANTENNA DIMENSIONS

Parameter	Dimension (mm)
W	40
W_0	5
L_0	8
W_f	3
L_f	28
W_i	30
L_i	20
a	1
b	17
c	6
d	1
g	0.5
h	1.6

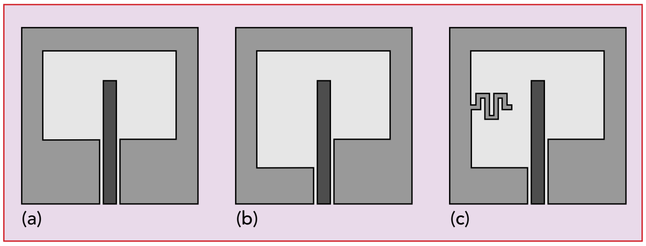

Fig. 2 **Design evolution: Antenna 1 (a), Antenna 2 (b) and Antenna 3 (c).**

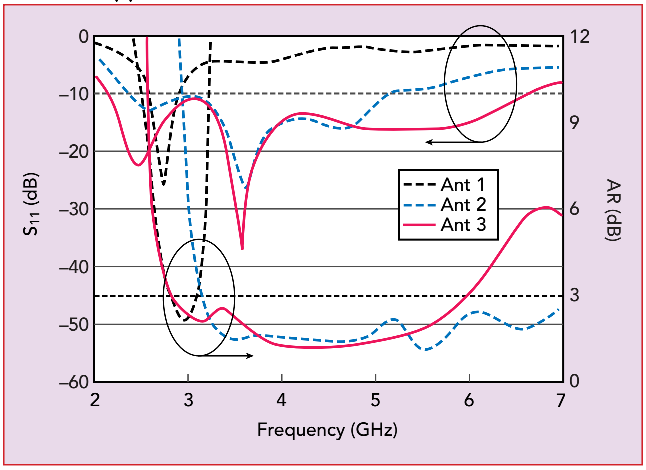

Fig. 3 **Simulated impedance bandwidth and ARBW of Antenna 1 (a), Antenna 2 (b) and Antenna 3 (c).**

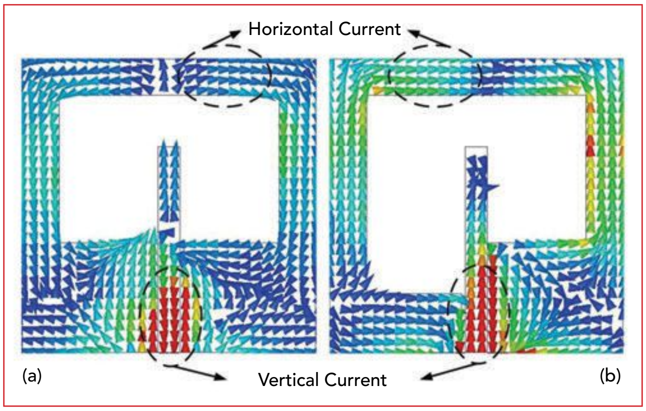

Fig. 4 **Surface current distribution of Antenna 1 (a) and Antenna 2 (b) at 5 GHz.**

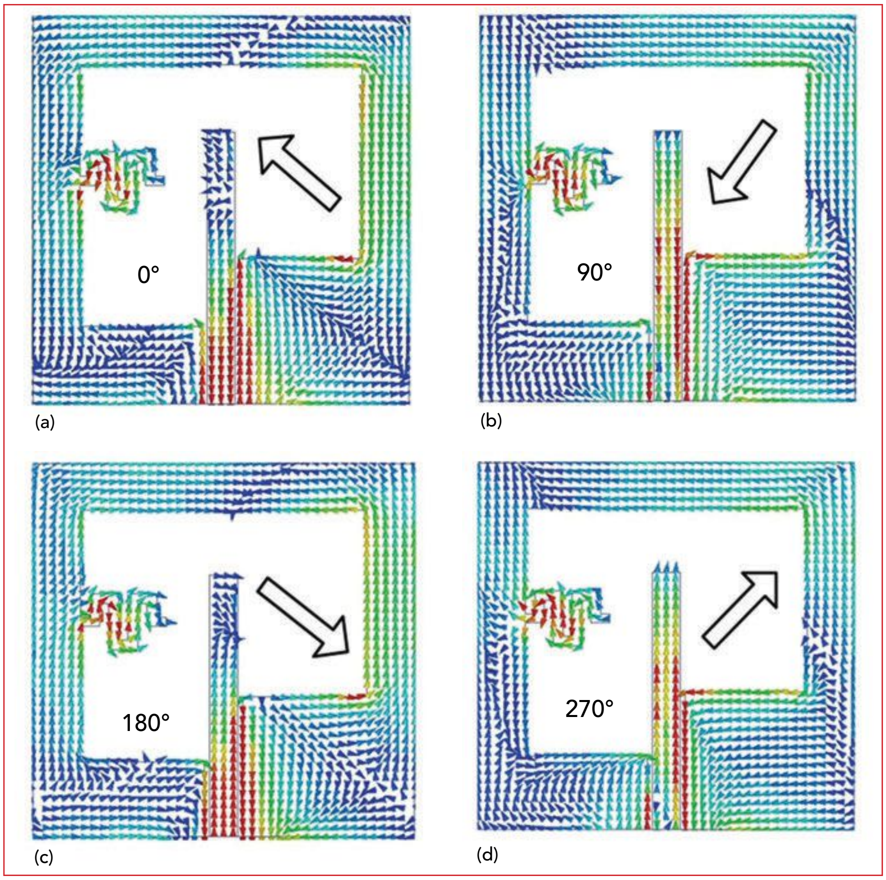

Fig. 5 **Time-varying current on the antenna conductive surface at 5 GHz: 0 (a), 90 (b), 180 (c) and 270 (d) degrees.**

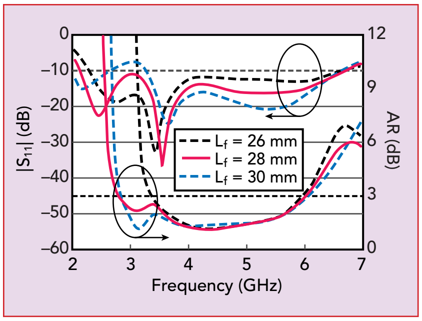

Fig. 6 **Simulated $|S_{11}|$ and AR with different L_f.**

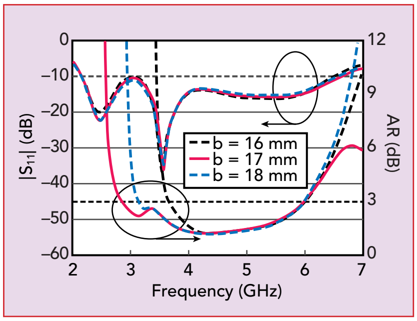

Fig. 7 **Simulated $|S_{11}|$ and AR with different b.**

wave in the +z direction. The dominance of surface current distribution on the feed line, the edge of the step-stairs ground and the meander line underscores the contribution of the meander line on CP radiation. To achieve the left-hand CP (LHCP), the meander line and step-stairs ground are simply positioned on the opposite side of the feed.

Simulations of $|S_{11}|$ and AR with key parameters of different dimensions are plotted in ***Figures 6*** through ***8***. Many references have pointed out that the elongated feed is an important factor affecting impedance matching. As seen in Figure 6, the optimum dimension produces the widest impedance bandwidth and ARBW. Figure 7 shows the effect of the meander line location on $|S_{11}|$ and AR. $|S_{11}|$ changes slightly, but with an optimum location, the widest ARBW is achieved. Finally, Figure 8 shows the effect of the L_0 dimension. The results clearly indicate that it has a great effect

MiCable

0.6~7.25GHz

High Accuracy Butler Matrices

NEW

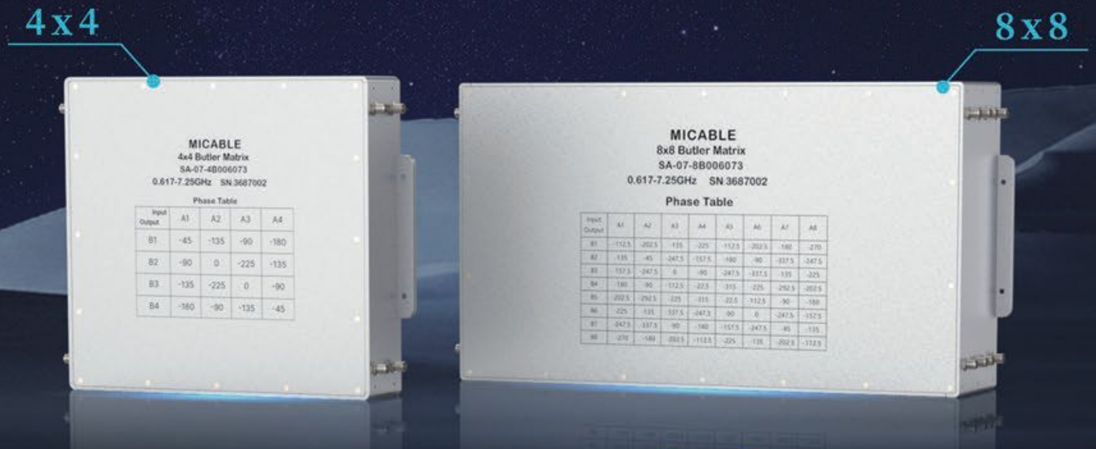

ONE MODEL COVER **5G NR(FR1) / WiFi 6E** Freq. Bands

Excellent Phase Accuracy & Amplitude Unbalance

Low VSWR / Low I.L. / High Isolation

Good Stability & Repeatability

P / N	Structure	Freq. Range (GHz)	VSWR Max. (:1)	Insertion Loss* Max. (dB)	Amplitude Unbal. Max. (dB)	Amplitude Flatness Max. (dB)	Phase Accuracy Max. (Deg.)	Isolation Min. (dB)
SA-07-4B006073	4x4	0.617-0.96	1.4	8.2	±1.1	±0.8	±11	17
		1.427-2.69	1.5	8.7	±1	±1	±10	14
		3.3-5	1.5	9.2	±1	±1	±12	14
		5.15-7.25	1.6	9.8	±1.1	±1.1	±12	13
SA-07-8B006073	8x8	0.617-0.96	1.4	12	±1.5	±1.4	±13	17
		1.427-2.69	1.5	13.2	±1.4	±1.6	±12	14
		3.3-5	1.5	14.6	±1.4	±1.6	±14	14
		5.15-7.25	1.6	15.9	±1.5	±1.7	±14	13

*Theoretical Insertion Loss Included

Typical Test Curve**

SA-07-4B006073

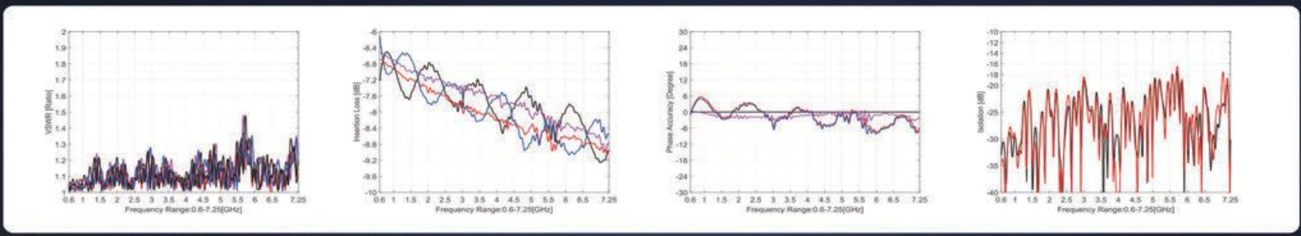

**Corresponding Channels: A1B1、A1B2、A1B3、A1B4

More Information-
Scan the QR Code

MIcable Inc.
www.micable.cn sales@micable.cn +86-591-87382856

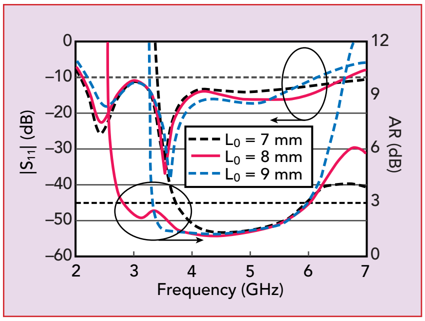

Fig. 8 Simulated $|S_{11}|$ and AR with different L_0.

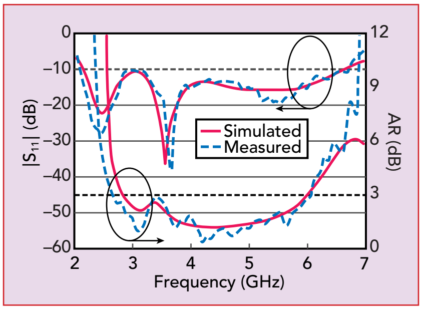

Fig. 9 Simulated versus measured results.

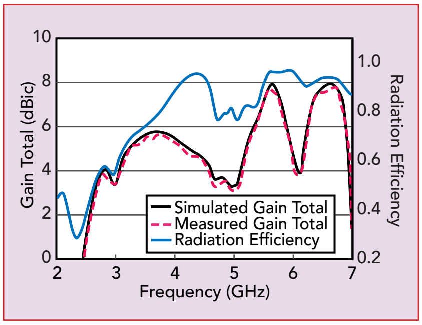

Fig. 10 Antenna gain and radiation efficiency.

on the impedance bandwidth and ARBW. As the size of L_0 becomes larger, the impedance and AR bandwidths become wider. However, due to the limitation of the distance between the meander line and the asymmetrical ground, its length is set as 8 mm.

EXPERIMENTAL RESULTS

Simulated and measured results are shown in ***Figure 9***. The simulated –10 dB impedance bandwidth is 4.52 GHz (2.12 to 6.64 GHz) and the ARBW is 3.17 GHz (2.82 to 5.99 GHz). For comparison, the measured impedance bandwidth is 4.65 GHz (2.10 to 6.75 GHz) and the ARBW is 3.40 GHz (2.65 to 6.05 GHz). The results are consistent with the simulation. Slight discrepancies are mainly due to material, measurement uncertainties and fabrication tolerances. These results show that the antenna has advantages in structure and bandwidth compared with those represented in the referenced work of ***Table 2***.

Figure 10 shows that the antenna's gain is higher than 3.8 dBic within the CP bandwidth with a maximum gain of 7.8 dBic. The radiation efficiency is a maximum of 96 percent occurring at 4.1 GHz.

Simulated versus measured radiation patterns in the xoz- and yoz-planes at 5 GHz (see ***Figure 11***) are bi-directional and in close agree-

TABLE 2

COMPARISON WITH OTHER ANTENNA STRUCTURES

References	Impedance BW (GHz, %)	3 dB AR BW (GHz, %)	Electrical Dimensions (λ)	Peak Gain (dBic)	Physical Dimensions (mm)
16	4.9 to 6, 20.18	5.1 to 6, 16.21	1×1×0.052 (f_0 = 5.5 GHz)	10.43	58×58×3.175
17	4.56 to 6.21, 30	5.23 to 5.7, 8.6	1×1×0.052 (f_0 = 5.4 GHz)	10.21	54×54×3.175
18	4.5 to 6.63, 38.2	5.0 to 5.7, 13	1×1×0.052 (f_0 = 5.6 GHz)	10.36	58×58×3.175
27	1.12 to 3.8, 108.9	1.6 to 4.36, 92.6	0.615× 0.615×0.0066 (f_0 = 2.46 GHz)	4.8	75×75×0.8
12	1.5 to 3.3, 72	1.98 to 3.02, 41.6	0.49×0.53×0.01 (f_0 = 2.5 GHz)	3.61	58.4×63×1.5
13	3.75 to 7.0, 60.5	4.33 to 5.90, 30.7	0.95×0.90×0.03 (f_0 = 5.2 GHz)	4.75	55×52×1.52
This work	2.12 to 6.64, 103.2	2.82 to 5.99, 72.0	0.47×0.47×0.02 (f_0 = 3.5 GHz)	7.8	40×40×1.6

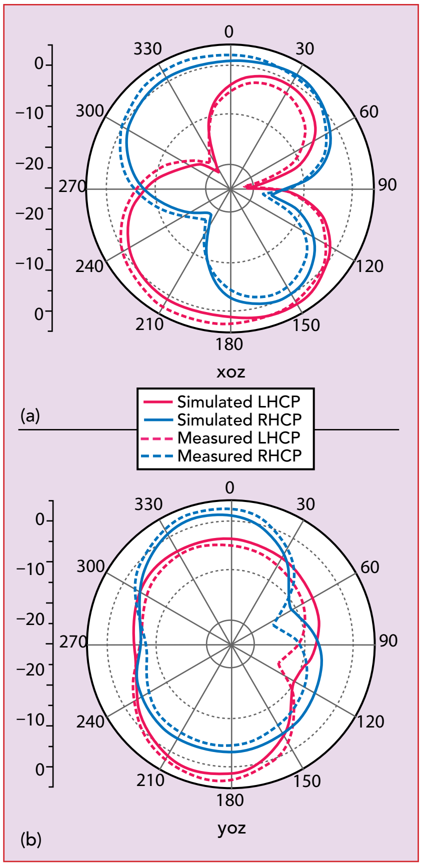

Fig. 11 Radiation patterns at 5 GHz: xoz (a) and yoz (b).

ment. Simulated results in ADS agree closely with those in HFSS as well.

CONCLUSION

A novel asymmetrical CPW-fed antenna with broadband circular polarization uses an asymmetrical ground and meander line to achieve circular polarization and improved bandwidth. After parameter optimization, the measured -10 dB impedance bandwidth is 103.2 percent (from 2.12 to 6.64 GHz) and the ARBW is 72.0 percent (from 2.82 to 5.99 GHz), which agrees well with the simulations. With a simple structure, wide ARBW and low profile, this antenna is suitable for many applications in modern communication systems. ■

References

1. Y. -Y. Chen, Y. -C. Jiao, G. Zhao, F. Zhang, Z. -L. Liao and Y. Tian, "Dual-Band Dual-Sense Circularly Polarized Slot Antenna with a C-Shaped Grounded Strip," *IEEE Antennas and Wireless Propagation Letters*, Vol. 10, September 2011, pp. 915–918.
2. M. Samsuzzaman and M. T. Islam, "Wideband Hook-Shaped Circularly Polarized Antenna," *Electronics Letters*, Vol. 50, No. 15, July 2014, pp. 1043–1045.
3. S. L. S. Yang, A. A. Kishk and K. F. Lee, "Wideband Circularly Polarized Antenna with L-Shaped Slot," *IEEE Transactions on Antennas and Propagation*, Vol. 56, No. 6, June 2008, pp. 1780–1783.
4. R. Ma R and Q. Feng, "Broadband CPW-Fed Circularly Polarized Square Slot Antenna for Universal UHF RFID Handheld Reader," *The Applied Computational Electromagnetics Society Journal (ACES)*, Vol. 36, No. 6, August 2021, pp. 747–754.
5. M. Y. Sai, S. Kavya, S. R. Bhimavarapu, M. Mudaliar and S. Sharma, "CPW Fed Microstrip Patch Antenna for Dedicated Short-Range Communication," *Wireless Personal Communications*, Vol. 122, September 2021, pp. 3859–3873.
6. J. -Y. Sze and S. -P. Pan, "Design of CPW-Fed Circularly Polarized Slot Antenna with a Miniature Configuration," *IEEE Antennas and Wireless Propagation Letters*, Vol. 10, December 2011, pp. 1465–1468.
7. T. Fujimoto and K. Jono, "Wideband Rectangular Printed Monopole Antenna for Circular Polarization," *IET Microwaves, Antennas & Propagation*, Vol. 8, No. 9, June 2014, pp. 649–656.
8. S. -W. Zhou, P. -H. Li, Y. Wang, W. -H. Feng and Z. -Q. Liu, "A CPW-Fed Broadband Circularly Polarized Regular-Hexagonal Slot Antenna with L-Shape Monopole," *IEEE Antennas and Wireless Propagation Letters*, Vol. 10, October 2011, pp. 1182–1185.
9. K. Luo, B. Chen, Y. Yi and Y. Wang, "Miniaturized Design of Coplanar Waveguide-Fed Broadband Circularly Polarized Slot Antenna," *IET Microwaves, Antennas & Propagation*, Vol. 9, No. 11, August 2015, pp. 1200–1204.
10. H. Tang, K. Wang, R. Wu, C. Yu; J. Zhang and X. Wang, "A Novel Broadband Circularly Polarized Monopole Antenna Based on C-Shaped Radiator," *IEEE Antennas and Wireless Propagation Letters*, Vol. 16, October 2016, pp. 964–967.
11. C. -J. Wang and Y. Lin, "New CPW-fed Monopole Antennas with Both Linear and Circular Polarizations," *IET Microwaves, Antennas & Propagation*, Vol. 2, No. 5, July 2008, pp. 466–472.
12. W. -C. Weng, J. -Y. Sze and C. -F. Chen, "A Dual-Broadband Circularly Polarized Slot Antenna for WLAN Applications," *IEEE Transactions on Antennas and Propagation*, Vol. 62, No. 5, May 2014, pp. 2837–2841.
13. F. Z. Marouf and K. D. Ziani, "Study and Design of Wristband RFID Antenna for Healthcare Applications," *Microwave and Optical Technology Letters*, Vol. 60, No. 2, February 2018, pp. 359–364.
14. R. -C. Han and S. -S. Zhong, "Broadband Circularly-Polarized Chifre-Shaped Monopole Antenna with Asymmetric Feed," *IET Electronics Letters*, Vol. 52, No. 4, February 2016, pp. 256–258.
15. T. V. Hoang, T. T. Le and H. C. Park, "Bandwidth Improvement of a Circularly Polarized Printed Monopole Antenna Using a Lumped Capacitor," *IET Electronics Letters*, Vol. 52, No. 13, June 2016, pp. 1091–1092.
16. S. Guthi and V. Damera, "High Gain and Broadband Circularly Polarized An-

Frontlynk®
Bridging Gaps
Multi Coax
Probe Multi Coax up to 67GHz
RF.Microwave Coaxial Connector
& Cable Assembly
1.0mm Series
Connectors, Adaptors, and Cable Assemblies up to 110GHz
1.0mm Connector
DC to 110GHz, VSWR≤1.2
1.35mm Connector
DC to 90GHz, VSWR≤1.2
1.85mm Connector
DC to 67GHz, VSWR≤1.2
2.4mm Connector
DC to 50GHz, VSWR≤1.2
2.92mm Connector
DC to 40GHz, VSWR≤1.15
3.5mm Connector
DC to 34GHz, VSWR≤1.15
1.35mm Series up to 90GHz
Test Cables up to 110GHz
Frontlynk Technologies Inc.
www.frontlynk.com
Tel: +886-6-356-2626
Fax: +886-6-356-6268
E-mail: info@frontlynk.com

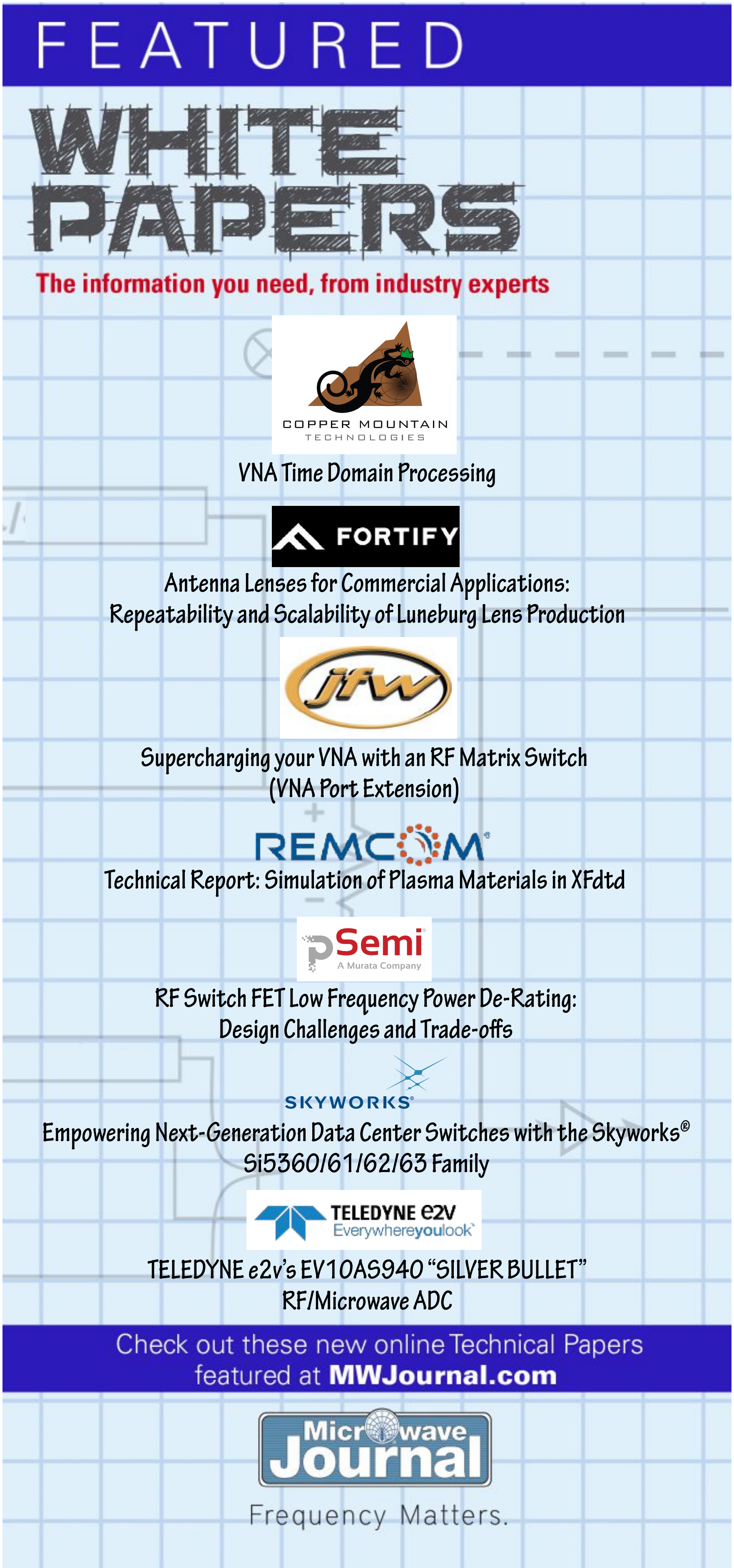

tenna Using Metasurface and CPW Fed L-Shaped Aperture," *AEU-International Journal of Electronics and Communications*, Vol. 146, No. 11, January 2022.

17. V. Damera and S. Guthi, "Aperture Coupled CPW Feed for High Gain and Broadband Circularly Polarized Slot Loaded Square Patch Metasurface Antenna," *Microwave and Optical Technology Letters*, Vol. 64, No. 4, April 2022, pp. 809–815.
18. S. Guthi and V. Damera, "Broadband and High Gain Circularly Polarized Truncated Corner Square Patch Metasurface Antenna Using Aperture CPW Feed," *Journal of Electromagnetic Waves and Applications*, Vol. 36, No. 18, July 2022, pp. 2601–2613.
19. S. -K. Lin and Y. -C. Lin, "A Compact Outer-Fed Leaky-Wave Antenna Using Exponentially Tapered Slots for Broadside Circularly Polarized Radiation," *IEEE Transactions on Antennas and Propagation*, Vol. 60, No. 6, June 2012, pp. 2654–2661.
20. X. L. Bao and M. J. Ammann, "Monofilar Spiral Slot Antenna for Dual-Frequency Dual-Sense Circular Polarization," *IEEE Transactions on Antennas and Propagation*, Vol. 59, No. 8, August 2011, pp. 3061–3065.
21. K. Agarwal, Nasimuddin and A. Alphones, "Wideband Circularly Polarized AMC Reflector Backed Aperture Antenna," *IEEE Transactions on Antennas and Propagation*, Vol. 61, No. 3, March 2013, pp. 1456–1461.
22. X. L. Bao and M. J. Ammann, "Wideband Dual-Frequency Dual-Polarized Dipole-Like Antenna," *IEEE Antennas and Wireless Propagation Letters*, Vol. 10, August 2011, pp. 831–833.
23. P. R. Prajapati, G. G. K. Murthy, A. Patnaik and M. V. Kartikeyan, "Design and Testing of a Compact Circularly Polarized Microstrip Antenna with Fractal Defected Ground Structure for L-band Applications," *IET Microwaves, Antennas & Propagation*, Vol. 9, No. 11, August 2015, pp. 1179–1185.
24. K. Ding, Y. -X. Guo and C. Gao, "CPW-Fed Wideband Circularly Polarized Printed Monopole Antenna with Open Loop and Asymmetric Ground Plane," *IEEE Antennas and Wireless Propagation Letters*, Vol. 16, September 2017, pp. 833–836.
25. R. Azim, M. T. Islam, H. Arshad, Md. Mottahir Alam, N. Sobahi and A. I. Khan, "CPW-Fed Super-Wideband Antenna with Modified Vertical Bow-Tie-Shaped Patch for Wireless Sensor Networks," *IEEE Access*, Vol. 9, December 2020, pp. 5343–5353.
26. M. Y. Sai, S. Kavya, S. R. Bhimavarapu, M. Mudaliar and S. Sharma, "CPW Fed Microstrip Patch Antenna for Dedicated Short-Range Communication," *Wireless Personal Communications*, Vol. 122, No. 4, February 2022, pp. 3859–3873.
27. L. Sun, W. Sheng, B. Yan and J. Cui, "Wideband Dual Circularly Polarized Coplanar Waveguide-Fed Slot Antenna with an Arrow-Shaped Strip," *International Journal of RF and Microwave Computer-Aided Engineering*, Vol. 32, No. 7, April 2022.


NSI MI
AMETEK®

Transforming Connectivity: Designing and Manufacturing Lens Antennas

Fortify
Boston, Mass.

In our hyperconnected world, reliable and high performance RF technology is no longer a luxury; it is essential. From satellite communications keeping us globally connected to the rise of private 5G fixed wireless networks powering Industry 4.0, the demand for innovative RF solutions that enhance connectivity across different platforms has never been greater. As the RF industry undergoes a generational shift to keep up with billions of data-hungry devices across multiple applications, Fortify is using cutting-edge design and advanced manufacturing to provide a new degree of freedom to device performance with gradient-index (GRIN)-enhanced apertures.

At the heart of Fortify's success lies its patented RF lens beamforming technology, which leverages a unique combination of design and manufacturing processes. This enables the company to create highly effective lenses that significantly enhance the capabilities of traditional antenna systems. These lenses often utilize GRIN lens technology, which is engineered with a dielectric permittivity that can be precisely tuned throughout the structure. This unique property allows GRIN lenses to bend, focus and manipulate RF waves, surpassing the performance of conventional lenses. These GRIN lenses can drastically improve size, weight, power and cost (SWaP-C) factors that are a crucial consideration for modern RF systems.

ADVANTAGES OF GRIN ANTENNAS

Enhanced directivity and efficiency: GRIN lenses can achieve drastically greater directivity than traditionally manufactured RF systems. This feature significantly enhances signal strength and reduces the likelihood of detection, which is crucial in defense applications where stealth and precision are paramount.

Wide field of view (FoV): GRIN lenses enable wide-angle beam scanning without a significant reduction in gain, providing superior spatial selectivity and range. This capability is essential for applications requiring detailed spectrum reconnaissance and enhanced survivability in hostile environments. ***Figure 1*** shows a GRIN phased array-fed lens that can steer to 90 degrees.

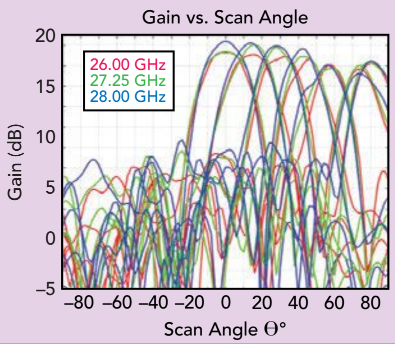

▲ Fig. 1 **GRIN phased array antenna and scan angle characteristics using a Qorvo development kit.**

Broadband performance: GRIN lenses support extremely wide operating bandwidths, making them suitable for a range of applications from fixed wireless access and 5G communications to multi-band, multi-orbit satellite communication applications. ***Figure 2*** shows a 13 in. diameter lens for wideband beamforming, along with the antenna patterns at 3.5 GHz and 8.2 GHz.

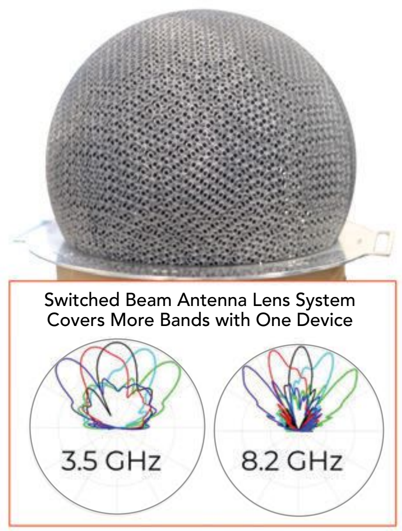

▲ Fig. 2 **GRIN switched beam antenna lens and antenna patterns.**

SWAP-C Optimized Parts for RADAR SYSTEMS

Radar systems are growing into multi-function, multi-mission systems that need to be contained in the smallest possible footprint.

Knowles Precision Devices' DLI Brand of RF and Capacitor components are designed to address your SWAP-C challenges by leveraging our decades of Aerospace and Defense expertise in:

Vertical Integration | Materials Science | High Performance

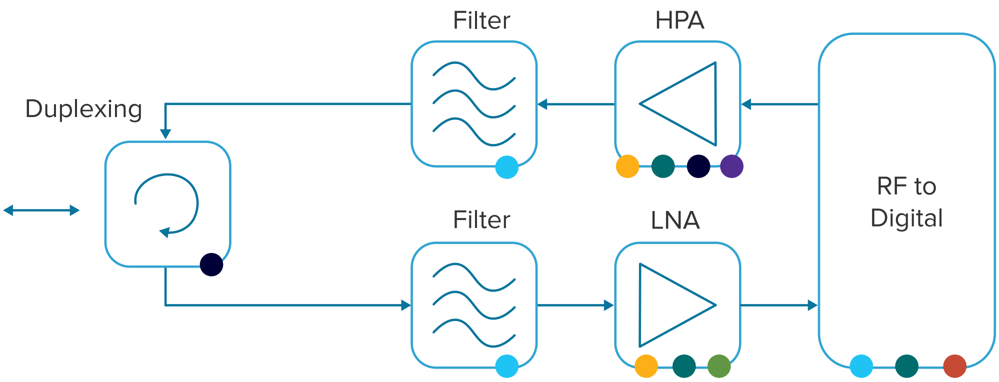

Knowles RF Components Support All Major Functions:

- Filter
- Low Noise Oscillators
- Bypass & Coupling Capacitors
- Bias Networks
- Hybrid Couplers
- Storage Capacitors
- Gain Equalizers

RF and Capacitor components have always played a key role in the success of radar systems as they have evolved over the years. At Knowles Precision Devices, we work closely with you to identify the filter solution you need to meet the challenges you face today.

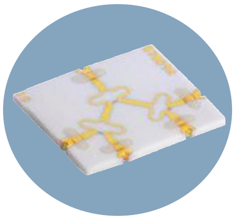

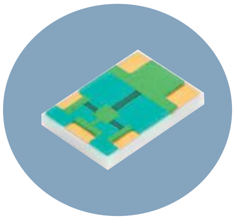

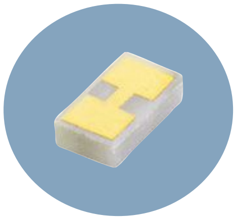

>> Learn more: rfmw.com/dielectric

Contact us today to explore a range of catalog and custom design options: **sales@rfmw.com**

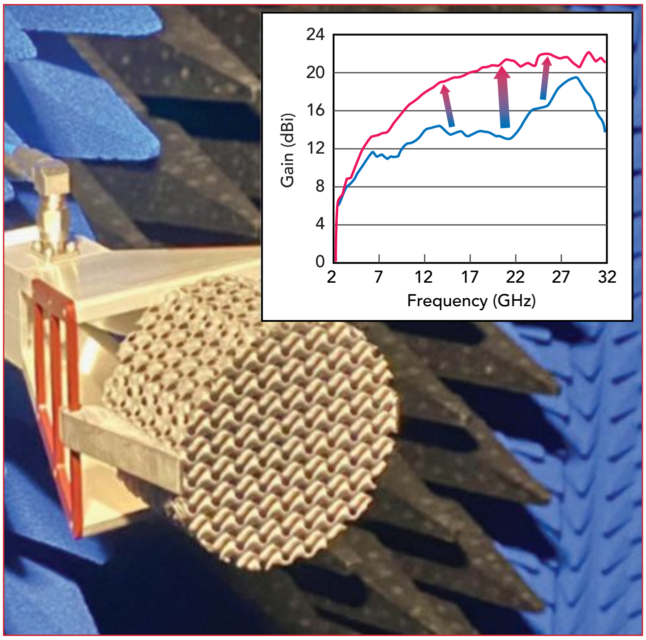

Fig. 3 **Gain characteristics of GRIN lenses.**

Figure 3 shows the increase in gain that can be expected from GRIN lenses versus traditional solutions.

ADVANCING GRIN TECHNOLOGY

Fortify's manufacturing technology plays a crucial role in advancing GRIN antenna manufacturing. The patented platform combines parallel manufacturing with high-throughput material processing, enabling the scalable production of high-quality GRIN media. Unlike traditional manufacturing methods, Fortify's approach allows for the duplication of parts at the same speed as single-unit production, drastically reducing production costs and time.

Fortify's design expertise and intellectual property reside in its innovative process and mastery of GRIN principles to enhance both existing and redesigned RF systems. Their vertically integrated approach leverages novel software developed in-house, which bridges traditional high frequency simulation tools like CST and HFSS with Fortify's manufacturing platform. This integration empowers engineers to unlock unprecedented performance across various RF applications, streamlining the design process and reducing the adoption curve for advanced RF solutions.

Fortify's end-to-end RF manufacturing solution, combined with its advancements in GRIN technology and unique design expertise, is poised to make a significant impact on the RF industry. The benefits of Fortify's innovations include:

Reduced total cost of ownership: Fortify's solutions can reduce overall system costs by increasing gain or enhancing the FoV. GRIN technology and efficient manufacturing processes enable the production of high performance RF systems that provide superior functionality at a lower total cost of ownership. As an example, fixed wireless operators can utilize GRIN lenses to effectively increase the gain of a standard radio. This allows operators to increase the distance between backhaul units to reduce the number of radios needed for point-to-point backhaul drastically.

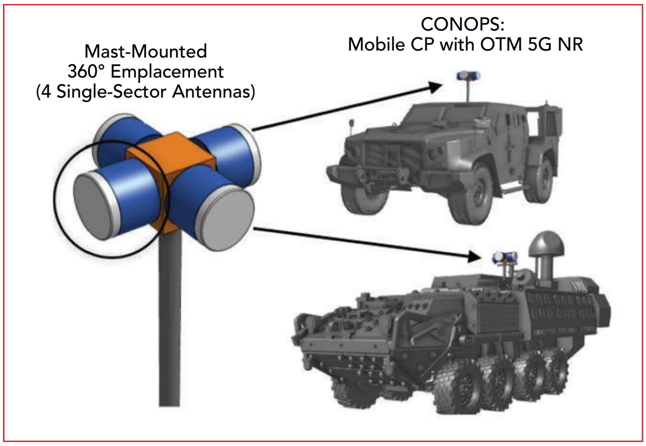

Fig. 4 **Bringing private and secure tactical communications to the battlefield.**

Increased efficiency: Fortify's integration enables systems with low and efficient SWaP-C. This enhances operational efficiency, making RF solutions more effective across various applications. The company's advanced design and manufacturing capabilities enable the creation of compact, lightweight and power-efficient RF systems that deliver exceptional performance. For example, large rotating parabolic dish antennas can be replaced by solid-state, lens-based antennas, drastically reducing the footprint and power consumption of these radar units.

Competitive edge: Fortify's innovative technologies and streamlined processes provide users with a distinct edge over competitors using traditional solutions. The ability to leverage cutting-edge GRIN technology, coupled with Fortify's unique design expertise and vertically integrated manufacturing approach, ensures that RF solutions are not only technologically superior but also highly reliable and cost-effective. This competitive advantage is crucial in industries where performance, reliability and cost-efficiency are paramount. ***Figure 4*** shows an example of using GRIN lenses and a switch matrix to reduce the total hardware by 85 percent with commensurate reductions in total power, cost and weight versus a traditional phased array approach.

Fortify's pioneering efforts in end-to-end RF manufacturing and GRIN technology are set to transform the RF industry. By providing a seamless, efficient production process and leveraging cutting-edge advancements in antenna design, Fortify is meeting the current needs of the market and paving the way for future innovations in RF technology. This holistic approach ensures that Fortify remains at the forefront of the industry, driving progress and setting new standards for excellence in RF manufacturing and production. Fortify's ability to deliver high performance, cost-effective RF solutions gives users a significant advantage, ensuring they stay ahead in an increasingly competitive and rapidly evolving market.

Fortify
Boston, Mass.
3dfortify.com/

Ultra Low Phase Noise
Phase Locked Clock Translators

Up to 27.5 GHz

Features
- Cost Effective
- Eliminates Noisy Multipliers
- Patented Technology

Applications
- Scanning & Radar Systems
- High Frequency Network Clocking (A/D & D/A)
- Test & Measurement Equipment
- High Performance Frequency Converters
- Base Station Applications
- Agile LO Frequency Synthesis

New!

Model	Frequency (Mhz)	Typical Phase Noise		Package
		@10 kHz	@100 kHz	
VFCTS100-10	100	-156	-165	
VFCTS105-10	105	-156	-165	
VFCTS120-10	120	-156	-165	
VFCTS125-10	125	-156	-165	
VFCTS128-10	128	-155	-160	
FCTS800-10-5	800	-144	-158	
FCTS1000-10-5	1000	-141	-158	
FCTS1000-100-5	1000	-141	-158	
FSA1000-100	1000	-145	-160	
FXLNS-1000	1000	-149	-154	
KFCTS1000-10-5	1000	-141	-158	
KFCTS1000-100-5	1000	-141	-158	
KFSA1000-100	1000	-145	-160	
KFXLNS-1000	1000	-149	-154	
FCTS2000-10-5	2000	-135	-158	
FCTS2000-100-5	2000	-135	-158	
KFCTS2000-100-5	2000	-135	-158	
KSFLOD12800-12-1280	12800	-122	-123	
KSFLOD25600-12-1280	25600	-118	-118	
KSFLO27R5-100-12	27500	-88	-98	

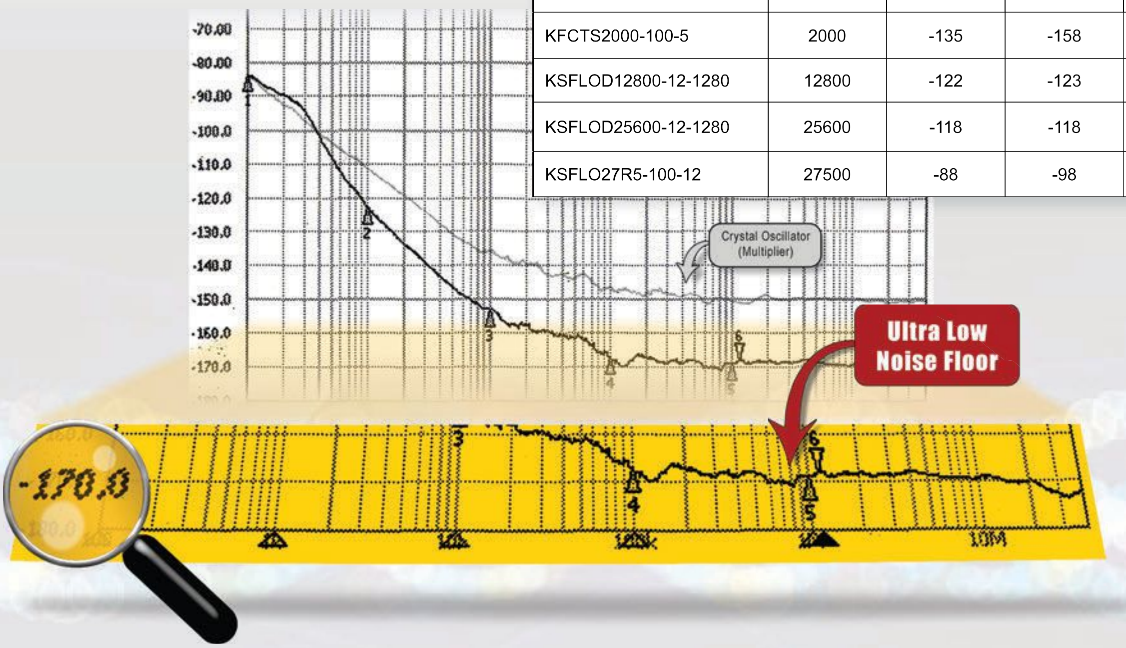

Talk To Us About Your Custom Requirements.

SYNERGY® MICROWAVE CORPORATION
Phone: (973) 881-8800 | Fax: (973) 881-8361
E-mail: sales@synergymwave.com | Web: www.synergymwave.com
Mail: 201 McLean Boulevard, Paterson, NJ 07504

Software Suite Update Improves Planar Filter Design

SynMatrix
Richmond Hill, Canada

The emerging growth of higher frequency applications is demanding smaller form factors, higher operating frequencies and thinner printed circuit board (PCB) layouts. Planar filters offer significant size and integration advantages, making them more efficient for compact designs. They can also operate at K-Band and beyond, which is critical for emerging new applications in 5G, satellite communications and automotive radar. With favorable and economical manufacturability on PCBs, planar filters also help reduce costs, have good production yields and offer R&D teams design flexibility, which is important when determining potential performance trade-offs.

To help address these emerging trends and growing design challenges, SynMatrix recently released a product update that features diplexer 3D geometry automation workflows and an end-to-end design workflow to support a variety of different microstrip filters.

The microstrip design suite features a powerful GUI interface to enable users to synthesize and generate their parameterized 3D geometries in Ansys HFSS automatically. They can also optimize their filter designs using AI and computer-aided tuning functions. Here is a quick summary of capabilities available to microstrip filter designers:

Lowpass filter applications: Filter synthesis support for Chebyshev, Butterworth and elliptic filters. Users can select from step impedance, open stub and elliptic design types.

Standard microstrip bandpass filters: Design workflow support for edge-coupled, end-coupled, interdigital and hairpin bandpass filters.

Microstrip open-loop coupled bandpass filters: SynMatrix now provides open-loop resonator modeling to help streamline and automate the coupled bandpass filter design workflow.

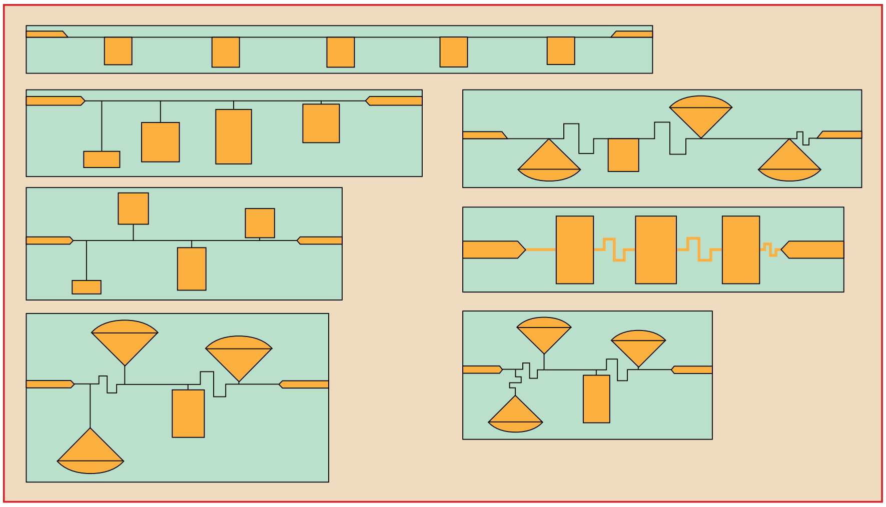

Fig. 1 **SynMatrix customizable tool for representative lowpass microstrip filter layouts.**

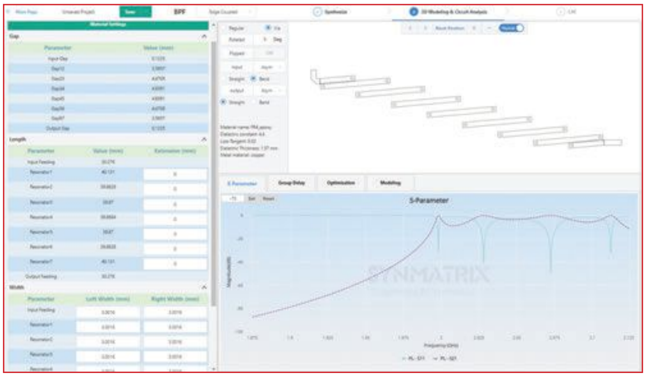

Fig. 2 **Example of edge-coupled bandpass filter design interface.**

Fig. 3 **AI-optimized results for edge-coupled bandpass filter structure.**

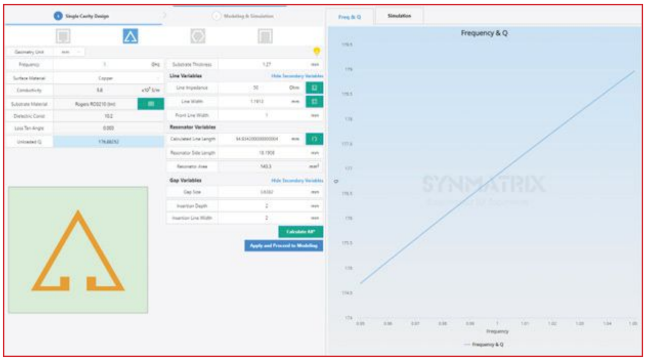

Fig. 4 **Example of a triangular resonator.**

AI and computer-aided tuning (CAT) optimization tools: SynMatrix has expanded the optimization functions and workflows to support all the microstrip filters previously mentioned.

LOWPASS MICROSTRIP FILTERS

SynMatrix now offers filter synthesis workflows to support lowpass microstrip filters. Users will enjoy a highly customizable environment featuring easy-to-edit circuit analysis pages and automation workflows to help quickly construct and model parameterized 3D geometries. ***Figure 1*** shows some representative geometries.

STANDARD PLANAR MICROSTRIP BANDPASS FILTER

SynMatrix now supports the entire design workflow, including synthesis, 3D modeling automation and optimization for edge-coupled, end-coupled hairpin and interdigital filters. ***Figure 2*** shows an example of this workflow for an edge-coupled bandpass filter. For edge-coupled and end-coupled bandpass filters, the SynMatrix design interface also supports end extension, angled with end via, flipped edge-coupled and end-coupled-line configurations.

Additionally, with automatically paired parameters, an AI-powered optimization workflow integrated with Ansys HFSS can be used to realize dramatic time savings. The results of this process for an edge-coupled bandpass filter analysis are shown in ***Figure 3***.

MICROSTRIP OPEN-LOOP COUPLED BANDPASS FILTER

SynMatrix now supports open-loop resonator modeling for coupled microstrip bandpass filters. Users can leverage SynMatrix's first principles design workflow, starting with single resonator analysis, coupling scheme analysis, input and output structure design and full 3D layout and modeling. Users can choose between rectangular, square, triangle hexagon and U-shape resonators; in addition, SynMatrix will enable users to customize and edit the resonator shapes and parameters, such as the line width and insertion depth, to fit design requests optimally. ***Figure 4*** shows the inputs and outputs for a triangular resonator.

Planar filter performance may not match cavity filter performance in scenarios demanding better insertion loss and power handling characteristics. However, the form factor and cost benefits help provide design alternatives for modern RF microwave systems. As planar technology evolves and improves and diplexer design volume and complexity demands continue to grow, productivity and advanced design tools will become increasingly important to help designers meet project timelines, engineering specifications and economic goals.

SynMatrix Technologies Inc.
Richmond Hill, Canada
www.SynMatrixtech.com/

50 Ohm 1:1 Transformer Operates to 3 GHz

MiniRF Inc. has introduced the MRFXF0589 miniature high performance transmission line transformer for RF wireless markets. The MRFXF0589 is a broadband 50 Ohm 1:1 transformer that covers a 5 MHz to 3 GHz frequency range. Its unique electrical characteristics provide RF designers with better return loss, lower insertion loss and a smaller package than our popular RFXF9503. Its footprint is 20 percent smaller than the RFXF9503, along with a 0.5 dB reduction of insertion loss at 3 GHz. Additionally, the MRFXF0589 return loss is improved to at least 15 dB across the band with improved amplitude and phase balance. This transformer targets synthesizers, mixers, output amplifiers and other balanced RF circuit applications. This next-generation 50 Ohm balun offers high performance without the need for circuit complexity.

MiniRF products are 100 percent RF tested. This, plus MiniRF's controlled manufacturing techniques and quality materials, inspire confidence in the company's ability to provide high volume, low-cost products. A ferrite core that provides sufficient low frequency inductance, along with low insertion loss over a broad operating temperature range, is a key element in this product design. This design incorporates other components and strict assembly techniques to ensure proper impedance and consistent high-frequency performance.

These and other design and manufacturing techniques ensure that the designer gets a reliable and effective component. Designing with the MRFXF0589 enables radio designers to develop high performance radio systems without costly components. This balun can be used in multiple applications to provide many advantages to wireless designers. Contact MiniRF or RFMW for this new broadband product.

MiniRF
Fremont, Calif.
www.minirf.com
www.rfmw.com//manufacturer/minirf

High-K Material for Microwave Circuits

Tecdia, a supplier of thin film substrates, diamond, ceramic and precision-machined products, has recently released another dielectric material for wire-bondable single-layer capacitors. This type of capacitor is proving to be critical for high performance microwave circuits. The K4200 material has an X7R temperature coefficient, a relative permittivity (K) of 4200 and an operating temperature range from -55°C to 125°C. This K4200 has been added to the company's list of proprietary materials. The updated list includes materials with K values of 10, 40, 90, 130, 280, 1600, 2800, 4200, 16,000, 30,000 and 50,000. Most of the dielectrics can be lapped to specific thicknesses and singulated as necessary to yield capacitance form factors that are ideal for customer requirements. This flexibility also enables Tecdia to provide drop-in replacement components to offer a secure and stable supply chain for second-source parts solutions. The new wire-bondable capacitor lineup ranges from capacitances of less than 0.1 pF to values up to 10 nF. These capacitors can be supplied with footprints ranging from 0.2 mm x 0.2 mm (0.008 in. x 0.008 in.) to 2 mm x 2 mm (0.080 in. x 0.080 in.). Thicknesses for these capacitors range from 0.1 mm (0.004 in.) to 0.3 mm (0.012 in.). In addition, Tecdia continues to develop more novel materials with characteristics tailored to meet the needs of innovative RF designs and provide optimal solutions to customers.

Tecdia's mission is to connect the world through technology, innovation and people with amazing ideas. Since its beginning, Tecdia has showcased innovative products, superior quality, outstanding customer care and their unique technological formula for success. Reach out to Tecdia for any of your wire-bondable capacitor needs.

Tecdia
Morgan Hill, Calif.
www.tecdia.com
sales@tecdia.com

Fetch Your Copy of Microwave Journal

Renew Today!

Ansys Releases Ansys 2024 R2

The latest release introduces two new products, Ansys TwinAI™ software for enhancing simulation with AI for accurate, evolving digital twins and Ansys HFSS-IC™ solver for deep electromagnetic analysis of ICs.

Ansys

www.ansys.com

DC-DC Optimizer

Coilcraft's MagPro DC-DC Optimizer is a complete converter application tool that finds the most efficient inductor solutions and analyzes their performance to optimize your Buck, Boost and Buck-Boost converters.

Coilcraft

www.coilcraft.com/en-us/tools/dc-dc-optimizer/#

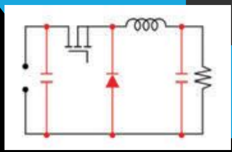

Mixer Measurement with a Vector Network Analyzer

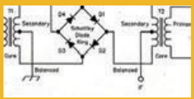

This app note gives an in-depth look at some of the common mixer measurement applications of VNAs. It covers conversion loss, compression, block converters, vector mixer calibration and much more.

Copper Mountain Technologies

buff.ly/3LNmjGz

Intro to RF Power Measurements

An assortment of instruments and methods are used for measuring power. In this article, the discussion is limited to electrical power, defined as voltage multiplied by current. Discussion is further narrowed to RF power, which implies higher frequency, say signals greater than 10 MHz, requiring more sophisticated instrumentation than a voltmeter due to the behavior of high frequency electrical signals.

Mini-Circuits

https://blog.minicircuits.com/intro-to-rf-power-measurements/

New Cable Configurator Tool

The new cable configurator tool enables users to select the exact product options for their design. The online tool allows for quick access to cable product families.

Smiths Interconnect

www.smithsinterconnect.com/products/cable-assemblies-harnesses/cable-configurator/

EMC Pre-Compliance Using Spike

EMC Pre-Compliance measurements are available for SM, SP and BB series devices in Spike Software. This mode provides measurement functions for testing emission regulation requirements.

Signal Hound

bit.ly/3Hu8Z7W

NEW PRODUCTS

FOR MORE NEW PRODUCTS, VISIT WWW.MWJOURNAL.COM/BUYERSGUIDE
FEATURING VENDORVIEW STOREFRONTS

DEVICES/ COMPONENTS/MODULES

Multi-Channel True Time Delay Unit

VENDORVIEW

Building off the success of its single channel time delay unit, the ADAR4002, ADI has expanded its True Time delay offerings. The ADAR4000 and ADAR4001 are highly integrated products, providing multiple channels operating from 2 to 18 GHz. The true time delay cores ensure beam-squint free wideband operations. Both devices have four channels, each with a 7-bit true time delay and a digital step attenuator. The total time delay range is 508 ps per channel and includes programmable amplifiers and on-chip memory, all in a 6 mm x 6 mm package.

Analog Devices
www.analog.com

GaAs MMIC Filters

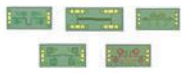

Electro-Photonics LLC announced the launch of their latest innovation in microwave and mmWave technology: the GaAs MMIC filters. Designed with precision and advanced engineering, these filters set a new standard in performance and reliability for high frequency applications. Measuring just 1.6 × 0.8 × 0.1 mm, these filters are perfect for space constrained designs, ensuring seamless integration into your compact electronic systems. Measuring just 1.6 × 0.8 × 0.1 mm, these filters are perfect for space constrained designs, ensuring seamless integration into your compact electronic systems.

Electro-Photonics LLC
www.electro-photonics.com

D-Band Down-Converter

VENDORVIEW

Designed for VNAs capable of cold-source noise figure measurements, model STC-11417400-06-C1 is a D-Band down-converter that includes an internal bypass switch. It converts signals from 110 to 170 GHz to a range spanning 5 to 65 GHz. Noise figures are measured when the down-converter is active. S-parameters are measured when the down-converter is bypassed.

Eravant
www.eravant.com

Waveguide Fixed Attenuators

VENDORVIEW

Fairview announced the launch of its new line of waveguide fixed attenuators. These advanced attenuators are designed to meet the rigorous demands of high frequency applications, offering unparalleled performance and reliability. The new waveguide fixed attenuators are available in a range of waveguide sizes, including WR-10, WR-12, WR-15, WR-19, WR-22 and WR-28. Their attenuation-levels of 3, 6, 10, 20 and 30 dB provide versatile options to suit various needs in signal attenuation and power control.

Fairview Microwave
www.fairviewmicrowave.com

0.7~6 GHz 50 W Surface-Mount 90° Hybrid

VENDORVIEW

MIcable just released the new 0.7 to 6 GHz high-power surface-mount 90-degree hybrid. It has low insertion loss (1.0 dB maximum), excellent VSWR (1.50:1 maximum), extremely good amplitude unbalance (±1.1 dB maximum) and phase unbalance (±9 degrees maximum), high isolation (15 dB minimum) and 50 W power handling capability with excellent stability and heat dissipation ability in a small package. It is suitable for power amplifier, power combining network, antenna feed network, modulator and phase shifter applications.

MIcable
www.micable.cn

High-Power RF Terminations

VENDORVIEW

Pasternack announced the launch of its new series of high-power RF terminations. They are designed for use in telecommunications, broadcasting, satellite communications and other high frequency applications where reliable signal termination is essential. The new high-power RF terminations are engineered for superior performance and reliability. They offer maximum power ratings of 5, 10 and 50 watts (continuous wave), making them ideal for a wide range of applications.

Pasternack
www.pasternack.com

Absorptive Switch

VENDORVIEW

Quantic PMI Model P1T-18G40G-90-1515-292FF-ROHS is an absorptive, high speed, single pole, single throw switch capable of switching within 15 to 25 ns. The frequency range is 18 to 40 GHz with a > 90 dB of isolation; insertion loss of 4.93 dB; VSWR 1.7:1; and input power 23 dBm. Housing size is 1.37 × 1.50 × 0.60 in. with 2.92 mm female connectors. ROHS compliant.

Quantic PMI
www.quanticpmi.com

26.5-40GHz 500W

Solid State Power Amplifier

Features

- Ultra Wide Band: 26.5-40GHz
- Gain: 57dB Min •
- Output Power: 57.5dBm Min
- High-efficiency GaN technology
- Low power consumption
- Low spurious signal
- Forward/reverse power monitoring
- Over voltage, over temperature, over current protection
- Optional overdrive protection

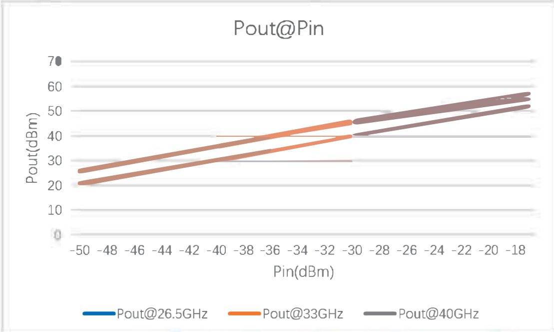

DC solid state power amplifier Modules

Fast Delivery!

- 26.5-40GHz Output Psat：47dBm
- Model：TLPA26.5G40G-47-47

- 2-18GHz Output Psat：45dBm
- Model：TLPA2G18G-45-45

AC Type Benchtop Power Amplifier up to 10KW

Three Years Warranty

- 0.5-6GHz 500W Solid State Power Amplifier
- 6-18GHz 250W Solid State Power Amplifier
- 2-18GHz 100W Solid State Power Amplifier
- 26-40GHz 500W Solid State Power Amplifier
- 40-60GHz 100W Solid State Power Amplifier
- 75-100GHz 10W Solid State Power Amplifier
- 8-18GHz 2000W Pulse Solid State Power Amplifier

NewProducts

0.1 to 20 GHz High-Power SPDT Switch

VENDORVIEW

Available now from RFMW, the Marki Microwave MSW2-1002HLGA is a 100 MHz to 20 GHz reflective SPDT switch with average insertion loss of 0.8 dB and 44 dB isolation. It has input power handling and hot switching capability of 33.5 dBm, all in a compact 2.25 × 2.25 mm LGA for surface-mount integration on circuit board-based systems.

RFMW
www.rfmw.com

Wideband 4-way Power Divider

Sigatek introduces a new addition to the family of 4-way power dividers covering the frequency range of 0.5 to 40 GHz. The SP70408 has an operating frequency range of 10 to 40 GHz with a typical performance of 1.5 dB loss, amplitude balance better than 0.4 dB and isolation greater than 15 dB. The return loss is better than 15 dB and phase balance is less than 6 degrees across all 4 output-ports. Dimensions are 2.30 × 0.75 × 0.40 in. with 2.92 female connectors.

Sigatek LLC
www.sigatek.com

TSX Wire Bondable Fixed Chip Attenuator Series

VENDORVIEW

Smiths Interconnect has extended its offering of high frequency surface-mount chip attenuators with the release of its new TSX wire bondable fixed chip attenuator series, a small, easy-to-implement, high-reliability product qualified for space and defence applications. The new TSX WB2 Series is qualified to MIL-PRF-55342 and designed to offer excellent broadband performance up to 50 GHz, while delivering increased power handling in a small 0404 wire bondable package. It allows wider coverage than traditional components while providing optimized return loss for multiple frequency ranges.

Smiths Interconnect
www.smithsinterconnect.com

CABLES & CONNECTORS

PT Test Cable

The Anoison PT test cable is designed for maximum ruggedness using a high-quality raw cable, connector and smart armoring module. Thus, Anoison offers top-grade test cables at a more reasonable cost. A great test cable must be durable. While most test cables in the market perform well in pulling and crushing, they often get damaged due to frequent twisting and bending at the cable end. Anoison has addressed this issue, and the PT cable can withstand frequent twisting and bending over the long term.

Anoison
www.anoison.com

EMI Filtered Connectors

Mobix Labs Inc. launched its latest EMI filtered ARINC 404 and ARINC 600 connectors for defense and aerospace applications. These versatile connectors can be customized with planar arrays, ceramic Pi tubes or chip capacitors to meet demanding military specifications. The new connectors are designed to deliver exceptional performance and reliability, featuring advanced EMI filtering options to ensure optimal signal integrity and minimal resonance. They offer insertion loss of 70 to 80 dB for Pi filters and 50 to 60 dB for C filters.

Mobix Labs Inc.
www.mobixlabs.com

New**Products**

Non-Magnetic Connectors

Withwave's non-magnetic connectors are widely used in applications that experience strong magnetic field can cause interference or introduce errors, such as quantum computing, magnetic resonance imaging (MRI) equipment and aerospace industry. They feature a DC to 40 GHz frequency range and are available in various interface sizes.

withwave co., ltd
www.with-wave.com

AMPLIFIERS

Solid-State LS-Band Amplifier

VENDOR**VIEW**

Exodus Advanced Communications' AMP2074P-LC-8 KW pulse amplifier is designed for pulse/HIRF, EMC/EMI MIL-STD 461/464 and radar applications. Providing superb pulse fidelity 1.0 to 2.5 GHz, 10 KW typical and up to 100 usec pulse widths. Duty cycles to 6 percent with a minimum 69 dB gain. Available monitoring parameters for forward/reflected power in watts and dBm, VSWR, voltage, current, temperature sensing for outstanding reliability and ruggedness in a compact configuration.

Exodus Advanced Communications
www.exoduscomm.com

Power Amplifier

Falcomm has sought to provide the next big leap in technology that will drastically improve energy efficiency over the state of the art. As part of their efforts, Falcomm has released their first power amplifier product, the FCM1401. The power amplifier product features Falcomm's proprietary technology, the ultra-efficient Dual-Drive™ architecture, and was implemented using the GlobalFoundries 130NSX1 process. It offers significant advantages in its exceptional performance, improved energy efficiency and thermal management cost reduction.

Falcomm
www.falcomm.com

Low Noise Amplifier

VENDOR**VIEW**

Richardson RFPD, Inc., an Arrow Electronics company, announced the in-stock availability and full design support capabilities for a new RF low noise amplifier from Guerrilla RF, Inc. The GRF2110 is a broadband, ultra-low noise linear amplifier designed for Wi-Fi 6/6E, small cell, wireless infrastructure and other high performance RF applications up to 8 GHz. The standard tune exhibits outstanding noise figure, linearity, return loss and gain flatness from 5 to 8 GHz.

Richardson RFPD
www.richardsonrfpd.com

RF Signal Amplifier

Model A10200 is an ultra-small footprint, ultra-wideband, high power amplifier designed for high frequency, high power, signal amplification. With an ultra-high bandwidth of almost 20 GHz and up to +28 dBm power into 50 Ohms, the A10200 is the ideal complimentary amplifier to any signal source that needs an extended power boost for demanding applications.

Tabor Electronics
www.taborelec.com

VHF to S-Band Low Noise Amplifiers

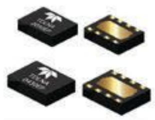

Teledyne e2v HiRel announced the availability of two enhanced plastic VHF to S-Band low noise amplifiers (LNAs), models TDLNA2050EP and TDLNA0430EP which are ideal for use in demanding high-reliability applications where low noise

figure, minimal power consumption and small package footprint are critical for success. These LNAs, developed on a 250 nm enhancement depletion mode pseudomorphic high electron mobility transistor (pHEMT) process, are available in an 8-pin dual-flat no-lead 2 × 2 × 0.75 mm plastic surface-mount package.
Teledyne e2v HiRel
www.teledynedefenseelectronics.com

TEST & MEASUREMENT

Thermoelectric Refrigeration Cooling/Heating System

VENDORVIEW

Cernexwave's thermoelectric refrigeration cooling/heating system is a great solution to bring your components to the optimum temperature for testing. They have a temperature control range of -45°C to +120°C with fast temperature change speed and high accuracy. The large cooling/heating plate dimensions and small overall footprint allow these units to be used for a great range of components in labs of any size.
Cernexwave
www.cernexwave.com

Multi-Channel Frequency Analyzer

The CNT-102 high performance frequency/time-interval analyzer supports parallel frequency, phase or time measurements on two input channels simultaneously. Gap-free technology, along with 14 ps resolution, up to 13 digits/s frequency resolution and 1M results/s sampling simplifies ADEV and related frequency stability measurements. Three timebase options and RF frequency support up to 15, 20 or 24 GHz via software upgrade on select hardware configurations satisfies a wide range of performance demands and/or budget.
Pendulum Instruments
www.pendulum-instruments.com

RF Microwave Generators

Saelig Company, Inc. has introduced Rigo DSG5000 Series RF microwave generators which can generate high-quality RF signals up to 20 GHz with amplitude, frequency, phase and pulse modulation capabilities. These generators are available with two, four, six or eight independent RF channels, housed in a 2U rack-mountable case. The DSG5000 Series of signal sources feature an impressive ±1-degree long-term phase stability between channels and they are designed for high frequency work in applications like radar and quantum research.
Saelig Company, Inc.
www.saelig.com

Reviewed by: Doug Jorgesen

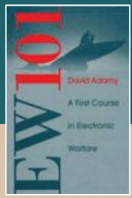

Bookend

EW 101: A First Course in Electronic Warfare

By David L. Adamy

EW 101: A First Course in Electronic Warfare by David Adamy stands as a cornerstone in the microwave aerospace and defense sector's library, distinguishing itself through its readability and practical approach. Originally a series of magazine articles, Adamy's text is notably more accessible than comparable academic texts, making it an ideal read, particularly for novice engineers in the field of electronic warfare (EW).

Adamy, a veteran in the EW arena, leverages his extensive experience to provide a comprehensive introduction to the field. The book covers crucial aspects of EW, including EW electronics like antennas, receivers and processing, as well as battlefield concepts such as jamming, emitter location, low probability of intercept signals and search strategies. It even delves into EW simulation, offering a rounded perspective on the subject.

Published initially in 2001, the book's continued relevance is impressive, given the advancements in technology such as GaN, MMICs and direct sampling architectures. Adamy focuses on fundamental principles and general rules of thumb rather than complex mathematical equations, which enhances the text's accessibility but may leave those seeking deep mathematical insights wanting more.

While some might find the book slightly verbose for an introductory overview and too basic for detailed technical study, it remains one of the few works on EW that is genuinely enjoyable to read. Its enduring relevance is a testament to the timeless nature of the subject matter, which remains pivotal in the world of radars, jets and countermeasures today.

EW 101: A First Course in Electronic Warfare is highly recommended for microwave and electrical engineers eager to gain insights into the dynamic field of EW. It serves as an excellent starting point for anyone looking to understand the complexities of this crucial aspect of modern defense technology.

ISBN: 9781580531696
Pages: 328
To order this book, contact:
Artech House (2001)
us.artechhouse.com

Advertising**Index**

Sales Representatives

Microwave Journal

Eastern and Central Time Zones
Michael Hallman
Associate Publisher
(NJ, Mid-Atlantic, Southeast, Midwest, TX)
Tel: (301) 371-8830
Cell: (781) 363-0338
mhallman@mwjournal.com

Susan Leppanen
Northeastern Reg. Sales Mgr.
(New England, New York, Eastern Canada)
Tel: (781) 619-1942
Cell: (508) 887-6360
sleppanen@horizonhouse.com

Pacific and Mountain Time Zones
Brian Landy
Western Reg. Sales Mgr.
(CA, AZ, OR, WA, ID, NV, UT, NM, CO, WY, MT, ND, SD, NE & Western Canada)
Tel: (831) 426-4143
Cell: (831) 713-9085
blandy@mwjournal.com

International Sales
Richard Vaughan
International Sales Manager
Tel: +44 207 596 8742
rvaughan@horizonhouse.co.uk

Germany, Austria, and Switzerland (German-speaking)
Victoria and Norbert Hufmann
victoria@hufmann.info
norbert@hufmann.info

France
Gaston Traboulsi
Tel: +44 207 596 8742
gtraboulsi@horizonhouse.com

Korea
Jaeho Chinn
JES MEDIA, INC.
Tel: +82 2 481-3411
corres1@jesmedia.com

China
Shanghai
Linda Li
ACT International
Tel: +86 136 7154 0807
lindal@actintl.com.hk

Wuhan
Phoebe Yin
ACT International
Tel: +86 134 7707 0600
phoebey@actintl.com.hk

Shenzhen
Annie Liu
ACT International
Tel: +135 9024 6961
anniel@actintl.com.hk

Beijing
Cecily Bian
ACT International
Tel: +86 135 5262 1310
cecilyb@actintl.com.hk

Hong Kong
Floyd Chun
ACT International
Tel: +852 28386298
floydc@actintl.com.hk

Taiwan, Singapore
Simon Lee
ACT International
Tel: +852 2838 6298
simonlee@actintl.com.hk

Japan
Katsuhiro Ishii
Ace Media Service Inc.
Tel: +81 3 5691 3335
amskatsu@dream.com

Submitting ad material?
Visit: www.adshuttle.com/mwj
(866) 774-5784
outside the U.S. call
+1-414-566-6940

Ed Kiessling
(781) 619-1963
ekiessling@mwjournal.com

Corporate Headquarters: 685 Canton Street, Norwood, MA 02062 • Tel: (781) 769-9750

FABS and LABS

Stellant Systems: Heritage & High-Power

Stellant Systems was founded toward the end of 2021, but they are not a newcomer to the electronics industry. The company traces its heritage back more than 90 years and includes some of the most recognizable names in the industry. What is now Stellant Systems started in Charles Litton's garage in 1932 and grew into Litton Industries. Howard Hughes' Electron Tube Laboratory got involved in 1959 and along the way to becoming Stellant Systems, there were multiple acquisitions and consolidations of divisions that operated under organizations like Sylvania, Loral, GM Hughes, Sperry, GE, RCA, Raytheon, Northrop Grumman and Boeing. Finally, after the merger of L3 Technologies and Harris Corporation in 2019, Arlington Capital Partners (ACP) bought the Electron Devices and Narda Microwave-West divisions from L3 Harris and renamed this entity Stellant Systems.

Stellant has expanded upon this heritage to become a $300 million manufacturer, employing nearly 1100 people. The company specializes in components and systems for critical spectrum and RF power applications. Befitting its origins in Litton Industries and the Hughes Electron Tube Laboratory, Stellant is the only vertically integrated supplier of traveling-wave tube amplifiers (TWTA) for space applications and the only U.S.-based manufacturer of space-qualified traveling-wave tubes (TWT).

However, Stellant manufactures more than tube-based products. In addition, the company develops and manufactures solid-state power amplifiers (SSPA) and active and passive control components from its 12 separate product lines that address four different markets. Stellant products are manufactured in five facilities in the U.S. and address opportunities in the space, defense, industrial and medical and scientific markets. In the space market, Stellant has been providing tube- and solid-state-based active products and passive components for more than 50 years. These products range from 1 to 70 GHz with output powers that can exceed 300 W. The product offering for the defense market is even broader, with frequencies to 95 GHz and power levels for some tube-based products reaching 6 MW. In the medical and scientific and industrial markets, Stellant tube-based products are used in a broad range of applications.

Stellant's rich heritage of acquisition and consolidation has enabled a diverse, full-featured facilities footprint. The company has two facilities in California. The Torrance headquarters addresses space and defense markets. This facility also offers specialized capabilities in metalization, deposition, chemical processing, brazing, inspection and analysis. A Folsom facility addresses space and defense applications and provides environmental testing laboratories, laser welding, RF chip-and-wire assembly, test and inspection service capabilities. This facility also offers metalization, chemical processing, welding, brazing, high-power and environmental testing capabilities. A facility in Williamsport, Pa., houses 10 of the Stellant product lines that address all markets except for space. A Power Systems Technology group became part of Stellant through the Comtech PST acquisition. This group manufactures high-power SSPAs and control components, along with receiver protection products in Melville, N.Y., and Topsfield, Mass. In total, these facilities occupy slightly more than 800,000 sq. ft. and provide multiple Class 100,000 cleanrooms. All facilities are ISO 9001:2015-certified and all the facilities, except Topsfield, are AS9100-certified.

With a rich heritage and deep roots in high-power RF products and applications, Stellant continues to expand its size and capabilities organically and through acquisition. Stellant prides itself on performance, precision and durability, along with understanding the needs of the ecosystem. These principles are perfectly reflected by the belief that "together we can go further."

https://stellantsystems.com/

2024 EW, Radar & MilCom

A SPECIAL SUPPLEMENT TO

Microwave Journal

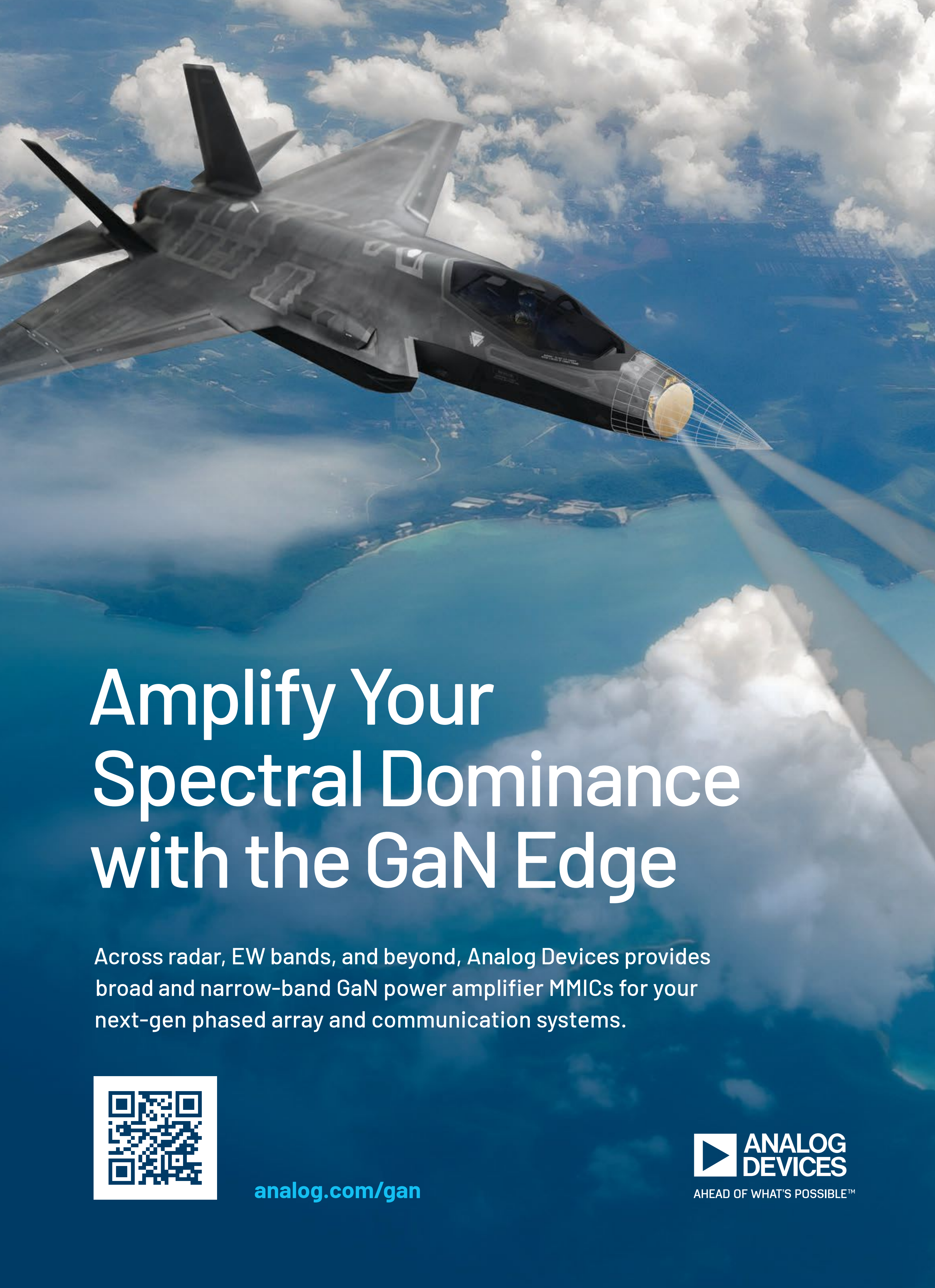
Amplify Your Spectral Dominance with the GaN Edge
Across radar, EW bands, and beyond, Analog Devices provides broad and narrow-band GaN power amplifier MMICs for your next-gen phased array and communication systems.
analog.com/gan
ANALOG DEVICES
AHEAD OF WHAT'S POSSIBLE™

Anokiwave Is Now qorvo

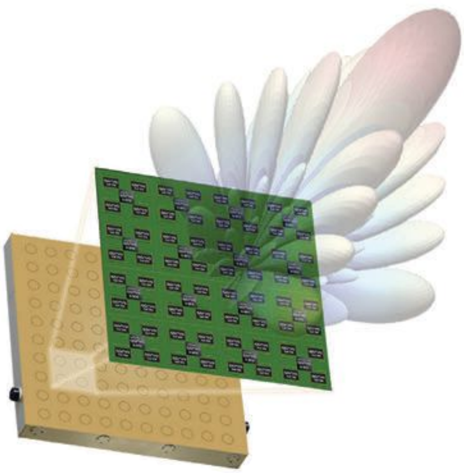

PROVEN PERFORMANCE

High Performing X-Band Radar ICs

Phased Array AESA Systems

- 4 channel beamformer IC with T/R duplex
- Dual Rx for dual polarity/monopulse capability
- Stable phase over temperature with digital phase shifters
- High efficiency, low current front-end modules with range of output power
- Low receiver noise with over drive power protection

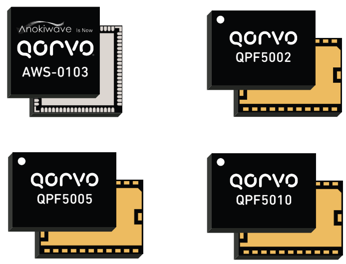

Visit to qorvo.com/go/xradar
to see our complete portfolio

Cover Feature

Perspective

Special Reports

Application Notes

Product Features

Tech Briefs

Company Showcase

Staff

Publisher: Carl Sheffres
Associate Publisher: Michael Hallman
Editorial Director: Patrick Hindle
Brand and Content Director: Jennifer DiMarco
Technical Editor: Eric Higham
Associate Technical Editor: Cliff Drubin
Editorial & Media Specialist: Kelley Roche
Associate Editor: Kaitlyn Joyner

Multimedia Staff Editor: Barbara Walsh
Electronic Marketing Manager: Chris Stanfa
Senior Digital Content Specialist: Lauren Tully
Director of Production & Distribution: Edward Kiessling
Art Director: Janice Levenson
Graphic Designer: Ann Pierce

EUROPE
Office Manager: Nina Plesu

CORPORATE STAFF
CEO: William M. Bazzy
President: Ivar Bazzy
Vice President: Jared Bazzy

Protecting Fully Digital, Multi-Mission Radar Receivers with Agile Filters

Peter Matthews
Knowles Precision Devices, Cazenovia, N. Y.

Radar plays a critical role in a variety of aerospace and defense applications. As the mission types evolve, fully digital phased array technology that can handle multiple radar, electronic warfare and communications functions with different frequency and bandwidth requirements is emerging. A fully digital phased array is software-defined, meaning each element can be controlled and tuned independently, making it possible to configure compact multi-mission radar systems. But there are new complexities, especially related to ensuring proper filtering in these increasingly tight spaces, that must be overcome when implementing a fully digital antenna design. This article explores how radar designers can overcome the complexities of using fully digital beamforming and how to address the new filtering challenges related to this evolving radar technology.

A Brief Review of the Evolution of Radar

Since the beginning of the 20th century, radar has rapidly evolved from a fairly simplistic device only capable of short-range object detection to the sophisticated systems of today that can stealthily provide detailed imaging and real-time data for objects thousands of miles away. As a result, radar systems have transitioned from passive detection to active detection techniques that use analog signal processing methods to the active digital technology we are familiar with today. ***Figure 1*** shows an overview of the evolution of radar systems.

Radar system architectures are also evolving to support the radar system transitions shown in Figure 1. These architectures give system designers a wide range of solutions that can be optimized to meet system requirements. ***Figure 2a*** shows a passive phased array. ***Figure 2b*** shows an active phased array. ***Figure 2c*** shows a subarray digital phased array and ***Figure 2d*** shows an element-level digital phased array.

The industry is experiencing a technological shift. It is evolving from subarray digital phased arrays to element-level digital arrays. In subarray digital phased arrays, antennas are divided into smaller subarrays that share common signal processing components and perform beamforming in the subarray at the RF or intermediate frequency (IF) level. Element-level digital arrays perform digital beamforming at the individual antenna element level. Element-level arrays, which are also known as fully digital phased arrays, have an analog-to-digital converter (ADC) connected directly to each antenna. As a result, this technology offers unparalleled flexibility, performance and scalability for radar systems.

The Benefits and Challenges of Fully Digital Phased Arrays

In a fully digital configuration, the functions of each antenna are software-defined. Each element can be controlled and tuned independently, allowing users to implement more complex beamforming algorithms that can split beams in multiple directions or detect and transmit beams at different frequencies simultaneously. Additionally, since the ADC is closer to the antenna element, the dynamic range is improved and more signals can be detected. With so many capabilities, one radar system can now be used for multiple missions; this saves space, which is crucial for tight environments such as on a ship.

However, like most applications, compact size and additional capabilities come with challenges. Locating devices closer to the antenna element imposes physical size constraints for the electronics and passive components needed behind every radiating element. Second, fully digital receivers pick up all signals from all directions since the antenna cannot be pointed away from a specific signal. Additionally, there is also the potential for the antenna to jam itself if the signal from one transmit beam impacts the reception of another, for example. Together, these challenges make it crucial to have high performance yet compact filters for these systems.

Simplifying Digital Receiver Design with Direct Sampling

Filters are essential components that protect a radar receiver. These small passive components do a big job; they clean up the signal "messes" created either outside the radar or made by the radar itself. While a typical heterodyne receiver requires multiple filters to clean up these messes, direct sampling is a technique that can be implemented in a digital array to directly convert analog signals to a digital format without using an IF conversion stage. As a result, direct sampling eliminates the need for a mixer and an amplifier in the receiver, along with the filtering required by those functions. This reduces the size of the receiver. To illustrate these benefits, ***Figure 3a*** shows a block diagram of a typical heterodyne receiver. ***Figure 3b*** shows the block diagram for a direct sampling receiver, which achieves the same system function with far fewer components.

In a direct sampling receiver, one filter selects the correct band of interest. It removes out-of-band interference and another filter cleans up any interference generated by the amplifier, along

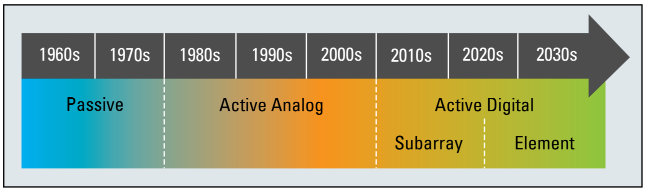

Fig. 1 A summary of the evolution of radar.

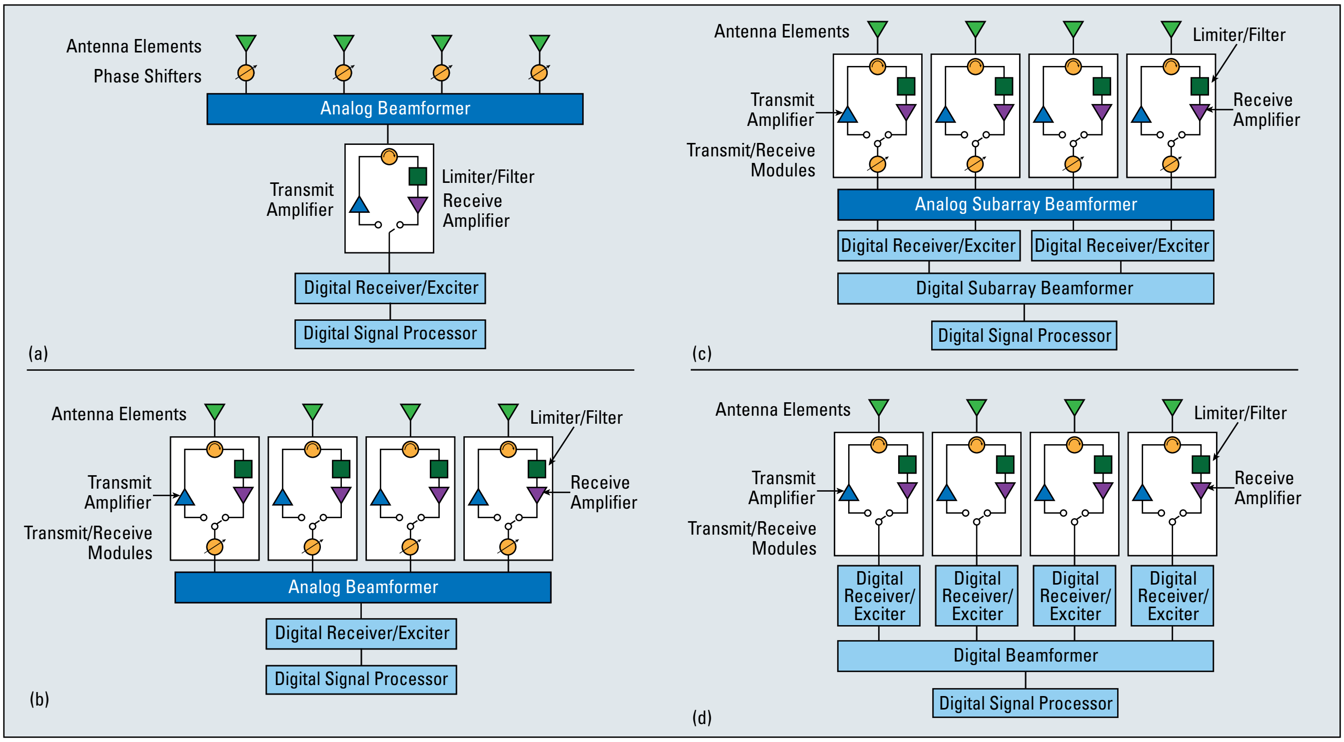

Fig. 2 (a) Representative passive phased array radar system block diagram. (b) Representative active phased array radar system block diagram. (c) Representative subarray digital phased array radar system block diagram. (d) Representative element-level digital phased array radar system block diagram.


WE TAKE YOU TO A PRIME POSITION
EN9100
CERTIFIED
Our proven track record with aerospace & defense primes is a testament to why you can trust ERZIA for your next EW project.
AIR FORCE
DC CTRL
ERZIA
ERZ-HPA-0200-2000-44
IN
OUT
ERZIA
WE TAKE YOU FURTHER
ERZIA.COM
RF & MICROWAVE | AMPLIFIERS | SWITCHES | MIXERS | FILTERS | CUSTOM INTEGRATED ASSEMBLIES

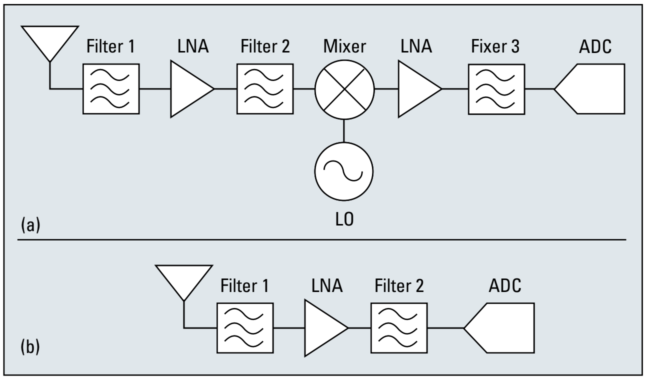

▲ Fig. 3 (a) Typical heterodyne receiver block diagram. (b) Typical direct sampling receiver block diagram.

with selecting the alias bands of the ADC. It is important to note that these filters should be small, under a half-wavelength at the frequency of interest. As radar systems move to higher frequencies, filters need to become even smaller. Additionally, a multi-mission receiver will typically require switching from wideband to narrowband coverage or keeping operating frequencies away from frequencies to avoid. Protecting the receiver over its range of applications requires a small, agile filter bank and the physical dimensions of the entire filter bank must be less than a half-wavelength.

Miniaturizing Filter Technology

As the operational frequencies of radar targets of interest increase, the wavelengths of these signals become shorter.

TABLE 1

UPPER-FREQUENCY HALF-WAVELENGTH SPACING FOR SOME COMMON BANDS

Band Designation	FL (GHz)	FH (GHz)	λ/2 (mm)
S	2	4	37.50
X	8	12	12.50
Ka	27	40	3.75

As described earlier, half-wavelength element spacing optimizes antenna performance, so arrays are also becoming denser as operational frequencies increase. ***Table 1*** shows half-wavelength distances in free space for the upper-frequency range for some common bands.

As array density increases, it becomes even more critical to have the ability to steer beams to avoid interference, especially when transmitting signals. This raises an interesting question: instead of solely relying on reducing the size of filters, what if a filter could alter the speed of the signal in the material? Doing this effectively changes the wavelength. ***Equation 1*** shows the classic equation that relates the frequency and wavelength of a signal to the speed of light in free space.

$$c = \nu\lambda \tag{1}$$

Where:
c = speed of light in free space
ν = frequency
λ = wavelength

Equation 1 shows how it is possible to change the speed of a signal in a material. Using different materials makes it possible to change c to the velocity of propagation in the ma-

terial. Changing the speed of the electromagnetic wave for a given frequency results in a different wavelength. Fortunately, when manufacturing distributed element filters on microstrip, for example, these filters will only occupy a fraction of a wavelength. If the wavelength in the material can be reduced, the size of the filter will decrease. For a microstrip line, the wavelength is determined using ***Equation 2***:

$$\Lambda = \frac{\lambda}{(\varepsilon_{eff})^{0.5}} \qquad (2)$$

Where:
Λ = Wavelength in microstrip
λ = Free-space wavelength
ε_{eff} = Effective dielectric constant, which depends on the dielectric constant of the substrate material and the physical dimensions of the microstrip line.

This equation shows how changing the substrate and the dielectric constant can impact the wavelength inside the microstrip filter.

Shrinking the Switched Filter Bank

While switched filter banks are traditionally associated with larger footprints, the same concepts described above can be applied to this technology as well. Filter manufacturers such as Knowles Precision Devices are leveraging materials science innovations to shrink the size of each filter. Then, using high-precision lithographic processes, these microstrip filters can be patterned onto custom ceramics, resulting in significantly reduced filter form factors. ***Figure 4*** shows an example of this technique and the size reduction possible with printed circuit board (PCB), alumina and three custom dielectric materials. Beyond miniaturizing filter components to meet emerging requirements, there is also an opportunity for innovation in the packaging of the switched filter bank. With consideration for input size and how narrow an output needs to be, a designer has room for more channels. ***Figure 5*** shows a four-channel filter bank design that features a 3D-stacked structure with alternating filters and interposer boards mounted directly to the PCB. This packaging concept

Relative Filter Size
Compared by Material

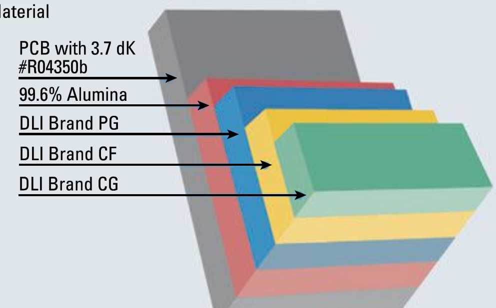

Filter Characteristics
Compared by Material

Material	dK	Effective K**	Wavelength at 10 GHz (in.) (mm)	Pct. Reduction
PCB with dK #R04350b	3.7	2.8	0.707 (17.96)	—
99.6% Alumina	9.6	6.5	0.462 (11.73)	34.7%
DLI Brand PG	12.5	8.2	0.412 (10.46)	41.7%
DLI Brand CF	25	15.1	0.304 (7.72)	57.0%
DLI Brand CG	67	36.8	0.194 (4.93)	72.6%

** Values are for Frequency 10 GHz on 0.010 in. Substrate

▲ Fig. 4 A comparison of the size and filter characteristics for different dielectric materials.

reduces internal spacing, which ultimately reduces the size of the filter bank.

Important RF Considerations for Radar Filters

Beyond bandwidth capabilities and size, several important factors must be considered when selecting the filters to include in a switched filter bank for a radar system. This next section explores how temperature stability, tolerance and phase performance can impact filter performance.

Temperature Stability

When selecting filter types and materials, the effects of the operating environment on filter performance must be considered. For microstrip filters, temperature stability is a crucial contributor to the frequency stability of the filter. In turn, the properties of the substrate materials are vital contributors to temperature stability. Let's consider this comparison of characteristics, including temperature stability, for filters built on two common substrates, alumina and PG and three custom Knowles Precision Devices ceramics. The results are shown in ***Table 2***.

Manufacturing Tolerances

It is also essential to analyze manufacturing tolerances when selecting filters for a switched filter bank in a radar system. Manufacturing tolerance refers to the acceptable deviation from the specified design parameters during the manufacturing process. For example, suppose a manufacturer specifies that a filter's center frequency is 2.4 GHz with a ±100 MHz tolerance. In that case, the actual center frequency can only range from 2.3 GHz to 2.5 GHz to still be considered acceptable. Manufacturing tolerances impact filter performance, especially at higher frequencies where tolerance impacts can become significant. If a radar system needs to operate precisely and reliably at higher frequencies, it is worthwhile to consider selecting filters with tighter tolerances.

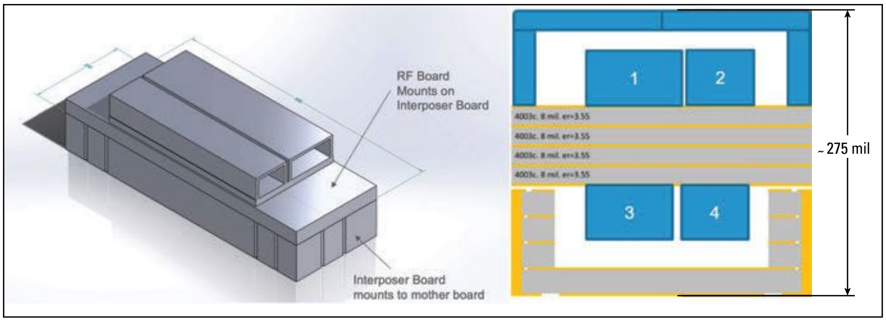

▲ Fig. 5 Using a 3D-stacked structure to reduce the size of a four-channel filter.

Phase Performance

Characterizing phase is an important and often overlooked aspect of assessing filter performance. Phase performance relates to how a filter affects the phase of the signals passing through the filter. Since filters can introduce phase shifts to the signals, good phase performance means

Accurate RF Analysis in the Field

Identify interference and signal degradation with ease.

Signal Hound's portfolio of real-time spectrum analyzers and monitoring receivers offers high-performance and reliability at an accessible price. With wide frequency ranges up to 43.5 GHz, ultra-fast sweep speeds up to 200 GHz/sec, and low phase noise, the SM435C, BB60D, and SP145 are ideal companions for your remotely located RF data analysis needs.

SP145
14.5 GHz Spectrum Analyzer

BB60D
6 GHz Spectrum Analyzer

SM435C
43.5 GHz Spectrum Analyzer

Signal Hound®

SignalHound.com

Made in the USA

not introducing much, if any, additional phase shift. This is essential for maintaining the integrity of the signals passing through a filter. Some factors to consider when specifying or characterizing phase performance:

- **Phase linearity:** This is a measure of the linearity of the filter's phase response across its passband. Any nonlinearity in the phase response can distort the processed signals.
- **Phase stability over temperature:** Minimizing the phase variability over a range of temperatures allows for more accurate measurements and reduces calibration requirements.
- **Phase length repeatability:** Consistency over variables such as temperature, frequency and repeatability contribute to increased signal coherence, image quality and measurement accuracy.

Embracing Fully Digital Phased Array Technology for Radar

To meet the challenges presented by modern signal monitoring, designers need to consider fully digital beamforming techniques. When using fully digital phased arrays, each antenna element becomes independently controllable, enabling complex beamforming algorithms and multi-mission functionality. The result is emerging and planned radar systems with unprecedented flexibility and capability.

As the article has discussed, this transition to fully digital beamforming presents its own set of challenges, particularly when it comes to filtering solutions that provide the required performance in these compact, multi-mission systems. However, with recent advancements in materials science, filter components can be made in much smaller form factors, allowing designers to develop compact switched filter banks without sacrificing performance. Now, agile radar systems that take advantage of fully digital beamforming technology hold tremendous potential for meeting the evolving demands of aerospace, defense and public safety applications. ■

TABLE 2

CHARACTERISTICS OF COMMON SUBSTRATES AND KNOWLES PRECISION DEVICES CUSTOM CERAMICS

Substrate Material	Dielectric Constant (Tolerance)	Typical Loss Tangent	Coefficient of Thermal Expansion (ppm/°K)	Temperature Coefficient of Capacitance (ppm/°C)	Surface Finish (minch)	Temp Stability
99.6% Alumina (Al203)	9.6 (± 0.15) at 1 MHz	0.0001	6.5 to 7.5	P120 ± 30	< 5	Poor
PG	12.5 (± 0.5)	0.0002	8.4	P22 ± 30	< 5	Good
SF	25 (± 1)	0.0003	10.6	0 ± 15	< 5	Excellent
CD	38 (± 1)	0.0004	5.8	N20 ± 15	< 5	Good
CG	67 (± 3)	0.0008	11.0	0 ± 30	< 5	Very Good

Analog Transformation: The Missing Link to Achieving Mass Affordability/Affordable Mass in Defense Systems

Ian Dunn
Spectrum Control, Fairview, Pa.

A key goal for next-generation defense systems is to achieve a new level of mass affordability and affordable mass that will allow for persistence and hedging in future conflicts. Digital transformation has been at the forefront of the defense community's initiatives to create systems that are lower cost, smaller and faster without compromising performance. This digital innovation has benefitted from catalysts, such as interoperability, software enablement and a full ecosystem of technologies, products and solutions.

These catalysts have seemed largely incompatible with the analog world, where most innovation has been associated with commercial volumes but has not been readily translatable to the defense sector. A new design approach is changing all of that. By focusing on the development, integration and deployment synergies between digital and analog technologies, the Department of Defense (DOD) can unlock previously unattainable levels of mass affordability.

Mass Affordability for Affordable Mass

The ability to manufacture at scale plays a critical role in preparing for conflict. Affordable mass refers to the capability to produce large quantities of weapons systems at a cost that is sustainable over long periods, especially in the face of prolonged conflicts. It ensures that military forces remain equipped and can sustain operations without the risk of munition depletion. Affordable mass supports sustained operational capability, deterrence through volume and versatility in response.

Mass affordability, conversely, focuses on minimizing the costs of individual units of weaponry to maximize production and deployment capabilities within fixed economic constraints. This approach allows for a broader distribution of technology and resources, ensuring that advanced capabilities are not only available but also sufficiently abundant to reach widescale adoption and utilization. Reduced cost enables the DOD to invest in newer technologies, increase production runs and stabilize ever-growing defense expenditures.

Analog Not Keeping Pace with Digital

Analog has been both the mass and backbone of weapons systems throughout contemporary history. However, the limitations of purely analog systems, inflexibility, manual errors and inefficiencies, are apparent and are coupled with an exquisite design-to-requirements flow-down process. This has raised costs and hindered much-needed productivity improvements and mission-driven innovations. Today, the backbone of most weapons systems has transitioned to all-digital with a design process that is almost entirely digital. Additionally, the increasing use of digital twins is easing integration and lessening the potential for errors.

Digital flexibility, however, is no longer a substitute for mass affordability. Cost per digital mission is not an economically viable choice if the dominance of the underlying analog platform is no longer assured. The inflexibility of the analog world becomes an affordability impediment once again in this scenario. According to a report from the Hudson Institute,[1] in the absence of dominance, bets need to be hedged to make mass as affordable as possible.

Analog Transformation

Analog transformation requires a funda-

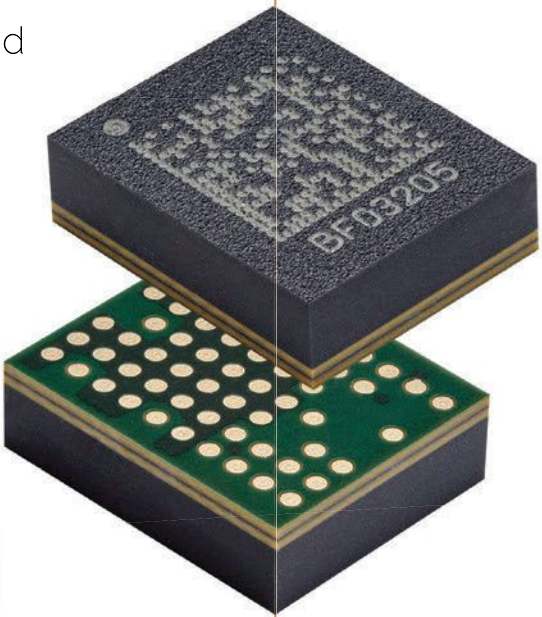
BF03205

mental re-envisioning of analog components and systems by incorporating digital capabilities to optimize and streamline integration. This will lead to automated test and tuning functions and, finally, enable real-time adaptability in the field. The outcome is that the analog function behaves more like a digital building block while retaining its high-fidelity analog performance.

This capability can be referred to as a digital gateway with a representative block diagram, as shown in ***Figure 1***. A digital gateway can be embedded into an analog circuit with minimal impact on the size, weight and power of the product. Customers can then conduct much of their integration in software, eliminating costly specification and technical negotiations typically required to translate and fix the analog performance for integration into a digital system/mission.

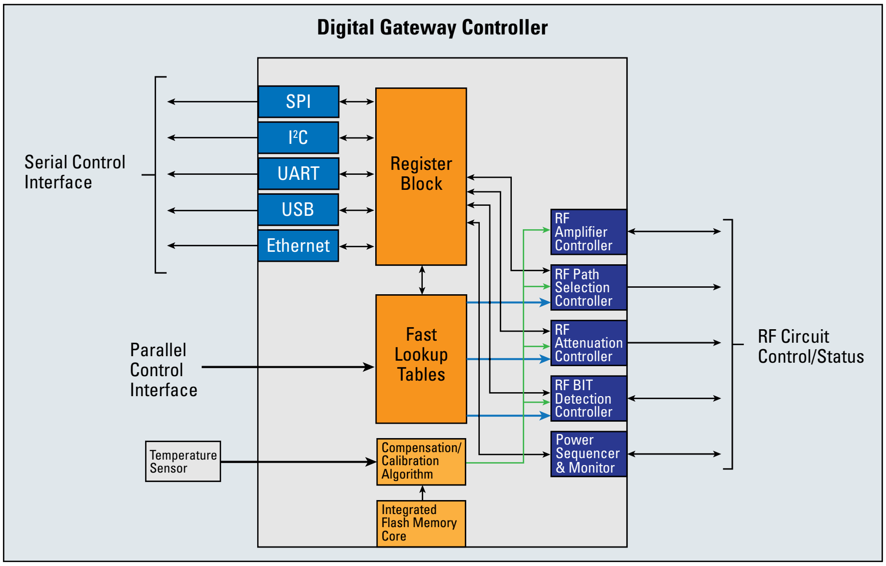

Fig. 1 Digital gateway controller block diagram.

Analog transformation seeks to enhance the inherent strengths of analog systems while seamlessly incorporating digital advancements. This hybrid approach leverages the precision, reliability, simplicity and mass of analog systems, complemented by the flexibility and data-rich capabilities of digital technologies. Rapid integration and adaptation of digitally-enabled analog building blocks into defense systems represents a transformative approach to affordable mass/mass affordability. Analog transformation is generating a three-fold improvement in the life-cycle cost of product development activities. The savings have manifested in three distinct categories:

Design velocity: The digital gateway is a framework for analog design. It is designed to control and power a set of standard analog building blocks that can be cascaded into a larger function. The physical size and power consumption of the gateway can be tailored to the analog function, but it is fundamentally very small. The framework includes a mechanical architecture that ensures proper isolation and thermal management of the analog and digital building blocks to ensure the overall performance of the function. More importantly, it drives and enables analog miniaturization. All of this, coupled with digital simulation, virtually eliminates the need for respins, saving three to six months.

Test and tune: The digital gateway is also an embedded, automated test stand that provides valuable, rapid insight into the fidelity of a design to meet its performance requirements. It comes with a software interface and basic GUI so that any member of the engineering and operations teams can manipulate the analog function to test and/or tune the device.

Rapidly emerging artificial intelligence (AI) and machine learning (ML) capabilities can quickly adapt the analog function to new missions. This is essential to delivering the speed and innovation required to realize the hedge force concept. Analog functions have rarely been associated with software, but the concept of an embedded digital gateway is being used across multiple industries and applications to make devices more reliable and adaptable

Dressed and Ready for Action

Custom Packaged Military Components

Micro Lambda Wireless, Inc offers a complete line of oscillators filters and harmonic generators for the military market. Whether you are designing for an Aircraft, Ship Board, Missile or Ground Based military system, check out the product capabilities available from Micro Lambda Wireless.

Oscillators covering 700 MHz to 40 GHz and filters covering 350 MHz to 50 GHz can be provided based on customer specific requirements. Individual components can also be provided utilizing industrial parts and the top levelcomponents can be screened and tested to specially designed test plans.

Micro Lambda is a ISO 9001:2015 Registered Company

- **MLFI and MLFP Series Bandpass filters**
- **MLFR and MLUN Series Bandreject (notch) filters**
- **MLOS, MLXS, MLOB, MLXB Series Oscillators**

www.microlambdawireless.com

MICRO LAMBDA WIRELESS, INC.

"Look to the leader in YIG-Technology"

46515 Landing Parkway, Fremont CA 94538 • (510) 770-9221 • sales@microlambdawireless.com

to the changing environment. This concept is being implemented in a range of applications, from water meters to implantable devices.

Systems engineer-ready: The ability of systems engineers and architects to interact directly with key elements of a design eliminates some need for specialized engineering functions in a design team. Translating an analog function into a digitally controllable asset at the system level can be very time-consuming and costly to the original equipment manufacturer (OEM) and integrator. The process typically starts with a hardware control specification. Then, the OEM and integrator must develop custom firmware to control the function. The use of simulation and digital twins can simplify testing but not necessarily firmware development. With the digital gateway, the analog functions have an out-of-the-box experience suitable for a systems engineer or a software engineer, a huge advantage in the speed of adoption and adaptation.

Interoperability and the Need for an Ecosystem

In the analog world, interoperability is largely a physical concept expressed in electromechanical terms. It is time to bring digital interoperability directly into analog building blocks. This has been a cultural issue at many companies with analog and digital assigned to separate teams as part of an integrated product development process. Digital architecture embedded within the analog building blocks needs to be viewed on equal footing, not simply as a necessary service for downstream digital integration. Digital enablement must be exposed to the integrator and possibly to the end-user via software to reap the benefits of speed, adaptability and, ultimately, affordability.

The concepts of interoperability and ecosystem development activities were largely made popular through the advent of digital communication systems. Related concepts have distinct differences that are important to understand in the context of analog transformation. Interoperability refers to the ability of different systems, applications or products to work together seamlessly. Information and functionality are exchanged without additional user effort. This is crucial in ensuring that diverse technologies can integrate and communicate efficiently, fostering a more unified user experience.

Conversely, an ecosystem encompasses a broader network of interrelated entities, including technologies, organizations and users, who interact and depend on each other from technology and commercial perspectives. An ecosystem often relies on interoperability to thrive, as the smooth interaction between its components ensures stability, growth and efficiency. An ecosystem includes the relationships, dynamics and synergies that develop within the network.

While interoperability focuses on technical compatibility, an ecosystem encompasses the broader context of collaboration, innovation and market presence. Bringing digital interoperability and the benefits of an ecosystem to the analog world can have profound consequences for mass affordability/affordable mass and analog transformation. Digital enablement of analog products is the precursor to that transformation.

Conclusion

As industries continue to evolve, the importance of analog transformation will only grow. The integration of analog and digital technologies offers a balanced approach to modernization, preserving the strengths of traditional systems while leveraging the advantages of digital innovation. It is most impactful in the speed and flexibility it brings to the design and deployment of analog technologies. Its impact could be greater as AI and ML start to adapt the analog components of subsystems to the threats and opportunities in front of the mission.

Analog transformation represents a pivotal shift in the way industries approach mass production. By enhancing analog systems with digital capabilities, unprecedented levels of efficiency, cost-effectiveness and scalability can be achieved. This hybrid approach is more than the key to affordable mass production. It is also a pathway to a more sustainable and resilient future. While it can be referred to as an analog transformation, the real missing link is the synergy between analog and digital transformations. Our competitiveness depends on it. ■

References

1. B. Clark and D. Patt, "Hedging Bets: Rethinking Force Design for a Post-Dominance Era," *Hudson Institute*, February 20, 2024, Web: https://www.hudson.org/defense-strategy/hedging-bets-rethinking-force-design-post-dominance-era-bryan-clark-dan-patt.

INVITED PAPER

From Radar to High-Power Weapons: Microwave Tubes Power Modern Warfare

Aniket Roy
Stratview Research, Detroit, Mich.

War is known for bringing pain and suffering, as it seldom brings anything good to humanity. Even if something positive comes from it, the benefits are often meager at best. However, one war drastically changed not just the art of warfare but also the way people live their lives.

World War II (WWII), which lasted from 1939 to 1945, led to the development of several technologies and products that have now become an irreplaceable part of our lives. Synthetic rubber, duct tape, flu vaccines, penicillin, electronic computers and radar all were developed or gained significant traction because of the war effort. In addition, the cavity magnetron that still powers microwave ovens in addition to providing high RF transmit power, was invented in the early part of WWII and became a mainstay of radar systems used by the Allied forces.

Though the name cavity magnetron implies that we are going to talk about some infamous leader of the Decepticon Army; it was one of the functional blocks that saw its first application in radar systems during WWII and proved to be crucial in enhancing the effectiveness of radar systems. The contribution was so significant that many experts consider it one of the major reasons behind the Allied forces winning the war.

Though originally designed for the generation of electromagnetic signals to be used in high frequency military applications, the cavity magnetron and other similar vacuum tubes gained more popularity after they found application in American households as microwave ovens. Currently, their applications stretch far beyond the defense domain to sectors including medical, household, space and many more. ***Figure 1*** shows some common applications that use tube-based transmitters, along with where they operate in the frequency spectrum.

From devices that cook food, to devices that jam military communications with a frequency band ranging from 1 to 1000 GHz, microwave tubes offer different solutions at different frequency ranges. If we consider the entire microwave band, the consumer microwave oven emerges as the biggest application of microwave tubes. According to the Residential Energy Consumption Survey 2020, more than 95 percent of U.S. households had at least one microwave. This equates to approximately 126 million microwave ovens being used in household applications in the U.S. alone.[1] Considering just the high frequency or high-power applications, the defense industry becomes the largest user, accounting for more than 30 percent of the high-power microwave tube market, according to a report from Stratview Research.[2]

Microwave Tubes on the Battlefield

Defense applications for microwave tubes are very diverse. Radar systems, remote-sensing, electronic warfare (EW), satellite communications, improvised explosive device (IED) and infrared (IR) countermeasures are some of the most popular defense applications using microwave tubes. Of these applications, radars and satellite communication links were among the first applications to use microwave tubes.

The advent and growth of solid-state power amplifiers (SSPAs) are diminishing the market share of microwave tubes in all but the highest power applications. Recently, the industry has shifted focus toward utilizing tubes in high-power EW applications and innovations in microwave tube-based directed energy (DE) weapons. DE weapons use concentrated electromagnetic energy, rather than kinetic energy, to sabotage, damage or disable various

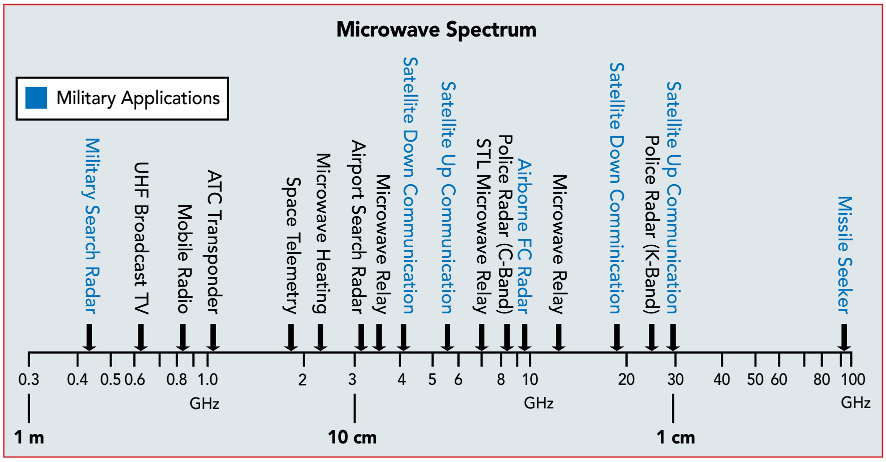

Fig. 1 The microwave spectrum and some common applications.

TABLE 1

SOME POPULAR HPM SYSTEMS

Platform Name	Ideal Application	Developer	Status
Tactical High-power Operational Responder (THOR)	DE counter-UAS weapon system for short-range defense	U.S. Air Force	Successful field tests completed June 2023
Phaser high-powered microwave system	DE counter-UAS weapon system for short-range defense	Raytheon	Prototype deployed for operational evaluation by the U.S. Air Force
Counter-electronic High-power Microwave Extended-range Air Base Defense (CHIMERA)	DE counter-UAS weapon system for long-range defense	Raytheon	Currently in the testing phase
Indirect Fire Protection Capability High-power Microwave (IFC-HPM)	DE counter-UAS system to counter Group 1 and Group 2 UAS	U.S. Army	Currently in the testing phase

electronic systems used by enemy forces. DE weapons are emerging as a popular EW option because of their ability to render enemy systems useless without the need to fire a bullet or cause any physical explosions.

Both lasers and microwave tubes can be used to launch a DE attack but tubes are preferred for wider attacks given the distance from the target is the same. DE systems based on microwaves are classified as high-power microwave (HPM) weapons and countries like Russia, China, France and the U.S. have been working on HPMs for more than a decade. However, only a few HPMs have seen field operations. ***Table 1*** shows some popular HPM systems.

Like any device that transmits RF power, HPMs require a source to convert the electromagnetic pulses to higher power signals with frequencies well into the GHz range. The output power and frequency capabilities of microwave generators are fairly broad. That allows almost every common microwave tube variant to be used for HPMs and the same flexibility makes tubes broadly applicable to a wide variety of defense applications. ***Table 2*** presents a high-level comparison of the common microwave tube types and indicates their suitability in HPM applications.

While each microwave generator is suitable to be used in a wide variety of defense applications, they each have disadvantages. For instance, Klystrons can provide the highest power outputs but they may be less preferred because of their complex operation. Similarly, BWOs, though extensively explored by the industry, become limited in high frequency applications because high frequency implies smaller sources.

Macro Opportunities for Microwave Tubes in the Defense Industry

Since defense is fundamental to national sovereignty, funding for procurement and innovation in the defense industry is often a large portion of a country's budget. The

DEFENSE & AEROSPACE

GaN Wideband Amplifiers

UP TO 6GHz

| **50W**, 500-2500MHz

| **25W**, 2000-3000MHz

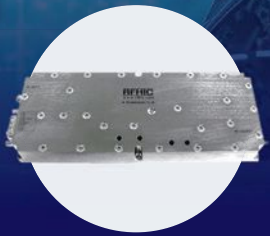

| **20W**, 2000-6000MHz

| **100W**, 2000-6000MHz

Part Number	Freq. [MHz]		Output Power	POUT	Gain	Dimensions
	Min	Max	[W]	[dBm]	[dB]	W x H x D [mm]
RWS03020-11	20	450	10	40	40	58 x 15 x 32
RWP03040-50	20	500	40	46	39	70 x 50.8 x 17.1
RWP03160-10	20	500	160	52	43	120 x 65 x 16.7
RWS02520-10	20	512	20	43	41	63 x 38 x 14.4
RWS02540-10	20	512	40	46	44	63 x 38 x 14.4
RWP03060-10	20	512	80	49	38	72 x 50.8 x 16.8
RWP03040-10	20	520	40	46	42	70 x 50.8 x 17.3
RWM03060-10	20	520	80	49	55	162.6 x 86.4 x 27
RWM03125-10	20	520	125	51	55	162.6 x 86.4 x 27
RWP03160-2R	20	800	150	51.8	41.8	120 x 65 x 16.7
RWP05020-10	20	1000	20	43	40	70 x 50.8 x 17.3
RWP05040-10	20	1000	40	46	38	70 x 50.8 x 17.3
RFW2500H10-28	20	2500	4	36	17	38 x 50.8 x 12.5
RWM03125-20	50	520	125	51	55	162.6 x 86.4 x 27
RWS02520-1K	100	600	20	43	46	63 x 38 x 14.4
RWP0106300-55	100	600	300	54.8	55	310 x 50 x 165
RWM05080-10	200	470	100	50	40	160 x 23 x 135
RWS05520-10	420	470	40	46	40	63 x 47 x 14.4
RWP06040-10	450	880	30	45	40	70 x 50.8 x 17.1
RWP06040-60	500	1000	40	46	42	90 x 75 x 25
RWP15040-10	500	2500	50	47	38	72 x 50.8 x 16.8
RWP15040-1H	500	2500	50	47	38	98.8 x 75 x 25
RWP15080-10	700	2500	100	50	53	134 x 105 x 30
RWP17050-10	700	2700	50	47	37	72 x 50.8 x 16.8
RWP15080-20	700	2700	100	50	53	134 x 105 x 30
RWP0809300-55	800	900	300	54.8	55	220 x 27.1 x 180
RWP0810500-55	800	1000	500	57	55	220 x 31.1 x 196
RWP15020-50	1000	2000	20	43	29	70 x 50.8 x 17.1
RWP1027200-53	1000	2500	200	53	50	223 x 131 x 30
RWP20050-10	1000	3000	50	47	38	72 x 50.8 x 16.8
RWP25020-50	2000	3000	25	44	25	70 x 50.8 x 17.1
RUM43020-10	2000	6000	20	43	35	170 x 64 x 21.5
RWP2060050-48	2000	6000	65	48	48	175 x 90 x 23
RWP2060080-50	2000	6000	100	50	50	175 x 90 x 23
RUM43010-10	2500	6000	10	40	29	130 x 64 x 21.5

WIDEBAND AMPLIFIERS ADVANTAGE

- High Efficiency
- Broad Frequency Coverage
- Versatile Amplification
- Signal Stability
- Compact Design

APPLICATIONS

- Milcom
- Jammers
- EW

ABOUT RFHIC

RFHIC is a global leader in providing radio frequency (RF) & microwave (MW) solutions utilizing Gallium Nitride (GaN) for various applications in wireless infrastructure, commercial and military radar, and industrial / scientific / medical (ISM) industries. Our product capabilities range from device to high-power microwave systems all within our One-Stop GaN facility.

RFHIC®

Please visit our website for more information and feel free to contact us for any inquiries.
www.rfhic.com or www.rfhic.com/contact

TABLE 2
MICROWAVE TUBE COMPARISON

Microwave Generator	Power Output	Defense Applications	Efficiency	Complexity	HPM Suitable
Magnetron	Low to high	Airborne and naval radar systems, electronic warfare jamming, ECM/ECCM and electronic support measures (ESM)	Moderate	Low	Yes
Klystron	Moderate to high	High-power ground-based radar systems, electronic warfare jamming and ECM/ECCM	Moderate to high	Moderate	Yes
Traveling wave tube (TWT)	Moderate to high	Radar transmitters, electronic warfare jamming, ECM/ECCM and satellite communication systems	High	High	Yes
Crossed-field amplifier (CFA)	Moderate to high	Airborne and ground-based radar systems, electronic warfare jamming, ECM/ECCM and radar altimeters	High	Moderate	Yes
Backward wave oscillator (BWO)	Moderate to high	Electronic warfare signal generation and simulation, radar systems, ECM/ECCM and threat simulation	Moderate	High	No

goals and strategies may be different, but defense spending is a critical part of the budget for developed and developing countries. Global defense expenditures have risen continuously since 2015 and from 2013 to 2022, expenditures grew by 19 percent, according to SIPRI.[3]

The U.S. has the largest defense budget, by far, so it is not surprising that they are also the biggest consumer of microwave tubes. This is a numbers game with the U.S., given the growth in combat aircraft, warships, missiles and electronic countermeasures (ECM)/electronic counter-countermeasures (ECCM) equipment. We estimate that more than 40 percent of the microwave tubes shipped in the defense industry go to U.S. equipment.

While SSPA solutions, particularly GaN, are making fast inroads into the RF power market, some of the very highest power applications require power levels best served by tube-based amplifiers. Naval applications, with long-range search radars, are a prime example of the need for high-power transmitters. Despite their expense, the number of ships is growing quickly. The Chinese Navy, the largest in the world, currently stands at approximately 350 ships, but they are planning to expand to 400 ships as soon as 2025.[4] Most of these ships will be surface combatants likely employing several different types of radars. The U.S. Navy has announced another major expansion that will see it acquire between 282 and 340 ships over the 2023 to 2052 period.[5]

Despite the threat from solid-state power technology, microwave tubes will continue to occupy a niche and play a vital role in defense applications. Their versatility and innovation potential make them an integral part of the ever-evolving defense industry. As technologies advance and new challenges emerge, microwave tubes are poised to keep contributing significantly to future defense capabilities. ■

References

1. "U.S. Household Growth Over Last Decade was the Lowest Ever Recorded," *Pew Research Center*, October 2021, Web: www.pewresearch.org/short-reads/2021/10/12/u-s-household-growth-over-last-decade-was-the-lowest-ever-recorded/.
2. "Microwave Tubes Market Size, Share, Trend, Forecast, Competitive Analysis, and Growth Opportunity: 2022-2027," *Stratview Research*, February 2023, Web: www.stratviewresearch.com/2981/microwave-tubes-market.html.
3. "Trends in Military Expenditure, 2022" *SIPRI*, April 2023, Web: www.sipri.org/sites/default/files/2023-04/2304_fs_milex_2022.pdf.
4. "Pentagon: Chinese Navy to Expand to 400 Ships by 2025, Growth Focused on Surface Combatants," *USNI* News, November 2022, Web: news.usni.org/2022/11/29/pentagon-chinese-navy-to-expand-to-400-ships-by-2025-growth-focused-on-surface-combatants.
5. "An Analysis of the Navy's Fiscal Year 2023 Shipbuilding Plan," *Congressional Budget Office*, November 2022, Web: www.cbo.gov/publication/58745.

INVITED PAPER

The Post-Quantum/AI Threat: RF Must Adapt to Increasingly Sophisticated Attacks at the Tactical Edge

Michael Redding
Quantropi, Ottawa, Canada

John Dames
Reticulate, Palm Bay, Fla.

The modern battlefield depends on secure wireless for voice, data and increasingly, in the era of autonomous vehicles and drones, streaming video. Soldiers need to quickly access video footage even in low bandwidth environments without it being tracked, intercepted or manipulated by adversaries. Video is key to seeing and identifying threats, opportunities and obstacles, but the only way to get the video from the sensor to the observer is radio. The challenges facing today's RF systems are three-fold: the need to avoid being observed, intercepted or jammed.

The U.S. Air Force dogma that has been in use since the 1950s of Observe, Orient, Decide, Act (OODA) is just as applicable today as it was during the Cold War. If you can get inside your adversary's decision-cycle loop, you can win. Maximum situational awareness hinges on the number of sensors you can access to drive intelligence on the ground and in the sky.

The U.S. has enjoyed the sensor advantage over the last two decades, fighting wars in Iraq and Afghanistan. However, adversaries have quickly advanced their capabilities. As witnessed in Ukraine, Russia's jamming of tactical radio communications over the airwaves has hurt Ukrainian defenses and disrupted tens of thousands of commercial flights[1] because of interference with the GPS navigational systems of planes in European air space.

Adversarial radio signals are overwhelming communication links between drones and troops. This is causing difficulties in locating targets and tricking guided weapons, reports the *New York Times*. In an article,[2] they quote a senior fellow at the Hudson Institute think tank as saying, "Electronic warfare has impacted the fighting in Ukraine as much as weather and terrain."

Operational Constraints at the Tactical Edge

Digital communications-over-RF at the tactical edge faces many constraints today. These range from the need for low power consumption to limited CPU and RAM to constrained and congested bandwidth. Deployed troops rely on radios to communicate their position and coordinate their operations but often face issues of limited battery power and connectivity challenges.

These issues are compounded by cybersecurity threats, especially the looming threat of quantum computing and hybrid quantum plus AI capabilities. Understanding this latest threat requires first understanding the evolution of quantum technologies. In the 1990s, Nobel Prize-winning MIT mathematician Peter Shor de-

Q Microwave
An Amphenol company

Ensuring Quality, Precision, and Reliability: Your Trusted RF Partner

INDUSTRY-LEADERS IN MICROWAVE SUBSYSTEMS & FILTERS FOR OVER 25 YEARS

Looking for high-performance and reliable microwave subsystems and filters for your system?

- Applications for Radar, EW, Sigint, Communications, IFF, and Satcom
- 25 years of expertise in RF filters, converters, switch filter banks, and amplification.
- RF Multifunction Modules in 6U or 3U Package, custom hermetic housings, or SMT configurations.
- Optional VITA standard interfaces and FPGA digital controls using UHART or TCP/IP through RS-422 or RS-485.

ITAR compliant & Cybersecurity compliant

AS 9100D CERTIFIED ISO 9001

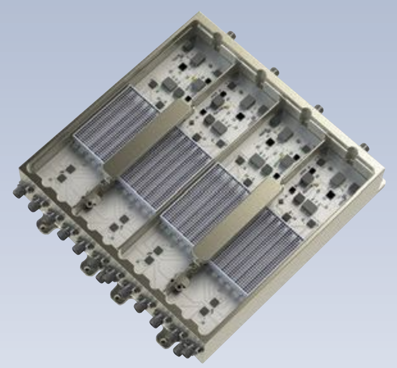

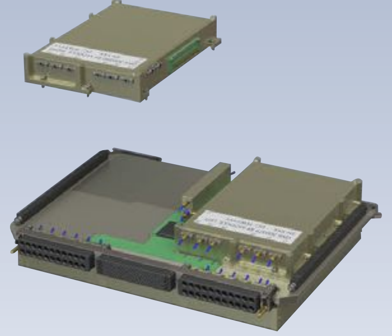

Switch Filter Bank Modules

- Switch filter banks customized for filters centered between 0.5 and 18 GHz, with bandwidth from 1% to 100%. Our modules are packaged in a rugged housing with hemetrical seals and internal potting in order to provide high reliability in difficult environments.

Frequency Converter Modules

- Frequency-agile FR converters, capable of converting FR frequencies between 0.5 & 18 GHz, with 500 MHz of Instantaneous Bandwidth, for an IF Range centered at 1200 MHz (950 to 1450 MHz).

www.qmicrowave.com

veloped what is now called Shor's Algorithm, which showed that a quantum computer could efficiently factor prime numbers well beyond the capability of a classic computer. At the time, his idea was theoretical. However, once realized, Shor's Algorithm gives the world a pathway to break current asymmetric encryption because it is based on the prime factorization of very large numbers. A sufficiently capable quantum computer using Shor's Algorithm would be able to break asymmetric encryption almost instantaneously.

This means that traditional encrypted communication networks and legacy encryption methods like the RSA 2048 and Elliptic-curve cryptography (ECC), considered the gold standard as the U.S. government's recognized encryption methods, are no longer sufficient on their own. Quantum advances are moving much faster than anyone guessed. Leading industry sources, including Gartner Group, Ernst & Young and Cloud Security Alliance, predict that quantum will overtake existing encryption methods this decade.

In the last two years, with the surge in AI and machine learning (ML), quantum experts have pointed out that using ML could lower the amount of quantum computing power needed to break encryption. That is why combining quantum with AI could make breaking current asymmetric encryption a reality much sooner than anticipated. AI runs on classic GPUs, while other calculations are run on a quantum processor. This hybrid combination accelerates the time window when an effective attack on this type of encryption will be possible.

For decades, the quantum threat to encryption was presumed to be primarily related to asymmetric encryption. However, a recent IBM research paper[3] suggests that AI running on a quantum computer could also attack symmetric encryption, such as the Advanced Encryption Standard (AES-256). An accelerated path to break asymmetric encryption means bad actors can intercept and interpret digital communications transmitted over RF while also opening the door to the possibility of injecting deep fakes and flooding the airwaves with noise. Deep fakes already threaten the authenticity of video content as commonly seen on the internet today. Even before a quantum or quantum/AI hybrid attack is successful, battlefield compromises of radio communications using legacy encryption have been reported.[4] A report by the Royal United Services Institute for Defence and Security Studies on Russian tactics in Ukraine found that Russia was able to preemptively warn its units of an artillery strike based on Ukrainian troops calling in a fire mission after decrypting transmissions coming from Motorola radios that featured 256-bit encryption in near real-time. Such attacks are not targeted at the radio signals themselves but at the payloads that the radio waves are carrying. Even microwave transmissions, which frequently are limited to narrow-beam point-to-point connections, are still vulnerable since there can be beam spread. ***Table 1*** shows the challenges that quantum computing poses for classic encryption algorithms.

Why the Quantum/AI Threat Matters to Military RF Users

RF communications, the lifeblood of tactical warfare, is at risk from quantum/AI threats. The U.S. has 500,000 military radios that use current classic, symmetric encryption that would all be vulnerable to this compromise. In addition to handheld applications, radios operate in ground vehicles and on military aircraft.

The quantum/AI threat extends to all

TABLE 1

IMPACTS OF QUANTUM THREATS ON ENCRYPTION ALGORITHMS
(Source: NISTIR 8105)

Cryptographic Algorithm	Type	Purpose	Quantum Impact
AES-256	Symmetric	Encryption	Larger Key Sizes Needed
SHA-256,SHA-3		Hash Functions	Larger Output Needed
RSA	Asymmetric	Signatures, Key Establishment	No Longer Secure
ECDSA, ECDH	Asymmetric	Signatures, Key Exchange	No Longer Secure
DSA	Asymmetric	Signatures, Key Exchange	No Longer Secure

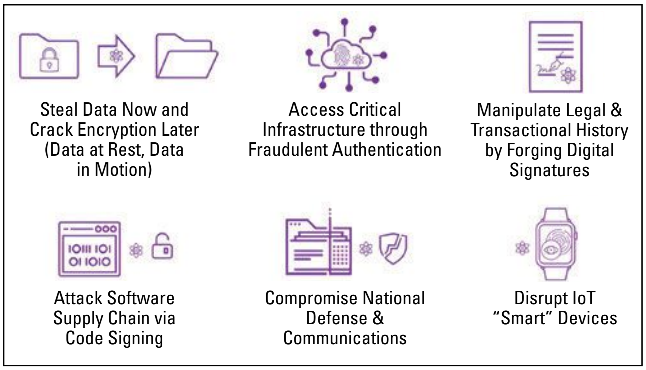

Fig. 1 Potential threats from quantum computing/AI.

devices that touch the public internet, including mobile phones and computers in the Department of Defense. To appreciate the scale of the threat, consider that the global digital economy is estimated at over $30 trillion.[5] Quantum and AI have the potential to disrupt that economy and the trillions of online transactions occurring every day. Some of the potential areas for quantum computing-/AI-based disruption are shown in ***Figure 1***.

Addressing security issues can drain the military's limited resources. However, the overhead costs of protecting against the quantum threat should not hinder the military's ability to conduct surveillance, mission coordination and reconnaissance. Electronic warfare environments demand maximum security while respecting the resource constraints of that environment, both for encryption and for video and radio data transmissions.

Addressing the Threat: New Quantum & Encoding Advances

A common question is, "How do we fight the next battle?" If we build a big fortification, the enemy will drive around it. If we construct a wall, the enemy will fly over it. Just as our allies in Ukraine have learned, technologies must be deployed now that provide immediate benefits and protection for the next emerging threat. The RF sector, along with the cryptography and encoding communities, needs to pivot to address this new threat environment. But the challenge becomes determining the best way to add a layer of protection against a near-term threat that will find its way to the battlefield while still addressing the pressing constraints of operating at the tactical edge.

Fortunately, the cybersecurity community is actively researching and developing new encryption methods to resist quantum computing attacks. The U.S. National Institute of Standards and Technology (NIST) is executing a process to standardize new post-quantum cryptographic algorithms (PQCs).[6] These algorithms are designed to secure data against the capabilities of future quantum computers.

Fighting Quantum with Quantum

The best approach is to fight quantum with quantum. There are new mathematical approaches from companies like Quantropi that continue to advance the science to find solutions that provide security against these new attacks. However, these approaches must also balance the needs of RF communications in the current battlefield environment.

In cryptography, a perfect form of encryption is called a one-time pad, where the secret is as big as the data and it only gets used one time. This scenario is called "perfectly secret." Quantropi's encryption is based on a permutation group that is constructed from quantum gates, which make up a "quantum permutation pad" or the quantum equivalent of a one-time pad, which achieves perfect secrecy. The company then represents this quantum permutation group mathematically. Once this mathematical expression is derived, it can be translated into computer code that will run on a "classic" CPU. This holy grail of encryption can then be used to protect against symmetric attacks and can be further leveraged to strengthen asymmetric algorithms. ***Figure 2*** introduces the concepts of key spaces and shows the big improvement in Shannon entropy that comes from

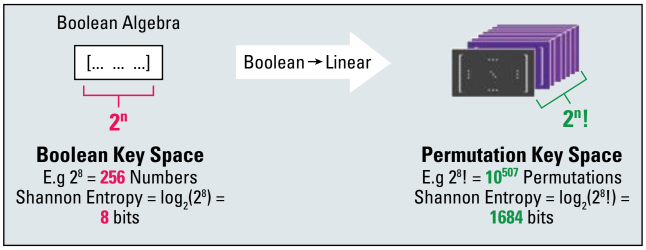

Fig. 2 Permutation groups: key space and Shannon entropy expansion vs. Boolean.

EXODUS ADVANCED COMMUNICATIONS

Powerful Solutions!
Superiority begins with Exodus Ingenuity!

Model Number	Frequency Range	Rated Power Watts	Gain dB
10KHz-250MHz, Low Frequency Amplifiers			
AMP2080B	10kHz-250MHz	100	50
AMP2080C-1	10kHz-250MHz	150	52
AMP2080C	10kHz-250MHz	300	55
AMP2080D	10kHz-250MHz	600	58
80-1000MHz, VHF, UHF Range Amplifiers			
AMP2032	80-1000MHz	300	55
AMP2071-2	80-1000MHz	500	57
AMP2071A-LC	80-1000MHz	750	60
AMP2115-LC	80-1000MHz	1300	61
AMP2121-LC	80-1000MHz	2000	63
700MHz-6.0GHz, Broadband Amplifiers			
AMP2070C	0.7-6.0GHz	100	50
AMP2070A	1.0-6.0GHz	150	52
AMP2030-LC	1.0-6.0GHz	300	55
AMP2030-600-LC	1.0-6.0GHz	600	58
AMP2030D-LC	1.0-6.0GHz	750	59
AMP2030LC-1KW	1.0-6.0GHz	1000	60
2.0-8.0GHz, SC Band Amplifiers			
AMP2085-1	2.0-8.0GHz	120	51
AMP2085C	2.0-8.0GHz	200	53
AMP2085E-1LC	2.0-8.0GHz	250	54
AMP2085E	2.0-8.0GHz	400	56
6.0-18.0GHz, High Frequency Amplifiers			
AMP2118	6.0-18.0GHz	40	46
AMP2111	6.0-18.0GHz	50	47
AMP2033-LC	6.0-18.0GHz	100	50
AMP2065A-LC	6.0-18.0GHz	200	53
AMP2065B-LC	6.0-18.0GHz	300	55
AMP2065E-LC	6.0-18.0GHz	500	57
18-26.5GHz, K-Band, Millimeter Amplifiers			
AMP4032	18.0-26.5GHz	10	40
AMP4065LC-1	18.0-26.5GHz	20	43
AMP4065-LC	18.0-26.5GHz	40	46
AMP4065A-LC	18.0-26.5GHz	100	50
AMP4065B-LC	18.0-26.5GHz	200	53
26.5-40.0GHz, Ka-Band, Millimeter Amplifiers			
AMP4072	26.5-40.0GHz	10	40
AMP4066LC-1	26.5-40.0GHz	20	43
AMP4066-LC	26.5-40.0GHz	40	46
AMP4066A-LC	26.5-40.0GHz	100	50
AMP4066B-LC	26.5-40.0GHz	200	53
18.0-40.0GHz, Millimeter Amplifiers			
AMP2145A-LC	18.0-40.0GHz	10	40
AMP2145B-LC	18.0-40.0GHz	25	44
AMP2145C-LC	18.0-40.0GHz	50	47
40.0-50.0GHz, Q-Band, Millimeter Amplifiers			
AMP4076-1	40.0-50.0GHz	5	37
AMP4076A	40.0-50.0GHz	20	43
AMP4076B	40.0-50.0GHz	40	46
AMP4076C	40.0-50.0GHz	80	49

RF & Microwave Amplifiers

10KHz-75GHz

Amplifiers CW & Pulse

EMC APPLICATIONS

MILITARY APPLICATIONS

COMMERCIAL APPLICATIONS

3674 E. Sunset Road, Suite 100, Las Vegas, Nevada 89120 USA
Tel : 1-702-534-6564 Email : sales@exoduscomm.com

www.exoduscomm.com

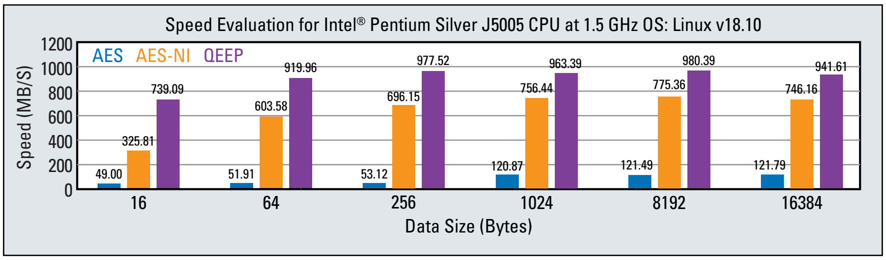

▲ Fig. 3 Data transmission rate comparison.

the permutation group concept just described.

Emerging Success: Post-Quantum-Protected Radios

An example of tactical capabilities receiving a post-quantum boost can be found with the Ukraine-based tactical radio supplier, Himera. Himera and its U.S. distributor, Reticulate Micro, recently unveiled the company's G1 Pro. This is their newest lightweight and low-power radio and it comes integrated with post-quantum symmetric encryption from Quantropi.

These new capabilities represent an impressive leap from the first-generation voice-only radio, already widely deployed in the Ukraine defense forces and proven effective against Russian jamming. The G1 Pro incorporates quantum security to future-proof the radio against the looming quantum/AI threat. It also offers enhanced frequency hopping as an additional defense mechanism. The new radio offers standard AES with a 256-bit cryptographic key and Quantropi QEEP quantum symmetric cryptography with a stronger 1024-bit key. In addition, the quantum algorithm running in the radio uses 80 percent less battery power. It also decreases encryption overhead by 80 percent, leaving more room to maximize data transmission rates. ***Figure 3*** shows the improvement in data transfer rates that the QEEP quantum symmetric cryptography produces versus standard AES-256 and AES-256-NI hardware-accelerated methods.

In cryptography, plaintext refers to unencrypted, readable information input into an encryption algorithm while ciphertext refers to the output of the algorithm that has been encrypted and rendered undecipherable. As mentioned previously, entropy measures the randomness and uncertainty in a set of data. Higher levels of uncertainty and randomness of ciphertext indicate more complete security and the inability for hackers and adversaries to learn anything about the original plaintext. ***Figure 4a*** shows a plaintext signal with a very low entropy value of 5.827504/16 bits, meaning the signal is easily interpreted. ***Figure 4b*** shows that the entropy for the same plaintext signal has increased to 15.999077/16 bits after the application of QEEP encryption, making this an effectively impossible signal for adversaries and other unintended recipients to decode.

Future: Encrypting the Transport Layer

Current advances in this area are focused on data-level quantum protec-

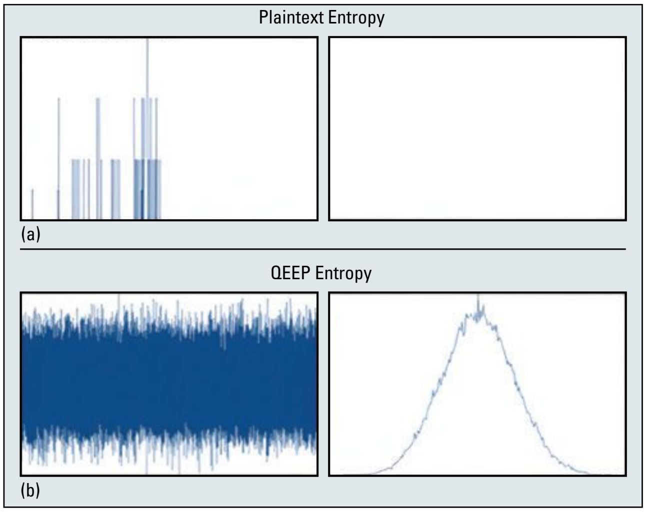

Fig. 4 Plaintext entropy before QEEP encryption (a) and entropy after QEEP encryption (b).

tion on a device-by-device or application-by-application basis. A promising area of emerging research looks at bringing post-quantum protection to the physical transport layer. Focusing on the transmission itself would protect anything that is broadcast. This would make everything inherently secure. McGill University in Montreal, Quebec, is leading this research with industry partners such as Quantropi. The initial focus of this research is on photonic communications and applying quantum permutations to phase and amplitude. Future work will be applied to the radio component of the electromagnetic spectrum.

Conclusion

Quantum and AI threats are coming to today's contested battlespace, which is increasingly reliant on capabilities at the edge. As video and data intelligence become more accessible to warfighters on the ground, we must ensure RF systems are protected, hardened and secure. Effective quantum-based defense can serve as a powerful weapon and prevent encrypted data from being exploitable or valuable to anyone but the intended recipient. ■

REFERENCES

1. "Russia GPS Jamming 'Thousands Of Flights In Europe'," *TalkTV*, April 23, 2024, Web: youtube.com/watch?v=iEWxSo8FnEA.
2. "The Invisible War in Ukraine Being Fought Over Radio Waves," *The New York Times*, November 19, 2023, Web: nytimes.com/2023/11/19/technology/russia-ukraine-electronic-warfare-drone-signals.html.
3. D. R. Campbell, D. W. Diffie and C. Robinson, "Advancements in Quantum Computing and AI May Impact PQC Migration Timelines," *Preprints*, 2024, Web: preprints.org/manuscript/202402.1299/v1.
4. J. Watling and N. Reynolds, "Meatgrinder: Russian Tactics in the Second Year of Its Invasion of Ukraine," *Royal United Services Institute for Defence and Security Studies*, May 19, 2023, Web: static.rusi.org/403-SR-Russian-Tactics-web-final.pdf.
5. UNCTAD, "Digital Economy Report 2024," Web: unctad.org/publication/digital-economy-report-2024#:~:text=New%20data%20from%2043%20countries,digital%20economy%20is%20resource%20intensive.
6. "Post-Quantum Cryptography Standardization," *NIST*, Web: csrc.nist.gov/projects/post-quantum-cryptography/post-quantum-cryptography-standardization.

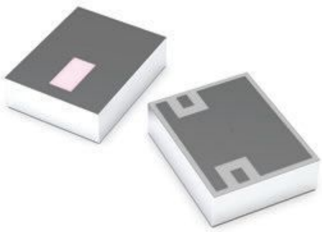

INVITED PAPER

Using Advanced DFM Analysis to Future-Proof PCBs for Defense Applications

Amit Bahl
Sierra Circuits, Sunnyvale, Calif.

Printed circuit boards (PCBs) designed for radar and military communication applications are complex and must adhere to strict IPC standards. They must undergo rigorous testing to ensure their reliability and stable performance under demanding conditions. These boards operate at radio frequencies, so maintaining good signal integrity is crucial. Perfecting high frequency board designs often requires multiple iterations, which are expensive and time-consuming. The best way to tackle this challenge is to identify and resolve potential manufacturing issues through design-for-manufacturing (DFM) analysis. The standard DFM checks include trace and drill spacing, pad size and solder mask clearances. But in RF boards, you must also consider the probability of issues arising from hybrid stack-up, antennas, ground-stitching, differential pairs and controlled impedance.

DFM Analysis Process

During the quote process, PCB designers determine the expected deliverables, testing requirements and comprehensive production documentation that will be sent to the contract manufacturer. Once the required data is received, DFM analysis is conducted at the fab house. After checking the production files for missing data, a tool number is assigned to the project. Next, the CAM team runs design rule checking (DRC) to identify any design errors. They ensure that all the design specifications align with their capabilities. For example, they check if the desired microvia aspect ratio is achievable. CAM engineers will also identify potential DFM issues that DRC may overlook, such as copper or solder sliver formation, as shown in ***Figure 1***.

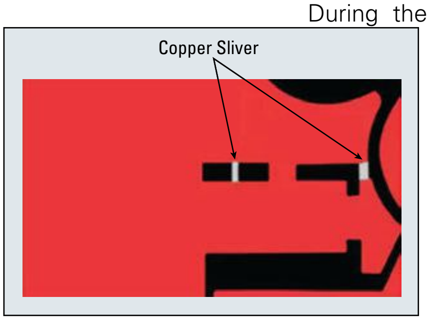

▲ Fig. 1 Copper slivers in a PCB design.

During DFM analysis, the manufacturer will conduct an in-depth board layout analysis, adding or removing features to increase the yield. For instance, a copper thieving pattern is added to an empty space on signal layers to avoid plating or etching issues. Snapshots of all the errors and required modifications are documented in a DFM report and sent to the customer/designer. After the designer's approval, the fab house proceeds with the manufacturing process.

Essential DFM Factors of Radar and Military Communication PCBs

Design Files for Class 3 Boards

Conveying precise design specifications to your PCB manufacturer is crucial for military-grade PCBs. The fabrication drawing should include a board outline with dimensions, stack-up details, a drill chart and fab notes.

Clearly define the following in your fabrication notes:

- IPC Class 3 or MIL-PRF-31032 standard requirements
- Material details with UL ratings, T_g and RoHS compliance
- Manufacturing tolerances
- Presence of via-in-pad and buried or blind vias
- Via plating and filling details (e.g., Type VII fill-

TREXON

Mission Critical Connections

When it comes to solving intricate connectivity challenges, look no further than Trexon. Our cutting-edge connector and cabling solutions are meticulously designed to exceed expectations.

- Built to remain secure and reliable, in the harshest environments.
- Wide range of options to cater to your specific needs.

Discover the Trexon difference today and unlock a world of seamless connectivity solutions!

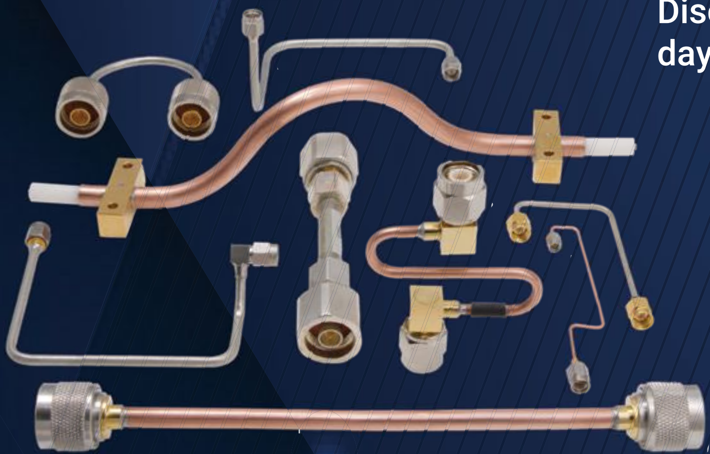

Designed for Durability. Engineered for Excellence.

trexon.com

EZ FORM CABLE | CEPA C.E. Precision Assemblies | IntelliConnect | 603 MANUFACTURING | CICOIL

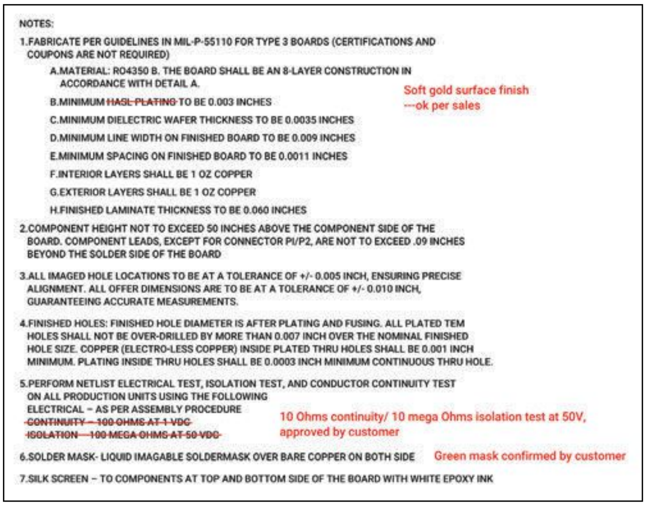

NOTES:

1.FABRICATE PER GUIDELINES IN MIL-P-55110 FOR TYPE 3 BOARDS (CERTIFICATIONS AND COUPONS ARE NOT REQUIRED)

A.MATERIAL: RO4350 B. THE BOARD SHALL BE AN 8-LAYER CONSTRUCTION IN ACCORDANCE WITH DETAIL A.

B.MINIMUM ~~HASL PLATING~~ TO BE 0.003 INCHES — Soft gold surface finish ---ok per sales

C.MINIMUM DIELECTRIC WAFER THICKNESS TO BE 0.0035 INCHES

D.MINIMUM LINE WIDTH ON FINISHED BOARD TO BE 0.009 INCHES

E.MINIMUM SPACING ON FINISHED BOARD TO BE 0.0011 INCHES

F.INTERIOR LAYERS SHALL BE 1 OZ COPPER

G.EXTERIOR LAYERS SHALL BE 1 OZ COPPER

H.FINISHED LAMINATE THICKNESS TO BE 0.060 INCHES

2.COMPONENT HEIGHT NOT TO EXCEED 50 INCHES ABOVE THE COMPONENT SIDE OF THE BOARD. COMPONENT LEADS, EXCEPT FOR CONNECTOR PI/P2, ARE NOT TO EXCEED .09 INCHES BEYOND THE SOLDER SIDE OF THE BOARD

3.ALL IMAGED HOLE LOCATIONS TO BE AT A TOLERANCE OF +/- 0.005 INCH, ENSURING PRECISE ALIGNMENT. ALL OFFER DIMENSIONS ARE TO BE AT A TOLERANCE OF +/- 0.010 INCH, GUARANTEEING ACCURATE MEASUREMENTS.

4.FINISHED HOLES: FINISHED HOLE DIAMETER IS AFTER PLATING AND FUSING. ALL PLATED TEM HOLES SHALL NOT BE OVER-DRILLED BY MORE THAN 0.007 INCH OVER THE NOMINAL FINISHED HOLE SIZE. COPPER (ELECTRO-LESS COPPER) INSIDE PLATED THRU HOLES SHALL BE 0.001 INCH MINIMUM. PLATING INSIDE THRU HOLES SHALL BE 0.0003 INCH MINIMUM CONTINUOUS THRU HOLE.

5.PERFORM NETLIST ELECTRICAL TEST, ISOLATION TEST, AND CONDUCTOR CONTINUITY TEST ON ALL PRODUCTION UNITS USING THE FOLLOWING
ELECTRICAL – AS PER ASSEMBLY PROCEDURE
~~CONTINUITY – 100 OHMS AT 1 VDC~~
~~ISOLATION – 100 MEGA OHMS AT 50 VDC~~
10 Ohms continuity/ 10 mega Ohms isolation test at 50V, approved by customer

6.SOLDER MASK- LIQUID IMAGABLE SOLDERMASK OVER BARE COPPER ON BOTH SIDE — Green mask confirmed by customer

7.SILK SCREEN – TO COMPONENTS AT TOP AND BOTTOM SIDE OF THE BOARD WITH WHITE EPOXY INK

Fig. 2 Sample of corrected fab notes after DFM analysis.

ing as per IPC 4761)
- Controlled impedance with impedance value, trace width, layer number and type of trace (single-ended or differential pair)
- Solder mask color and surface finish
- Types of tests and their standards (e.g., IPC-TM-650).

After downloading the production documentation, ensure that no data is missing and that all the files are in the required format:
- Artwork data: IPC-2581, ODB ++ or Gerber 274X
- Embedded aperture information: IPC-2581, ODB ++ or Gerber 274X
- Netlist in IPC-356 format
- N/C drill and route data: Excellon or Plotter format
- Fabrication drawings: HPGL, AutoCAD, PDF or Postscript
- Pick and place file: CSV, text or ASCII.

Choose a file format compatible with your manufacturer's system. The manufacturer will contact you if any modifications are needed in your design. ***Figure 2*** shows an example of a CAM engineer suggesting changes to the customer's fab notes after performing a DFM analysis.

Dielectric Material For Military-Grade PCB Designs

Military-grade PCBs are expected to provide high-level, uninterrupted performance in extreme environments. Heat-resistant and high-quality materials are always preferred to ensure circuit board reliability. Choose the substrate listed under the qualified parts list (QPL) on the Defense Logistics Agency (DLA) database.[1] These materials are tested and approved to meet specific military standards.

Radar and milcom PCBs usually operate at radio frequencies, so the material experiences substantial insertion losses. PTFE materials like Rogers Duroid and RO4350 B are commonly used as they exhibit low D_k, low loss tangent and consistent electrical characteristics over a wide range of frequencies. IPC-4103 defines standards for copper-clad, laminates and bond ply in high frequency applications.

The following material parameters are checked during the DFM analysis of radar or milcom PCBs:
- The chosen materials are listed under the QPL and meet the design's thermal, mechanical and electrical requirements
- Dielectric constant and loss tangent are within the specified ranges for signal integrity and controlled impedance needs

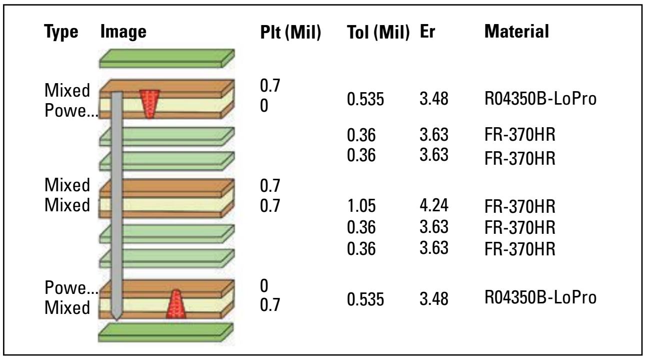

Fig. 3 Example of a hybrid stack-up.

- The thermal conductivity and coefficient of thermal expansion (CTE) are within the required range so that the materials can withstand thermal cycles and soldering processes without degrading
- The materials are compatible with the manufacturing processes, including lamination, drilling, plating and soldering
- The selected materials are readily available in the required quantities
- Whether they are compatible with HDI and fine-pitch components if present in the design.

Note that PTFE materials need different drilling methods, hole treatment (plasma etch) and etching processes due to their fragile and non-stick properties. This will eventually increase the manufacturing cost. Always consult your fab house before choosing the material.

Hybrid Stack-Up

A hybrid stack-up is built using a combination of mixed materials. By combining different substrates in different layer configurations, the circuit's electrical properties can be tailored to specific needs. This customization allows for better signal integrity, impedance control and power distribution performance. It also reduces the production cost as the desired electrical characteristics can be achieved without relying solely on expensive materials.

Consequently, manufacturing a mixed-material stack-up is complex. If the expansion rates of the substrates differ, it causes registration issues and cracks in the stack-up. Adhesion properties vary between materials; hence, choosing a suitable bonding material is necessary to avoid delamination problems. The choice of material also affects the drilling rate, hole treatment and plating process.

Any stack-up error will cause the PCB to fail reliability tests like highly accelerated life test (HALT) and highly accelerated stress screening (HASS), which are usually conducted on military-grade PCBs. Hence, the manufacturer ensures the materials are compatible with matching CTEs and bonded with the appropriate materials during the DFM process. They also check the feasibility of building the stack-up with available equipment and established processes.

Figure 3 shows an example of a hybrid stack-up of Rogers 4350-LoPro and Isola 370HR. The build includes blind and buried vias with an overall board thickness of 0.065 in.

Controlled Impedance Traces and Differential Pairs

When performing DFM analysis for controlled impedance, the following parameters are considered:
- Trace width and spacing conform to the calculated values of the desired impedance
- Trace shapes (microstrip, stripline, coplanar waveguide) match the impedance requirements

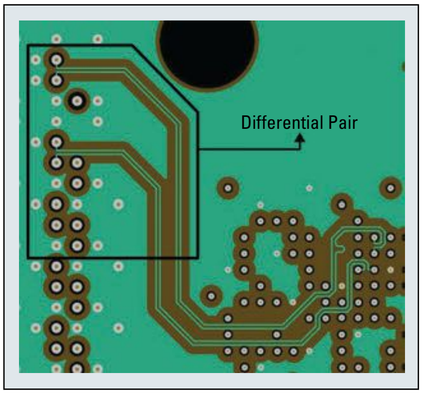

Fig. 4 Differential pairs matched in length.

- Line edges are smooth and free from irregularities
- Meandering is done at the appropriate section of the trace
- A continuous return path (ground plane) is beneath or alongside the traces
- Vias and pads do not disrupt the impedance
- Traces are isolated from noisy components, ground pours and guard traces
- Differential pair traces are length-matched within the specified tolerance to prevent skew
- Trace bends use appropriate radii to minimize impedance discontinuities.

Generally, the fab house modifies the trace width or dielectric spacing to achieve the desired impedance value. Before making the changes, the designer gives consent to the fab house. ***Figure 4*** shows an example of matching the length of a differential pair of transmission lines.

Contouring Traces

In EDA tools, when a trace or pad is contoured, the entire feature will be locked and it can no longer be edited. This option should be used for oddly shaped traces and copper fill in your layout. Having features that are unnecessarily contoured does not create manufacturing issues, but it does hinder the DFM analysis. In addition, the CAM engineers cannot add test points to the contoured pads. To resolve the issue, they must individually add small pads to the test point, which increases the time required to complete the task. ***Figure 5a*** shows a non-contoured trace and ***Figure 5b*** shows the trace after contouring. It should be noted that all the features can be contoured if the design is created using AutoCAD and later converted into Gerber using CAM software.

PCB Antenna

Whether to build it or buy it is a common dilemma every layout engineer faces when considering an RF PCB antenna design. Many factors, such as board quantity, layout, cost and available resources, come into play. Antenna design requires extensive knowledge, advanced design tools and simulation software. Designing an antenna is only feasible for mass production. For low quantity production or prototype volumes, purchasing an antenna may be the best choice. This build or buy decision is crucial as you must tailor your entire PCB design according to the antenna.

If you choose to design, consider the operating frequency, radiation patterns, gain, bandwidth and polarization. After designing, create and simulate a model antenna to verify its performance. Share the simulation results with your PCB manufacturer.

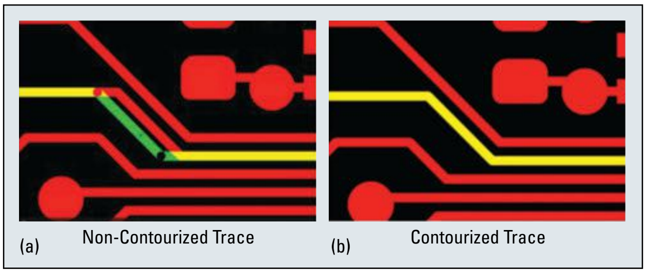

Fig. 5 (a) CAM snapshot of non-contoured trace. (b) CAM snapshot of contoured trace.

TABLE 1

TYPICAL RECOMMENDATIONS FOR A PCB DESIGN

Via parameter	Recommended values
Aspect ratio for microvias	6:1
Aspect ratio for through-holes	10:1
Minimum laser drilled hole size before plating	0.007 in.
Minimum through-hole size before plating	0.010 in.
Minimum conductor width/spacing	0.004 in.
Minimum annular ring on internal layers	0.006 in.
Minimum annular ring on external layers	0.007 in.

If the choice is to purchase, a designer must follow the exact specifications provided by the antenna OEM in the design and communicate these specifications to the PCB fabricator. The designer must also double-check the manufacturer name and the part number in the BOM. Monopole, printed dipole, patch, wire, ceramic and inverted F antennas are commonly used in circuit boards.

Key antenna design aspects checked during DFM analysis include:

- Board material and thickness
- Stack-up arrangement (usually, the region below the antenna should not have any components or conductors)
- Antenna position and orientation
- Clearance from the board edge
- Uniform impedance (matching impedance) between the antenna and the connecting trace
- Isolation from other nets and components.

Via Design

Multiple rules apply to vias and their pads in military-grade PCBs, which are prone to damage in extreme environments. According to IPC standards, burrs and stubs are not allowed in drilled holes. To avoid them, positive etch-back and back drilling procedures are typically used. Copper wrap plating for plated vias is mandatory to improve reliability because this procedure minimizes the possibility of cracks in the via-in-pad during thermal cycling.

If the filled vias are copper-plated, no voids should be exposed in the filling. However, bumps and dimples are allowed. The inner and outer annular rings should be a minimum of 0.001 in. and 0.002 in., respectively. Teardrops need to be added to the pads and the non-functional pads on the internal layers can be removed. This decreases unnecessary spacing issues and increases yield.

Table 1 shows the recommended values for common via parameters for a military-grade design. It should be noted that values can vary among different manufacturers.

All plated through-holes, pads and hole-to-pad ratios are examined in the DFM process to ensure that they comply with the capabilities of the fab house. The minimum drill size and final board thickness are checked to see if they meet the required aspect ratios. The design must allow modifications for tooling requirements. Some PCB suppliers offer PCB design tools to assist designers in building reliable boards. Sierra Circuits, as an example, offers Stack-Up Designer, Impedance Calculator, Material Selector, Better DFM and BOM Checker as free tools for circuit board design.

Ground-Stitching Vias

Although it is not the norm, most RF designs have copper pours on the top and bottom layers stitched with vias to avoid EMI issues. This helps maintain a constant impedance in sensitive traces when they transit through different layers. Additionally, stitching vias can be used to connect a multi-ground plane design across multiple layers. ***Figure 6*** shows an example of this technique with ground-stitched vias across a coplanar circuit trace.

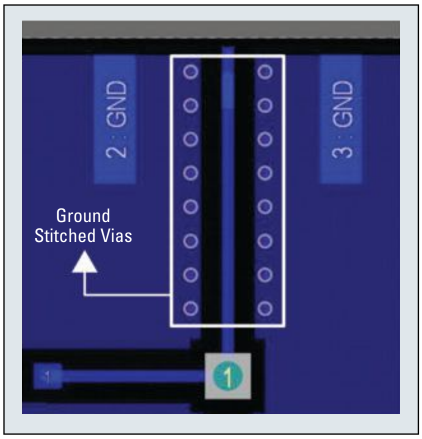

Fig. 6 Ground-stitched vias placed across a coplanar trace.

For military applications, stitched vias can facilitate better heat dissipation, which can help them operate better in harsh environments. However, designing ground-stitched vias presents many challenges. These challenges include:

- The unintentional creation of copper islands on the inner layers of the board. If these are not identified and grounded, they will become floating copper and cause EMI issues.
- Insufficient spacing between the vias can lead to crosstalk and signal degradation. Maintaining a spacing of λ/10 for high frequency designs is recommended, where λ represents the signal's operational wavelength.
- Holes too close to the board's edge can get easily fractured, so keep a minimum clearance of 0.008 in. between the hole and the board's edge.
- Less drill-to-copper clearance will

TABLE 2

RECOMMENDATIONS FOR A TYPICAL PCB DESIGN

Parameter	Recommended values (in.)
Minimum solder mask web clearance	Green/red color: 0.004 Other colors: 0.005
Minimum coverage	Standard board: 0.002 Advanced board: 0.001
Minimum clearance from surface features	Standard board: 0.0015 Advanced board: 0.001
Maximum via pad diameter to tent	0.012
Minimum clearance between solder mask and silkscreen features	0.0045

cause signal integrity issues. Maintain a minimum drill-to-copper clearance of 0.008 in. for 8+ layer PCBs and 0.007 in. for 4-6 layer boards.

- Unplanned via placement can create hotspots instead of dissipating heat. So, place the vias strategically around the heat-generating components and traces.

All these clearances are double-checked during the DFM analysis to avoid issues during the manufacturing stages.

Surface Finish, Solder Mask and Silkscreen

Surface finish protects PCBs from contamination and chemical exposure. Hence, the IPC standard clearly defines the thickness, uniformity, coverage and solderability criteria for surface finish. The choice of surface finish and its thickness should be mentioned in the fab notes.

Recommended surface finishes for military-grade PCBs are:

- Electroless nickel immersion gold (ENIG)
- Soft gold
- Electroless palladium immersion gold (EPIG)
- Immersion silver.

IPC-6012 defines standards for solder resists:

- Copper features where a solder mask is required should not be exposed
- Edge board connectors, golden fingers and surface-mount lands should be free of solder masks
- Solder mask adhesion should be 100 percent for bare copper and laminates
- No voids are allowed if a solder mask is used to tent vias.

Recommended values for solder mask coverage and clearance parameters are shown in ***Table 2***. Note that these values can vary among different manufacturers.

The silkscreen should be legible to facilitate the assembly process, repair and rework. The recommended minimum text height is 0.025 in. and the minimum line width is 0.004 in. The text must not overlap on adjacent pads or it might create solderability issues. A minimum 0.005 in. clearance should be provided between the silkscreen and other copper features.

Conclusion

PCBs for radar and milcom applications demand adherence to stringent IPC standards and meticulous attention to detail. The article has presented a number of factors, along with guidelines and recommended values for important considerations in the DFM process. By considering these factors and recommendations in a PCB design and closely collaborating with the fabricator, the number of iterations needed to achieve reliability and stable performance can be reduced and the process can be optimized. ■

REFERENCES

1. Qualified Products Database or Qualified Products List, *Defense Logistics Agency*, Web: https://www.dla.mil/Working-With-DLA/Applications/Details/Article/2923127/qpdqpl-qualified-products-database-or-qualified-products-list/.

INVITED PAPER

Calming Clock Jitter in Data Converter Noise

Russell J. Hoppenstein
Texas Instruments, Dallas, Texas

The signal-to-noise ratio (SNR) is the primary noise characterization parameter for analog-to-digital converters (ADCs). The three main contributors to SNR performance are quantization noise, thermal noise and clock jitter. While most of these parameters are inherent to the device, the clock jitter performance contribution from an external clock can be controlled by the user. This article will provide calculations to predict overall SNR performance from measured clock phase noise sweeps and show practical techniques to achieve the best performance when operating with high frequency clocks for RF sampling converters.

Introduction

High-end communication and radar systems require a clock source with very low phase noise for data converters. SNR specification characterizes the noise performance of an ADC. A higher SNR translates to a device with a better opportunity to detect a small signal in the presence of noise. A good clock is vital to getting the best performance from the data converter.

Noise Contributions

ADC noise comes from three core elements: quantization noise, thermal noise and clock jitter. Each element contributes to the overall SNR performance, as shown in ***Equation 1***:

$$SNR_T = -10 \times \log \left[10^{\left(\frac{-SNR_Q}{10}\right)} + 10^{\left(\frac{-SNR_N}{10}\right)} + +10^{\left(\frac{-SNR_j}{10}\right)}\right] \quad (1)$$

Where:
SNR_T = Total SNR
SNR_Q = Quantization SNR
SNR_N = Thermal noise SNR from the number of bits (N)
SNR_j = Jitter SNR

Quantization Noise

The ADC resolution (number of bits) determines the quantization noise. ***Equation 2*** shows the standard SNR calculation for quantization noise based on the number of bits, N:

$$SNR_Q = 6.02 \times N + 1.72 \quad (2)$$

Where:
SNR_Q = Quantization SNR
N = Number of bits

High-end radar systems or communication systems use high speed data converters sampling at over 1 GSPS. These converters are typically 12 or 14 bits. Per the standard equation, the quantization noise of a 14-bit converter is about 86 dB, which is usually two orders of magnitude better than the remaining factors in practical devices. As such, you can ignore the quantization noise contribution.

Thermal Noise

ADCs have an underlying thermal noise component, but the device's datasheet does not explicitly specify that parameter. Instead, it is best to use the published SNR performance data at very low input frequencies, 10 MHz, for example, to gauge the thermal noise contribution. At very low input frequencies, the clock jitter component has minimal impact, so thermal noise is the dominant factor. Noise output is proportional to signal output amplitude, and the convention is to measure from 1 to 3 dB below the full-scale output.

Clock Phase Noise

The SNR contribution from the clock, expressed by ***Equation 3***, depends on the clock jitter and input frequency but not the clocking frequency:

$$SNRj = -20 \times \log(2\pi f_{in} \tau_j) \qquad (3)$$

Where:
SNR_j = Jitter SNR
f_{in} = Input frequency
τ_j = Clock jitter

It is a bit counterintuitive to realize that it does not matter how fast a device is clocked. When thinking about high-sampling speed converters, what matters most is the speed or frequency of the input signal. ***Figure 1*** illustrates this concept. For a given amount of clock jitter, the variation in the crossover points where an actual sample is taken creates more error from ideal on a faster-moving, higher frequency signal than a slower, lower frequency signal. There is an indirect relationship to sampling speed because designers typically use high-sampling converters to pass high bandwidth, high frequency signals. As such, clock jitter performance is an important performance metric.

Slew Rate Impact on Jitter Performance

Ideally, the clock signal would be a perfect square wave, as depicted in textbooks. A perfect square wave represents an infinite slew rate of a clock transition from low to high. This is not possible with real-world clock signals because of bandwidth limitations. High frequency clocks are generally pure sine waves.

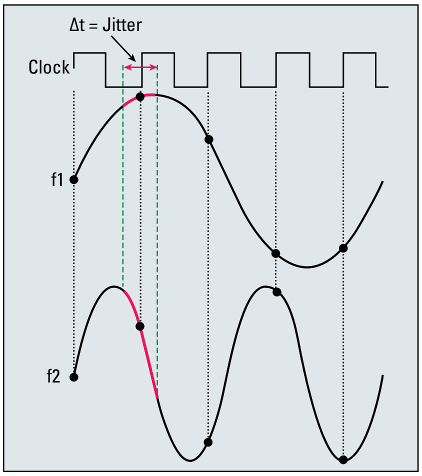

▲ Fig. 1 SNR impact related to input frequency.

Assume that the ADC samples the signal at the zero-crossing of a clock pulse. Traditional timing jitter is the random variation of a clock with respect to time. This means that zero-crossings occur at a slightly different offset location from the ideal location. Thermal noise on the clock produces an equivalent effect because it generates random fluctuations in the amplitude of the signal. As the clock signal approaches the zero-crossing, a sufficiently high amplitude fluctuation causes the sample to trigger slightly prematurely.

A low-amplitude sinusoid clock approaches the zero-crossing at a relatively shallow angle, representing a low slew rate and is more susceptible to thermal noise impacting jitter. By increasing the amplitude of the clock, the transition becomes steeper. Accordingly, an equivalent thermal noise fluctuation on the higher slew rate clock translates to a lower timing error. This is shown in ***Figure 2***, where the signal with the higher slew rate undergoes a smaller timing error versus a lower slew rate signal in the presence of the same thermal noise fluctuation (Δn). The takeaway is to drive the clock inputs to the ADC hard, on the order of 10 to 15 dBm, to keep the slew rate as sharp as possible.

Measuring Clock Jitter

The clock jitter comprises two components: aperture jitter and sample clock jitter. Aperture jitter is the contribution from the ADC device itself within its clock distribution circuitry. This parameter is extracted directly from the device's datasheet. Sample clock jitter comes from the external clock source. The total clock jitter is the root mean square sum of each component, as expressed by ***Equation 4***:

$$\tau_j = \sqrt{\tau_a^2 + \tau_{Clk}^2} \qquad (4)$$

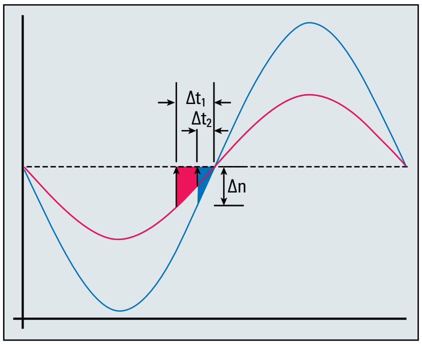

▲ Fig. 2 Benefits of a high slew rate clock.

Where:
τ_j = Total clock jitter
τ_a = Aperture jitter
τ_{Clk} = Sample clock jitter

Sample clock jitter is not a parameter that is readily provided. It is calculated from the clock source's phase noise performance. ***Equation 5*** expresses the clock noise by integrating the phase noise performance (L(f)) over the desired frequency limits:

$$N_{Clk} = \int_{f1}^{f2} 10^{\left(\frac{L(f)}{10}\right)} df \qquad (5)$$

Where:
N_{Clk} = Clock noise
L(f) = Phase noise (dBc)

The integration limits for Equation 5 depend on the application. The start frequency, f_1, should be the location where the information is important. If using the information to estimate the error vector magnitude (EVM) of a communication signal, the best choice would be to start integrating on the lowest subcarrier frequency, which is usually a few kilohertz. For adjacent channel power ratio measurement calculations, the best choice might be to start near the frequency edge of the signal, which may be several megahertz. The final frequency, f_2, should be set to the maximum signal bandwidth or the maximum measured frequency offset if the instrument limits are below the maximum signal bandwidth.

Equation 6 shows the jitter calculated from the clock noise at a specific frequency of operation:

$$\tau_{Clk} = \frac{\sqrt{2 \times N_{Clk}}}{2^{\pi f}{}_{Clk}} \qquad (6)$$

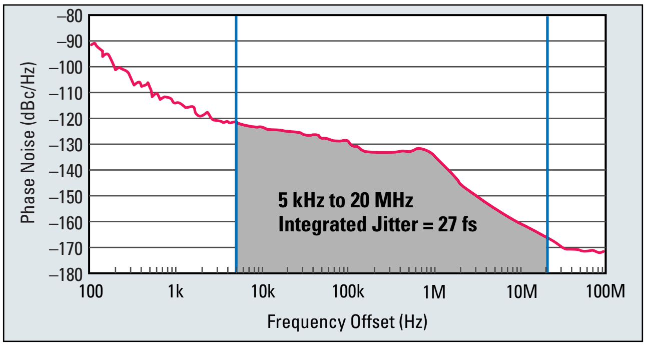

Fig. 3 Clock phase noise and jitter measurement.

Where:
τ_{Clk} = Clock jitter
N_{Clk} = Clock noise
f_{Clk} = Clock frequency

The factor of 2 in Equation 6 accounts for converting the single-sideband (SSB) phase noise analyzer measurement to a full double-sideband (DSB) parameter. Theoretically, the clock jitter should remain constant. When doubling the frequency, the phase noise should ideally become 6 dB worse, indicating that it doubles as well. In practice, other contributions come into play as the frequency is modified, so an actual measurement is prudent for the best accuracy.

Example Calculations

As an example, the following analysis measures clock phase noise performance and estimates the corresponding ADC SNR performance. The ADC device is a Texas Instruments ADC32RF45 operating in decimate-by-4 mode with an external clock at 2457.6 MHz. The input frequency is 1.75 GHz, operating at -3 dBFS. Assume that the SNR from thermal noise is 65 dBFS, derived from the low frequency performance of the ADC in the datasheet.

Figure 3 shows the phase noise measurement of the clock source. The phase noise integration lower limit is set to 5 kHz, which is roughly the smallest bin size in the ADC capture fast Fourier transform (FFT) plot. The high end of integration is set at 20 MHz, which is near the maximum of the instrument. Within the limits of integration, the clock jitter is 27 fs. From the ADC device data sheet, the aperture jitter is 70 fs. The composite clock jitter from Equation 4 is about 75 fs. Note that the external clock jitter is quite good and contributes only a slight increase over the device's aperture jitter in this case.

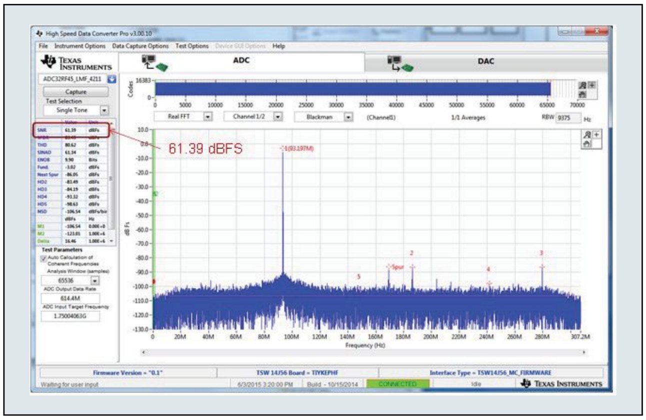

Fig. 4 ADC32RF45 FFT capture and SNR measurement.

The SNR from the composite clock jitter is about 61.7 dBc at the desired input frequency. The next step is to adjust the value for the given carrier level to get a clock SNR of 64.7 dBFS. Next, combine the SNR from the clock with the SNR attributed to thermal performance from Equation 1 to get a composite SNR performance of 61.8 dBFS. ***Figure 4*** shows the actual FFT measurement under this condition, where the reported SNR performance is 61.4 dBFS. The calculations match the measured results within a few tenths.

Conclusion

Most of the parameters affecting a data converter's SNR performance are set for a given device, but a user can influence the choice of the data converter clock. Maintaining the best clock phase noise performance leads to the best performance from the device. The jitter calculations assist in cascading clock performance to an overall data converter SNR performance to ensure that system specifications are met. ■

Capturing and Identifying RF Threats

Anritsu
Morgan Hill, Calif.

The RF spectrum is becoming increasingly crowded as more technologies use radio signals for sensing, control and communications. Commercial communications systems, including public cellular, first responder radios, digital mobile radio and Bluetooth/wireless LAN, crowd the spectrum below 6 GHz. These technologies compete for spectrum allocation with satellite communication in the 1 to 4 GHz bands and air traffic control and commercial weather radar operating just below 3 GHz.

Fig. 1 Remote spectrum monitors.

Deploying military communications in the field requires knowledge of background RF activity to ensure smooth and reliable communications. The very high frequency and ultra-high frequency bands are fundamental frequencies for military communications, but these individual radios are commonly networked using mobile ground-based satellite terminals. When deploying resources into new or threatening environments, the local RF environment is commonly analyzed. Networked mobile spectrum analyzers provide the building blocks for this activity. The survey typically includes monitoring RF background activity and gaining insight into the origin of unknown signals.

LOCAL AREA SPECTRUM MONITORING

Monitoring the background RF environment requires spectrum monitors located at strategic positions around the site of interest. The analyzers continuously sweep frequency bands of interest and spectrum traces are logged and recorded over an extended time. Anritsu MS27101A Remote Spectrum Monitors are ideal for this application, with a frequency range of up to 6 GHz. Formats include standard half-rack

Fig. 2 Multiple-source signals in Vision software.

chassis, IP67 outdoor chassis or 24 RF port rack-mount chassis for multiple antennas. ***Figure 1*** shows a representative equipment location for a secure compound.

Anritsu's Vision Software controls the remote spectrum monitors, schedules spectrum captures and archives the spectrum traces into a database. Vision is PC-based, using an Ethernet connection to communicate with spectrum monitors. Vision software on one PC can control multiple monitors. Monitoring a large compound requires many networked monitors that archive a spectrum trace at a scheduled time interval. The number of traces in the database can quickly become too large to analyze manually. Tools within the Vision software enable filtering by signal level or the sudden appearance of a new signal. ***Figure 2*** shows a representative multiple-source spectrum display.

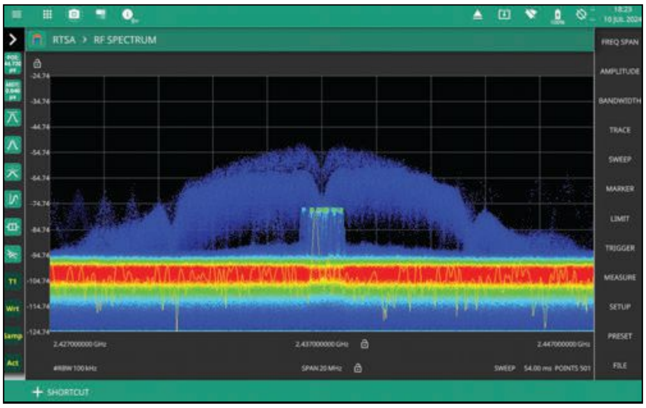

Fig. 3 Pulsed signal hidden in an ISM-band Wi-Fi carrier.

When signals of interest, such as potential interfering or nefarious signals, are identified in background testing, their source is located and purpose identified. Nefarious signals are often transmitted at the same frequency as desired transmissions but at lower power levels using spread spectrum modulation to hide their presence. These signals are difficult to find and the best detection tool is a real-time spectrum analyzer (RTSA). An RTSA displays RF power spectral density and highlights the presence of an RF transmitter, even if there is a larger signal at the same frequency. These hidden signals are not visible on a traditional swept frequency spectrum analyzer

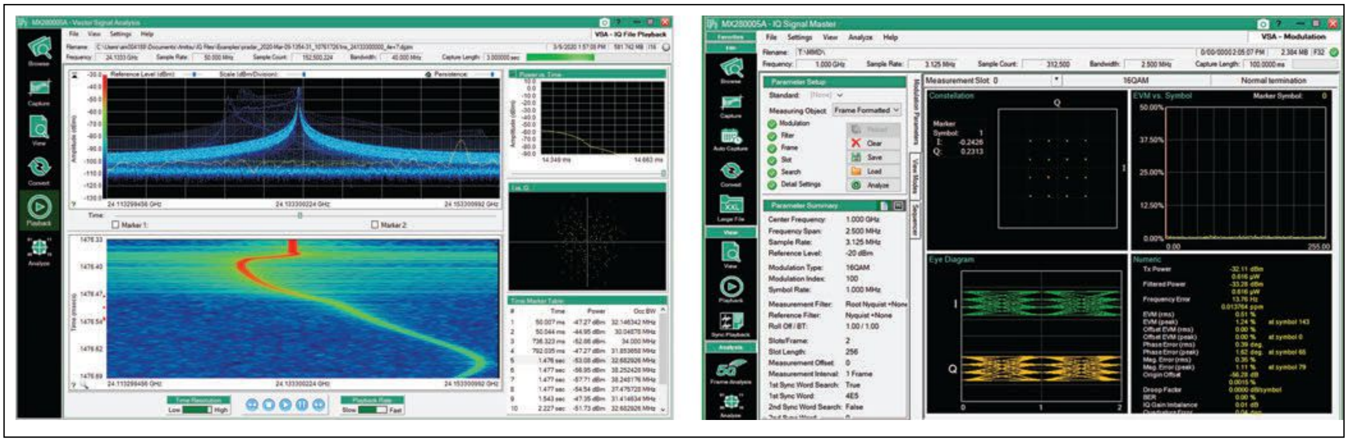

Fig 4. I/Q Signal Master showing the frequency signature of a transmitter power-up and 16QAM signal data.

that detects the peak or average power at each frequency point. Anritsu's MS27201A remote spectrum monitors and Field Master spectrum analyzers all offer an RTSA option with frequency ranges up to 54 GHz and analysis bandwidths up to 110 MHz. ***Figure 3*** shows an example of this hidden signal.

SIGNAL IDENTIFICATION

Once a signal of interest has been spotted, further insight must be gained into its characteristics. The best technique for analyzing signals of unknown origin is an I/Q signal capture coupled with post-processing using MATLAB or Anritsu's MX280005A I/Q Signal Master (see ***Figure 4***). Selecting a capture bandwidth matching the signal of interest's bandwidth can keep the I/Q data file size manageable. Sixteen bits of resolution is typically sufficient for signal processing.

I/Q files can be captured as single, time-limited events that are saved to the internal instrument memory or as a continuous data stream to an external USB 3.0 SSD drive or a PC with a PCIe interface (required to capture and manage the data flow). Replaying the I/Q data using MATLAB or Signal Master provides insight into the signal characteristics. For pulsed or TDD signals, the RF turn-on and frequency lock time are displayed. These parameters give a unique signature for each transmitter technology. By comparing these characteristics with a library of known threats and signals, the signal origin often becomes clear.

DATA SECURITY

In all the use cases described, sensitive information is distributed over a network, typically Ethernet. Hostile agencies can easily detect an unsecured Ethernet network, collecting control commands between the PC and the spectrum monitor and copying traces and files. This provides those agencies with knowledge of the RF activity on a site, hostile and legitimate.

Anritsu remote spectrum monitors provide a secure communications option to prevent access to sensitive frequency, spectrum and I/Q data. When connecting the remote spectrum monitor to a network, Option 17 creates a secure tunnel and closes unused communication ports to all traffic. As an additional layer of security, the ports can be password-protected, preventing simple connection by searching for active IP addresses.

Remote spectrum monitors are the ideal instrument for monitoring and safeguarding RF activity at sensitive locations. In addition to monitoring basic spectrum and creating RF background activity databases, an RTSA can detect hidden signals and I/Q data capture enables detailed insight into signals of interest. Data integrity and security are expectations of monitoring networks and the Anritsu Remote Spectrum Monitors offer secure encrypted communications to meet these needs.

Anritsu
Morgan Hill, Calif.
anritsu.com/en-us/


INSULATED WIRE
INCORPORATED
When system engineers call for ultra-reliable, high performance military grade cables & connectors, the obvious choice is...
Today's advanced military platforms depend on the quality, selection, support and service that are the hallmarks of IW's product lines. We offer a range of jacket materials, armoring, and a wide variety of connectors including SMA, TNC, N, SC, 2.4 mm, and 7 mm to provide highly reliable, application specific solutions.
we're exhibiting with IMCA at the SAHA show and SACA Europe at MSPO
SAHA EXPO
SEE US AT
SAHA EXPO 2024!
October 22-26
İstanbul, TÜRKİYE
SEE US AT
MSPO 2024
September 3-6
Kielce Poland
MSPO
CALL US TODAY
with your project specs and we'll show you the most reliable way to get connected in the industry.
AS9100 Rev. D & ISO9001:2015 certified.
SCAN THIS CODE
TO FIND OUT HOW YOU CAN GET CONNECTED
We're how the microwave industry gets connected!
www.insulatedwire.com
t + 1 631 4724070
e nysales@insulatedwire.com

D38999 Connectors and Cable Assemblies in Military Applications

ConductRF
Methuen, Mass.

Named for MIL-DTL D38999N, the applicable military standard, the "D38-Triple-9" cable assemblies have played an important role in various military applications, from communication systems to radar and electronic warfare equipment since World War II. These robust and versatile RF and microwave single-action interconnects are critically important for engaging and disengaging multiple lines of communication in the field of battle. Long used as rugged, high performance connectors in military and aerospace applications, D38999 connectors and cable assemblies are resurging as dependable favorites in high frequency multi-port/multi-signal applications. The D38999 design capably meets the demanding requirements of high frequency performance, multi-signal management, flexibility and durability in tough land and sea environments.

High Frequency Performance

Military operations often rely on high frequency communication and data transfer capabilities, especially in emerging warfare scenarios. D38999 cable assemblies are designed to deliver exceptional performance up to Ka-Band. The D38999's ability to handle high frequencies with minimal signal loss ensures reliable and secure communication channels for military personnel in the field. ***Figure 1*** shows individually terminated cables in (a) and examples of populated D38999 shells in (b).

Table 1 shows applications for D38999 connectors and cable assemblies.

Benefits

Multi-Signal Management

Military settings commonly require simultaneous transmission of multiple signals and signal types. D38999 cable assemblies excel in managing these complex signal configurations, whether it involves combining data, voice and video streams or integrating various sensor inputs into a centralized system. Their advanced design and shielding capabilities prevent signal interference while maintaining signal integrity and accuracy even in highly dynamic operational environments.

Application Flexibility

D38999 assemblies can be customized to accommodate specific multi-signal interconnection requirements. These requirements may address connector and cable styles, along with distance specifications, to ensure seamless integration with existing military equipment and infrastructure. Their flexibility extends to harsh environmental conditions, with options for ruggedized and water-resistant designs that withstand extreme temperature, vibration and mechanical stress.

Challenges

For the untrained specifier/purchaser, ordering D38999 cable assemblies can be tricky. Housings are offered in nine different shell sizes and each size has many insert arrangements. Users can fully or partially load them with coax, twinax, quadrax, signal, power, fiber and more. These technologies can be mixed within a single interface or keyed to the same interface in four different ways. This level of customization requires a trusted and experienced supplier to assist and ensure best practices in the ordering/production stages of assembly. Additionally, material and plating choices offer more options that can be tailored to various mechanical and environmental needs.

D38999 coax solutions come in standard contact sizes: #8 (largest), #12 and #16 (smallest). The standard back shell solutions are more diverse than the insert arrangements and shell options. These options include straight, angled, clamp, crimp and strain relief styles. There are also several material and plating options to consider.

Ordering D38999 Connectors and Cable Assemblies

A D38999 connector and cable assembly integrates, bundles or harnesses multiple signals to allow single-action connections and disconnections in the field. If the required assembly mates to a predetermined configuration, much of the specification is defined. In these cases, electrical parameters on the mating side of the solution and factors

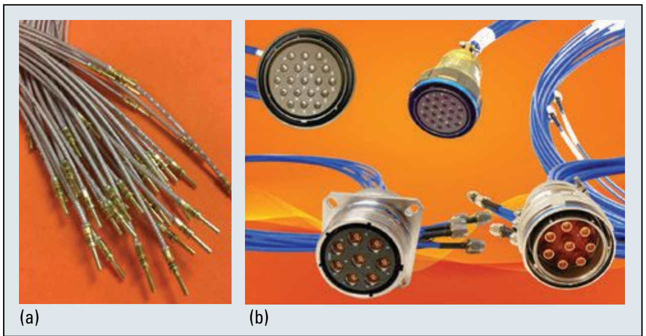

(a) (b)

▲ Fig. 1 ConductRF terminated cables (a) and ConductRF D38999 shells (b).

TABLE 1

COMMON D38999 APPLICATIONS

Band (GHz)	Applications
L- (1 to 2)	Satcom Systems Remote Sensing and Surveillance
S- (2 to 4)	Radar Systems EW Equipment
X- (8 to 12)	High-Resolution Imaging Systems Precision-Guided Munitions (PGMs)
Ku- (12 to 18)	Broadcasting and Multimedia Communication Remote Sensing and Earth Observation
K- (18 to 27)	Secure Communication Networks mmWave Sensors
Ka- (26.5 to 40)	High Speed Data Links Next-Generation Radar Systems

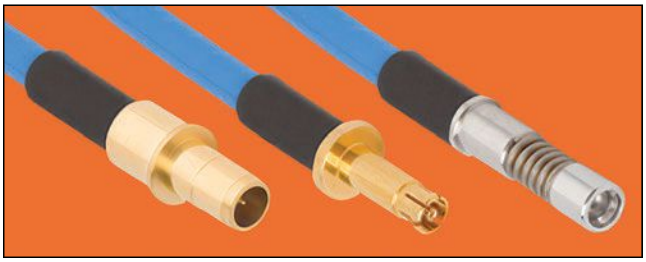

Fig. 2: Standard D38999 contacts.

like loss and power handling capability of the cable and assembly still need to be defined.

If the entire solution needs to be specified, the designer must consider the performance of each signal in the combined interconnect uniquely. This is important because each strand of cable that gets terminated in the final integration carries a signal. Each of these signals is terminated with a D38999 socket or pin contact that is inserted into the shell in a specifically keyed position.

To properly specify the assembly, the following performance requirements are important:

- Operating frequency range
- Insertion loss
- Maximum CW power
- VSWR
- Return loss
- Attenuation
- Impedance (50, 75 or 95 Ohm)
- Shielding requirements.

In addition to these parameters, ConductRF can assist designers with specifying cable type and size and selecting the best cable contact or termination style and size from a variety of options. Additional requirements to consider include phase matching, passive intermodulation (PIM) testing and other RF-related testing of key performance characteristics. It is also important to consider the need for strain relief, further wrapping and/or ruggedization, environmental sealing, thermal management and EMI/RFI protection.

Figure 2 shows examples of standard D38999 RF contacts. In this example, there are two pin-type contacts and one socket-type contact. It is important to note that not every RF cable style can be terminated to all the RF contact styles. This is a common miscue when specifying assemblies. Custom-designed contact solutions are possible but uncovering any potential cable/contact incompatibility early is important.

Conclusion

D38999 connectors and cable assemblies continue to be indispensable in military applications due to their versatility and reliability. Since ordering the connectors and cable assemblies can be complex, this article has highlighted tips to simplify this process for users. With proper education and in collaboration with an experienced RF cable assembly provider, users can specify key electrical, mechanical, environmental and assembly parameters and constraints to configure the appropriate D38999 connector and assembly solution. ConductRF will help users configure the best solutions for each unique challenge. The company also has a range of D38999 RF plug-in assembly solutions that provide field replacements in existing systems or turnkey solutions for users who want to avoid specifying a custom solution.

VENDORVIEW

ConductRF
Methuen, Mass.
www.conductrf.com/
+1 978 374 6840

Flexible X-Band Radar Module Delivers 250 Watts

The Empower 1222 is a high performance X-Band pulsed GaN solid-state power amplifier (SSPA) designed for advanced radar applications. Operating in the 9 to 10 GHz frequency range, this compact module delivers over 250 W peak power, making it ideal for portable radar systems requiring extended range. This fielded and proven module is also used as a building block in Empower's air- and liquid-cooled multi-kilowatt X-Band amplifiers.

Utilizing 48 V GaN-on-SiC technology, the Empower RF1222 offers exceptional efficiency and power density in a lightweight, reliable and rugged package. Its flexible design accommodates pulse widths ranging from 500 ns to 500 µsec with a duty cycle of up to 20 percent, providing versatility for various radar configurations. One of the standout features of the Empower 1222 is its rapid response time, with an enable/disable time of less than 250 ns.

The amplifier offers an RS-485 digital interface for control and monitoring in state-of-the-art implementations. To accommodate legacy implementations, the module also provides an analog interface. This flexibility, combined with its compact form factor, makes the Empower 1222 well-suited for new radar applications where portability and extended range are key requirements.

The 1222 offers comprehensive protection features to ensure optimal performance and reliability. These include safeguards against excessive pulse width or duty cycle, over temperature, power supply overvoltage, reverse polarity and overcurrent conditions. Empower RF has designed this SSPA to meet the demands of contemporary X-Band radar applications, offering a COTS solution that balances high performance with reliability. The Empower 1222 represents a significant advancement in radar technology, enabling longer-range detection and improved system capabilities in a compact package.

Empower RF Systems designs RF and microwave power amplifier solutions for EW, radar, satcom, threat simulation, communications and product testing.

VENDORVIEW

Empower RF Systems
Inglewood, Calif.
www.empowerrf.com

1.85 mm Adapter Supports Frequencies to 34.5 GHz

Fairview Microwave, an Infinite Electronics brand and a leading provider of RF, microwave and mmWave products, now offers a versatile 3.5 mm to 1.85 mm adapter to address a wide range of RF and microwave applications. The SM3980 from Fairview Microwave is part of a large selection of in-stock interconnect RF components. This 3.5 mm to 1.85 mm coaxial adapter features a 50 Ohm impedance and is manufactured to precise RF adapter specifications with a maximum VSWR of 1.25:1. The passivated stainless steel design resists corrosion and holds up to rugged environments, providing years of use.

This female-to-female inline adapter features a 1.85 mm connector on one end and a 3.5 mm connector on the other, which can be used to connect different cable assembly types or to various RF test, measurement and communication devices. These RF adapters can be used in a variety of applications, including military, aerospace, satcom and test and measurement. They are compact and can be used in confined spaces, making them useful for wiring equipment and connecting subassemblies.

The Fairview SM3908 3.5 mm to 1.85 mm adapter is part of over one million RF, microwave and mmWave components that are in stock and available for same-day shipping. Fairview also stocks and/or can custom-build 3.5 mm and 1.85 mm coaxial cables that ship quickly from our U.S.-based facility to address all your RF and microwave application requirements.

VENDORVIEW

Fairview Microwave
an Infinite brand
Lewisville, Texas
fairviewmicrowave.com/

MiCable

0.3~18GHz High Power
Directional & Dual-Directional Coupler

- High power handling **600W CW**
- Excellent coupling, flatness and directivity which will significantly improve the signal acquisition accuracy
- Environment conditions meet MIL-STD-202F
- Low VSWR & insertion loss
- Custom-design & narrow band is available
- Arbitrary customization of 30-40dB nominal coupling

Test Curve of D3008H010180

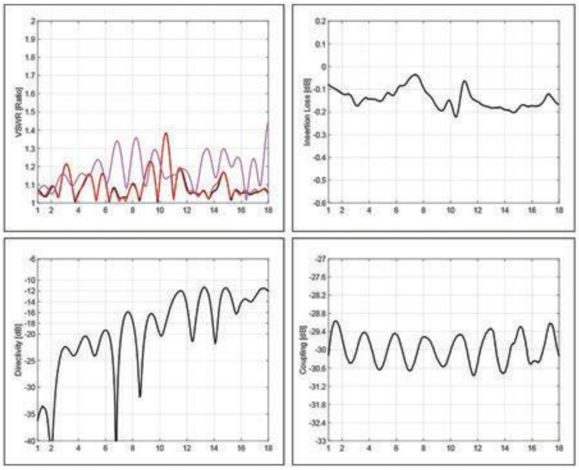

Freq. Range (GHz)	P/N	Coupling Max.(dB)	Main Line VSWR Max.(:1)	Coupling VSWR Max.(:1)	Insertion Loss* Max.(dB)	Flatness Max.(dB)	Directivity Min.(dB)	Power Max.(W)
High Power Directional Coupler								
0.3-6	D3012H003060	30±0.9	1.4	1.4	0.6	±1.2	15	600
	D4012H003060	40±1.0	1.4	1.4	0.6	±1.3	15	600
0.5-6	D3012H005060	30±0.7	1.3	1.3	0.4	±1.0	15	600
	D4012H005060	40±0.8	1.3	1.3	0.4	±1.1	15	600
0.5-18	D3008H005180	30±1.2	1.5	1.6	1.0	±1.2	10	400
	D4008H005180	40±1.2	1.5	1.6	1.0	±1.4	10	400
0.7-8	D3012H007080	30±0.8	1.4	1.4	0.5	±1.0	14	600
	D4012H007080	40±0.8	1.4	1.4	0.5	±1.0	14	600
1-8	D3012H010080	30±0.8	1.4	1.4	0.4	±0.9	14	600
	D4012H010080	40±0.8	1.4	1.4	0.4	±0.9	14	600
1-18	D3008H010180	30±1.2	1.5	1.6	0.6	±1.0	10	400
	D4008H010180	40±1.2	1.5	1.6	0.6	±1.0	10	400
6-18	D3008H060180	30±1.0	1.5	1.6	0.5	±0.7	10	400
	D4008H060180	40±1.0	1.5	1.6	0.5	±0.7	10	400
High Power Dual-Directional Coupler								
0.3-6	D3012HB003060	30±0.9	1.4	1.4	0.7	±1.5	15	600
	D4012HB003060	40±1.0	1.4	1.4	0.7	±1.6	15	600
0.5-6	D3012HB005060	30±0.7	1.3	1.3	0.6	±1.2	15	600
	D4012HB005060	40±0.8	1.3	1.3	0.6	±1.3	15	600
0.5-18	D3008HB005180	30±1.2	1.5	1.6	1.0	±1.5	10	400
	D4008HB005180	40±1.2	1.5	1.6	1.0	±1.7	10	400
0.7-8	D3012HB007080	30±0.8	1.4	1.4	0.6	±1.2	14	600
	D4012HB007080	40±0.8	1.4	1.4	0.6	±1.2	14	600
1-8	D3012HB010080	30±0.8	1.4	1.4	0.6	±1.1	14	600
	D4012HB010080	40±0.8	1.4	1.4	0.6	±1.1	14	600
1-18	D3008HB010180	30±1.2	1.5	1.6	0.8	±1.2	10	400
	D4008HB010180	40±1.0	1.5	1.6	0.6	±1.0	10	400
6-18	D3008HB060180	30±1.0	1.5	1.6	0.5	±0.9	10	400
	D4008HB060180	40±1.0	1.5	1.6	0.5	±0.9	10	400

*Theoretical Insertion loss Included

More Information - Scan the QR Code

MIcable Inc.

www.micable.cn sales@micable.cn +86-591-87382856

Cassegrain Monopulse Antenna Targets Ka-Band Applications

Eravant announces the SAY-3433634310-28-S1-MP, a monopulse Cassegrain antenna. Designed and manufactured for operation indoors or within an environmentally protected radome, the antenna covers a frequency range of 34 to 36 GHz. With a beamwidth of 1.0 degree and a gain of 43 dBi for the sum channel, the antenna provides E-plane and H-plane sidelobe levels of -16 dB. The minimum return loss is 13 dB on all RF ports.

The three waveguide ports provide channels for sum, vertical difference (elevation) and horizontal difference (azimuth) signals. The peak gain for the difference channels is 36 dBi. Minimum isolation between the sum and difference channels is 45 dB. The symmetrical feed structure yields excellent beam uniformity and a null depth of 30 dB for the difference channels.

The feed network includes E-plane and H-plane folded magic tees and machined waveguide sections that enable low signal loss and stable electrical performance. The antenna measures 26 inches in diameter and 14 inches in length. The reflector surface is painted and all waveguide components have a chemical finish for corrosion resistance. The WR-28 waveguide ports are compatible with UG-599/U waveguide flanges. A smaller version of the antenna, model SAY-3433632750-28-U5-MP, has a reflector that measures 4.0 inches in diameter and provides a gain of 27 dBi for the sum channel. The temperature range of both models is -40°C to +85°C.

Eravant, formerly Sage Millimeter Inc., offers a vast selection of mmWave and sub-THz antennas and components, as well as test and measurement accessories and services. Custom components and subsystems are also available with rapid quotes and fast delivery.

VENDORVIEW

Eravant
(formerly Sage Millimeter Inc.)
Torrance, Calif.
www.eravant.com

1 kW Pulse Solid-State Amplifier

Exodus Advanced Communications has developed a high-power solid-state amplifier (SSPA) system for C-Band pulse radar testing applications as well as general radiated susceptibility requirements such as EMI-Lab/RS103 and electronic warfare applications. The AMP4071P-1KW pulse amplifier covers 4.0 to 6.0 GHz, and it satisfies pulse requirements for radar applications with pulse widths up to 100 mS and duty cycles up to 10 percent. The AMP4071P-1KW produces at least 1 KW pulse power across the band with 2 dB maximum peak-to-peak power gain flatness. The system uses a class AB design, achieving less than -20 dBc harmonics at rated output and -60 dBc non-harmonic spurious. This system includes a gating feature with an 80 dB on/off ratio.

This SSPA features extensive control, monitoring circuits and optional calibrated power monitoring. Monitoring can be done via a seven-inch color display or various remote-control interfaces. The local color touchscreen features real-time readings of forward and reflected power levels, load VSWR, system voltages and currents, as well as the operating temperatures of the PA modules, heat sinks and internal system temperature. The incorporated gain control has a range of greater than 20 dB, which is accessible using the local screen or any of the remote interfaces. The AMP4071P-1KW is rack-mountable or may be used on a bench. The HPA has type N-female connectors for the RF input, output and optional RF sampling ports.

Exodus Advanced Communications' product lines use LDMOS, GaN HEMT and GaAs technologies with many devices manufactured internally. In addition to HPAs, Exodus designs low noise amplifiers, modules and multi-band systems for applications ranging from 10 kHz to > 75 GHz.

VENDORVIEW

Exodus Advanced Communications
Las Vegas, Nev.
exoduscomm.com

DC TO 50 GHz

MMIC Amplifiers

300+ Models Designed in House

Options for Every Requirement

CATV (75Ω)

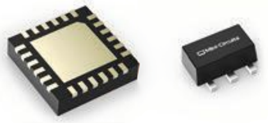

Supporting DOCSIS® 3.1 and 4.0 requirements

Dual Matched

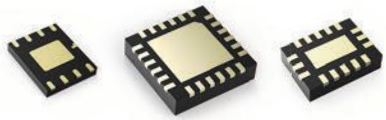

Save space in balanced and push-pull configurations

Hi-Rel

Rugged ceramic package meets MIL requirements for harsh operating conditions

High Linearity

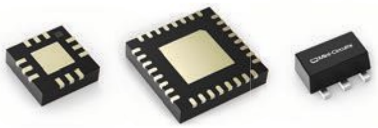

High dynamic range over wide bandwidths up to 45 GHz

Low Noise

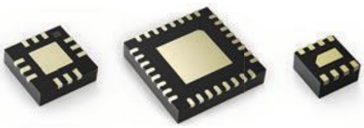

NF as low as 0.38 dB for sensitive receiver applications

Low Additive Phase Noise

As low as -173 dBc/Hz @ 10 kHz offset

RF Transistors

<1 dB NF with footprints as small as 1.18 x 1.42mm

Variable Gain

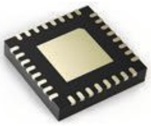

Up to 31.5 dB digital gain control

Wideband Gain Blocks

Flat gain for broadband and multi-band use

Mini-Circuits®

Analog Devices Expands True Time Delay Beamformer Portfolio

VENDORVIEW

The ADAR4000 is a highly integrated, single input, quad output time delay unit, operating from 2 to 18 GHz. Each of the four channels has an adjustable time delay unit (TDU) and digital step attenuator (DSA). The TDU can operate in a 508 ps mode with 4 ps resolution, or a 256 ps mode with 2 ps resolution. Each path also has an adjustable amplifier bias. All this functionality fits in a 6 mm x 6 mm package.

Analog Devices
www.analog.com/en/products/adar4000.html

Thermoelectric Refrigeration Cooling/Heating System

VENDORVIEW

Cernexwave's Thermoelectric Refrigeration Cooling/Heating System is a great solution to bring your components to the optimum temperature for testing. They have a temperature control range of -45°C to +120°C with fast temperature change speed and high accuracy. The large cooling/heating plate dimensions and small overall footprint allow these units to be used for a great range of components in labs of any size.

Cernexwave
www.cernexwave.com

Why CCDF is Better for Measuring P1dB

VENDORVIEW

Discover why Complementary Cumulative Distribution Function (CCDF) curves are the more effective method for measuring P1dB and P3dB in RF power amplifiers. This paper explains how CCDF curves provide a statistical description of power levels in digitally modulated signals, offering advantages over traditional methods, especially for amplifiers with soft compression characteristics. The paper outlines the process for using CCDF curves, provides examples and demonstrates how this approach accurately determines compression points for various amplifier classes.

Empower RF
www.empowerrf.com/amplifier-notes/Measuring-P1dB.php

Eravant's Space and Military Applications are Certified

VENDORVIEW

Eravant's quality management system has been certified by DEKRA to the AS9100D standard, based on and including ISO 9001:2015. Eravant's validation capabilities for space and military applications include thermal-vacuum test chambers and thermal-shock testing. Eravant offers components, subsystems and custom design services from 18 to 330 GHz.

Eravant
www.eravant.com

High Performance Passive Components

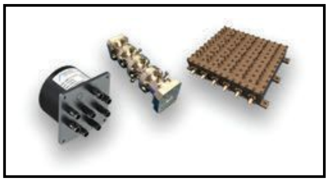

VENDORVIEW

Exceed Microwave provides custom high performance passive microwave component designs up to 110 GHz for defense, space and commercial applications. Exceed Microwave is AS9100 certified and ITAR registered, providing high-quality, high performance passive components. They provide various types of designs, each with its own unique values and are designed and made in the U.S. Many of Exceed's designs offer extremely high Q factor, allowing very low insertion loss and high-power handling.

Exceed Microwave
www.exceedmicrowave.com

Exodus AMP2033-LC, 6–18 GHz, 100 W, Another Outstanding TWT Replacement

VENDORVIEW

Exodus AMP2033-LC is designed for replacing aging TWT technology. A broadband, rugged EMC Class A/AB linear design for all modulations and industry standards. Covers 6.0 to 18.0 GHz, produces > 100 W minimum, with a minimum 50 dB gain. Excellent flatness, optional monitoring parameters for forward/reflected power, VSWR, voltage, current and temperature sensing for superb-reliability. Exodus Quiet-Cool technology in our compact 5U-chassis weighing a nominal 75 lbs.

Exodus Advanced Communications
https://exoduscomm.com

NEW Waveguide Standard Gain Horn Antennas

VENDORVIEW

Fairview Microwave offers a broad portfolio of in-stock standard gain horn (SGH) waveguide antennas with either waveguide or coax connectivity that offer increased precision in wireless test and measurement.

Fairview Microwave
www.fairviewmicrowave.com

Industry's Most Broadband DC Block

The HL8439 DC Block is a ceramic-based product offering that boasts a bandwidth of 16 kHz to greater than 110 GHz, with a voltage rating of 10 V. HYPERLABS has developed a proprietary ceramic-based transmission line topology that enables an entirely new lineup of ultra-broadband products as well as a wide range of other component offerings.

HYPERLABS INC.
www.HYPERLABS.com/product/hl8439/

Stable, Flexible Cables

IW presents low loss, phase stable cables for very high RF power applications! Our established 4806 and 7506-SP cables provide flexible solutions to replace corrugated coax and waveguide for high power systems up to 11 GHz (4806) and 6.5 GHz (7506), including communications, radar, EW and EMC test. Turn key assemblies are available with a wide range of connector options including C, SC, 7/16 DIN, 1 5/8 and 3 1/8 EIA flanges.

Insulated Wire
www.insulatedwire.com

Ultra-Compact High Performance SSPAs with Demonstrated Reliability

Kratos has an extensive portfolio of ultra-compact power amplifiers covering 1 to 50 GHz with power levels ranging from 50 W CW to 2 kW pulsed. We offer SWaP-C solutions and the fastest turn-around times for custom designs and production. Our capabilities extend into integrated microwave assemblies supporting various EW, radar and communications applications meeting unique mission specific electrical and environmental requirements. 2024 product development includes frequency coverage of V- and W-Bands.

Kratos Microwave USA
https://www.kratosdefense.com/about/divisions/microwave-electronics/us

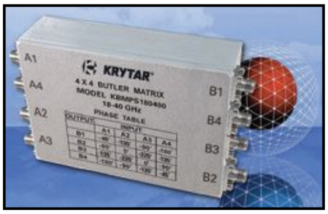

Ultra-Broadband Butler Matrix with Phase Shift

VENDORVIEW

KRYTAR Butler Matrix with Phase Shift family covers multiple microwave bands, from 0.5 to 40 GHz (L- thru Ka-Bands) with wide phase shift coverage, excellent amplitude imbalance, low insertion loss and VSWR and superior electrical performance. They are an ideal choice for antenna array beamforming, radar tracking and direction finding, 5G New Radio (NR), Wi-Fi 6, Wi-Fi 6E, mmWave, MIMO device testing, multipath simulation and performance evaluation. The advantage over other methods of angular beamforming is its simplicity of use.

KRYTAR
https://krytar.com/

Explore How Thermocouple RF Power Sensors Accurately Measure RF Signal Power

VENDORVIEW

LadyBug's thermocouple-based broadband power sensors deliver excellent performance, VSWR, flatness and linearity across a wide frequency range. These passive devices include a DC block and advanced protective circuitry to minimize damage from signal overloads. Encased in a waterproof package, they are ideal for system integration. The innovative architecture allows for low volume production of customized sensors tailored to specific customer requirements.

LadyBug Technologies
www.ladybug-tech.com/downloads/Articles/LadyBug%20Technologies-Thermocouple.pdf

MMPX-00002PSM: Passive MMIC DC-18 GHz Quadplexer

VENDORVIEW

The MMPX-00002PSM is a MMIC surface-mount quadplexer capable of multiplexing DC-6 GHz/8-10 GHz/12-14 GHz/16-18 GHz signals. Passive GaAs MMIC technology facilitates production of smaller filter constructions that replace larger form factor circuit board constructions. Tight fabrication tolerances allow for less unit-to-unit variation than traditional filter technologies, creating highly accurate simulations using the provided SnP files taken from measured production units. The MMPX-00002PSM is available as a 6x6 mm QFN. Available now.

Marki Microwave
www.markimicrowave.com

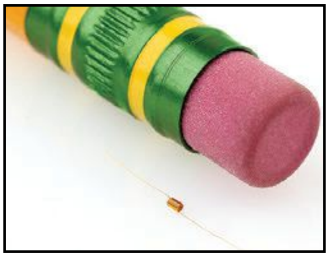

MCI Provides Custom Solutions

Microwave Components, Inc. (MCI) in Dracut, Mass., is a small veteran owned manufacturer of custom miniature air coils for Hi-rel applications. MCI has proudly been providing high Q, miniature coils to the aerospace, defense, and space markets since 1978. MCI will never obsolete a part number for convenience. Let MCI help "uncoil" your miniature inductor requirements.

Microwave Components, Inc.
www.mcicoils.com

MIcable 1-18 GHz 40 dB 400 W High-Power Directional Coupler

VENDORVIEW

MIcable 1 to 18 GHz 40 dB 400 W high power directional coupler has DC pass capability. With a nominal coupling of 40 dB, it can handle 400 W CW power at a wideband frequency and has 40±1.2 dB maximum coupling, 0.6 dB maximum insertion loss, ±1.0 dB coupling flatness, 1.6:1 maximum VSWR and 10 dB minimum directivity. It can be widely used in 5G, testing, instrumentation, power amplifier, transmitter and other fields.

MIcable Inc.
www.micable.cn

20 GHz to 36 GHz and 28 GHz to 40 GHz YIG-Based Notch Filters for EW and ECM

Breakthrough product line of notch filters that cover mmWave frequencies. This family of new yttrium iron garnet based filters provides superior notch depths over the 20 to 40 GHz frequency range. Two models provide tunable notches of 15 MHz minimum at 40 dB down across the 20 to 36 GHz (MLFR-2036) and 28 to 40 GHz (MLFR-2840) bands. Typical passband insertion loss is 3 dB and the passband range is 20 to 42 GHz.

Micro Lambda Wireless
www.microlambdawireless.com

Connecting and Protecting People® in EW, Radar and MilCom Applications

MPG proudly offers a full suite of cutting-edge filters, switches and solutions for a variety of demanding applications, designed to meet the highest standards of precision and reliability. Our latest innovations include Hercules™ switches, stacked filters, high performance miniaturized filters and more. Committed to global excellence, MPG leverages decades of expertise to deliver superior performance and security for defense and commercial sectors. Visit our website today and connect with our experts.

MPG
https://bit.ly/3Wm2wmq

See Norden's VPX Transceiver Specs

Norden's wideband VPX transceiver is used across military applications. It offers 2 to 18 GHz operation in a versatile OpenVPX platform. The NUDC2-18/1.3-2.3 includes internal LOs which provide an instantaneous IF bandwidth of 1 GHz and exceptional noise figure. The NUDC2-18_1.3-2.3 is currently in production. Contact Norden with your specific requirements and discuss custom configurations to meet your specification needs.

Norden Millimeter
https://nordengroup.com/wp-content/uploads/Norden-Transceiver.pdf

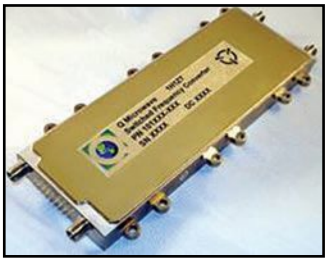

RF Wideband Converter, 0.5 to 18 GHz

Q Microwave's wideband frequency-agile RF converters, capable of converting RF frequencies between 0.5 and 18 GHz, with 500 MHz of instantaneous bandwidth, for an IF range centered at 1200 MHz (950 to 1450 MHz).

Q Microwave
www.qmicrowave.com/rf-subsystems

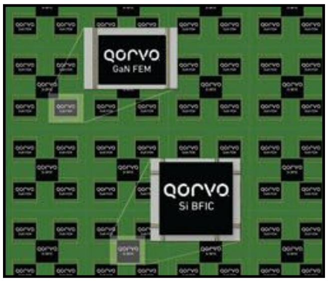

ICs that Power High Performing X-Band Phased Array AESAs

Qorvo provides the most capable components for high performing X-Band radars. Silicon quad core beamforming ICs from the Anokiwave acquisition feature selectable dual Rx beams to support monopulse or dual polarization operation. GaN T/R FEMs with a range of transmit output powers that complement and interface directly with the beamformer ICs. Independent phase/amplitude setting at each element is achieved through direct SPI control. These ICs are widely proven in military and commercial platforms and are available with short lead times.

Qorvo
https://www.qorvo.com

Q-Tech and AXTAL Crystal Oscillators

Q-Tech and AXTAL offer a full line of crystal oscillators designed for use in critical military and defense applications where precise timing, reliability, durability and performance are essential to meet the extreme operating conditions. Oscillators may be screened to MIL-PRF-55310, Level B as required. Combined, Q-Tech and its subsidiary AXTAL offer a full range of military/defense devices including XOs, VCXOs, TCXOs, OCXOs, MCXOs and SAWs.

Q-Tech
www.q-tech.com

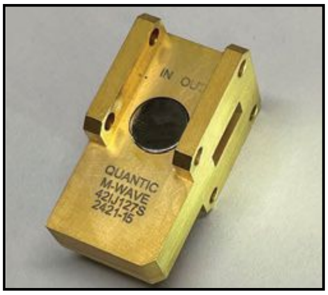

Ultra-Low Insertion Loss Isolators

Quantic M-Wave has 30+ years of passive ferrite product design experience in low loss applications. Our proprietary processes provide extremely high efficiency in our waveguide and coaxial isolator and circulators. The highlighted model #42IJ127S provides 0.08 dB typical insertion loss and a 0.12 dB maximum over the customer specified bandwidth in WR42. M-Wave is now part of the Quantic team, we are even better positioned to support your needs for high performance components. See what our design team can do for you.

Quantic M-Wave
www.mwavedesign.com/

RF and Microwave Filters and Integrated Assemblies

VENDORVIEW

Reactel manufactures a line of filters, multiplexers and multifunction assemblies covering up to 67 GHz. From small, lightweight units suitable for flight or portable systems to high-power units capable of handling up to 25 kW, connectorized or surface-mount — their talented engineers can design a unit specifically for your application.

Reactel, Inc.
www.reactel.com

Wideband Power Amplifier, RWP25020-50

VENDORVIEW

RFHIC's RWP25020-50 is a gallium-nitride on silicon carbide (GaN-on-SiC), S-Band, wideband amplifier suited for broadcasting and communication system applications. Covering from 2000 to 3000 MHz, the RWP25020-50 yields a small signal gain of 25 dB with 44 dBm at P3dB peak. The RWP25020-50 is designed using RFHIC's GaN-on-SiC on silicon carbide high-electron-mobility transistors (HEMT), providing high breakdown voltage, efficiency, and lower thermal dissipation. The device is fully matched for easier system integration.

RFHIC
https://hubs.li/Q02JHJzz0

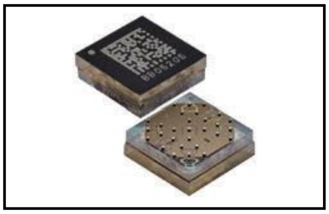

MM5130 26 GHz High-power SP4T RF Ideal Switch

VENDORVIEW

The Menlo Micro MM5130 high-power SP4T micro-mechanical switch provides ultra-low insertion loss and superior linearity as an SP4T from DC to 18 GHz, and greater than 3 billion switching cycles. The MM5130 can also be configured in Super-Port mode that extends the frequency operation to 26 GHz. This Ideal Switch® is an ideal solution for replacing large RF electromechanical relays, as well as RF/microwave solid-state switches in applications where linearity and insertion loss are critical parameters. Available now from RFMW.

RFMW
www.rfmw.com

RFS44 — 100 kHz to 44 GHz 4-Port RF Switch

Switch from LF all the way through the Ka-Band with Signal Hound's new RFS44 antenna switch. This single pole four throw (SP4T) absorptive solid-state switch, featuring silicon-on-insulator (SOI) technology, provides RF switching across four ports at up to 44 GHz. With blazing fast switch speed, 3 ns rise/fall times and direct access from Spike™, the RFS44 enables concise data acquisition when switching across varied frequencies in diverse RF environments.

Signal Hound
www.signalhound.com

Dielectric Materials for Wire-bondable Single-layer Capacitors

The new K4200 dielectric material for wire-bondable single-layer capacitors for high performance microwave circuits has a X7R temperature coefficient and wide operating range from -55°C to 125°C. The new wire-bondable capacitor lineup ranges from capacitances less than 0.1 pF up to 10 nF, footprints from 0.2 x 0.2 mm (8 x 8 mils) to 2 x 2 mm (80 x 80 mils) and thicknesses from 0.1 mm (4 mils) to 0.3 mm (12 mils). Tecdia continues to develop more novel materials with characteristics tailored to meet the needs of cutting-edge RF designs and provide optimal solutions to customers.

Tecdia
https://us.tecdia.com/

8 GHz Sapphire Loaded Cavity Oscillator

Saetta Labs' Sapphire Loaded Cavity Oscillators (SLCO) at X-Band are pure microwave oscillators exhibiting unparalleled low phase noise of -155 dBc/Hz at 10 kHz offset (8 GHz). Melding state of the art materials with meticulous engineering they are a complete sub-system operating free-running or external reference locked. 8 GHz, 10 GHz, 10.24 GHz, 12 GHz + Custom.

Saetta Labs
www.saettalabs.com/products

Solid-State Power Amplifiers (SSPAs)

Stellant Power Systems Technology (PST) (formerly Comtech PST) continues to revolutionize the solid-state RF amplifier industry. Our designs maximize amplifier performance by achieving higher power density, greater efficiency, improved thermal management and reduced size. We closely align ourselves with our RF device partners to be ahead of market trends in the aerospace and defense sectors. We also manufacture custom products for highly specialized medical, satellite and R&D laboratory markets. Our amplifier products operate to 18 GHz with output power levels to multi-kilowatt.

Stellant Systems, Inc.
https://stellantsystems.com/solid-state-power-amplifiers/

Customized Ceramic Solutions

Trans-Tech will provide customized ceramic solutions for your most difficult challenges. Trans-Tech manufacturers dielectric and ferrite materials and components, thermal barrier coating materials, RF bandpass filters, RF circulators and isolators, medical materials, patch antennas, phased array radar elements, radar absorbers and numerous other custom solutions for RF, microwave, thermal and high power, temperature stable and low dielectric loss uses. Your partnership with Trans-Tech will result in collaboratively developed products with unparalleled performance and value.

Trans-Tech
www.trans-techinc.com

Designed for Durability. Engineered for Excellence.

Trexon solves the world's most challenging connectivity problems with relentless innovation, industry expertise and constant collaboration. Formed from the combination of top wire and cable companies, Trexon provides an expanding range of specialized products and solutions designed for rugged and specific conditions. The Trexon Engineered Products Group consists of the following industry-leading companies; Cicoil, EZ Form Cable, The First Electronics Corporation, Hydro Group, Integrated Cable Systems and Power Connector Inc.

Trexon Company
https://youtu.be/n9ufNoBtJ9M
https://trexonglobal.com/engineered-products/

Directional Couplers

Introducing the cutting-edge X-Band 8 to 12 GHz 3 dB hybrid and 20 dB directional couplers, designed for broadband medium power applications in military, aerospace and commercial applications. The XMC0812F1-20G and XMC0812F1-03G models boast a 12 dB peak to average ratio, 50 W average power handling, and come in a compact 5 mm x 3.2 mm surface-mount package with a durable ENIG finish. Ideal for power/frequency detection, VSWR monitoring and signal combining/splitting. Available now for sampling.

TTM
https://ttm.com

Sales Representatives

Eastern and Central Time Zones
Michael Hallman
Associate Publisher
(NJ, Mid-Atlantic, Southeast, Midwest, TX)
Tel: (301) 371-8830
Cell: (781) 363-0338
mhallman@mwjournal.com

Susan Leppanen
Northeastern Reg. Sales Mgr.
(New England, New York, Eastern Canada)
Tel: (781) 619-1942
sleppanen@horizonhouse.com

Pacific and Mountain Time Zones
Brian Landy
Western Reg. Sales Mgr.
(CA, AZ, OR, WA, ID, NV, UT, NM, CO, WY, MT, ND, SD, NE & Western Canada)
Tel: (831) 426-4143
Cell: (831) 713-9085
blandy@mwjournal.com

International Sales
Richard Vaughan
International Sales Manager
Tel: +44 207 596 8742
rvaughan@horizonhouse.co.uk

Germany, Austria, and Switzerland (German-speaking)
Victoria and Norbert Hufmann
victoria@hufmann.info
norbert@hufmann.info

France
Gaston Traboulsi
Tel: +44 207 596 8742
gtraboulsi@horizonhouse.com

Korea
Jaeho Chinn
JES MEDIA, INC.
Tel: +82 2 481-3411
corres1@jesmedia.com

China
Shanghai
Linda Li
ACT International
Tel: +86 136 7154 0807
lindal@actintl.com.hk

Wuhan
Phoebe Yin
ACT International
Tel: +86 134 7707 0600
phoebey@actintl.com.hk

Shenzhen
Annie Liu
ACT International
Tel: +135 9024 6961
anniel@actintl.com.hk

Beijing
Cecily Bian
ACT International
Tel: +86 135 5262 1310
cecilyb@actintl.com.hk

Hong Kong
Floyd Chun
ACT International
Tel: +852 28386298
floydc@actintl.com.hk

Taiwan, Singapore
Simon Lee
ACT International
Tel: +852 2838 6298
simonlee@actintl.com.hk

Japan
Katsuhiro Ishii
Ace Media Service Inc.
Tel: +81 3 5691 3335
amskatsu@dream.com

Corporate Headquarters: 685 Canton Street, Norwood, MA 02062 • Tel: (781) 769-9750

eXclusive Digital Content >>>

mmWave Reflectionless Filters Using Advanced Thin Film Fabrication

Matthew A. Morgan and Tod A. Boyd
National Radio Astronomy Observatory, Charlottesville, Va.

Seng Loo and Miho Hunter
Anritsu, Kanagawa, Japan

Reflectionless lowpass and highpass filters on quartz in the mmWave band each have a cutoff frequency at approximately 60 GHz. The absorptive stopband of the lowpass filter and passband of the highpass filter extend up to 120 GHz, the measurement equipment limit. These represent the highest operating frequencies ever reported for reflectionless filters and a landmark achievement for strictly lumped-element-based designs. This performance is made possible due to an advanced thin film fabrication process capable of extraordinary lithographic resolution, down to 2 μm, combined with integrated circuit (IC) elements like metal-insulator-metal (MIM) capacitors, bridges and thin film resistors. The process shows high yield, suitable for mass production and commercialization.

The concept of absorptive filters dates back at least to the 1920s, nearly a century ago, with the work of Zobel[1] and Bode,[2] when they were called constant-resistance networks and were based on image-impedance principles, bridged-tees and cascaded, first and second-order lattice sections. However, the practical limitations on the performance and realizability of such designs precluded them from becoming widely adopted. However, interest in absorptive, or reflectionless, filters has experienced a resurgence in recent years, owing initially to the discovery of lumped-element topologies that could theoretically achieve perfect impedance matches at both ports and all frequencies, from DC to infinity, with no added passband loss.[3,4]

At first, limited to a single response type, that of a third-order Chebyshev Type II filter, a broader theory of symmetric and self-dual circuit topologies was built upon this foundation until it was eventually found that any transfer function whatsoever that was realizable using lumped elements could likewise be implemented in a reflectionless form.[5-12]

Seeing the advantages of a filter that absorbs stopband energy instead of reflecting it, many researchers began searching for ways to duplicate these results using other circuit elements, such as transmission lines,[13-19] coaxial resonators[20,21] and surface acoustic wave (SAW) resonators[22] as well as other methodologies, most importantly coupling-routing diagrams.[20-27] These often resulted in somewhat larger filters for a given frequency with limited absorption bandwidth (theoretically as well as practically), and/or with stopband impedance matching at only a single port.

This work concentrates on lumped-element designs, as these are generally capable of the broadest absorption bandwidth in the most compact form. Originally fabricated at relatively low frequencies using discrete surface-mount elements, these topologies were eventually implemented in the microwave regime using an integrated passive device (IPD) fabrication process on GaAs wafers.[28]

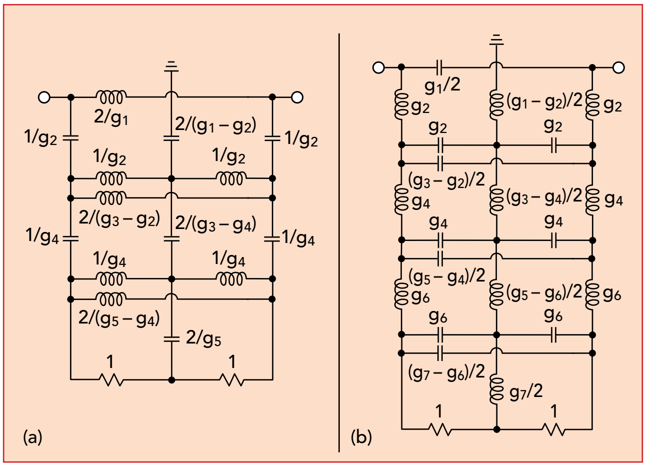

Fig. 1 Fifth-order lowpass (a) and seventh-order highpass (b) filters implemented in advanced thin film technology.

fifth-order lowpass filter, while Figure 1b is a seventh-order highpass filter. Both are Chebyshev Type II designs, having equal stopband ripple and are theoretically reflectionless at both ports and all frequencies. The prototype parameter values used for these designs are listed in ***Table I***.

The ripple factor is selected to achieve the maximum theoretical stopband rejection for these topologies (without requiring transformers, which are difficult to implement at such high frequencies in planar circuit technology). Ripple factor, ε, is given by ***Equation 1*** and ***Equation 2***:

$$\varepsilon = \sqrt{e^{4\tanh^{-1}\left(e^{-\beta}\right)} - 1} \cong \begin{cases} 0.2164, N = 5 \\ 0.2187, N = 7 \end{cases} \quad (1)$$

$$\sinh^{-1}\left(\sqrt{1/2\sin\left(\pi/N\right)\tan\left(\pi/N\right)}\right) \quad (2)$$

N is the order of the filter.[5,6]

Consequently, stopband rejection is theoretically limited to about 13.5 dB, as shown by their ideal, normalized frequency responses in ***Figure 2***. It has become common practice to cascade multiple stages of such designs to achieve the level of stopband attenuation desired for a given application, however, single-stage designs are sufficient for this present proof-of-concept.

Having been reduced to practice in a form suitable for cost-effective mass manufacturing, these devices are now distributed by Mini-Circuits and have become adopted by the industry as the preferred solution in several applications.[29-32] However, the difficulty of realizing good-quality lumped elements at short wavelengths has limited their cutoff frequencies, primarily to the cm-wave range (though passband and absorption bandwidths often extend much higher).

With the advent of sophisticated thin film fabrication that combines IC elements (MIM caps, bridges and thin film resistors) with photolithography having even better resolution than is generally achievable with commercial III-V semiconductor processes, we are now prepared to implement lumped-element circuits of this kind for the first time in the mmWave regime. This capability is demonstrated by the development of two prototypes: a fifth-order Chebyshev Type II lowpass filter and a seventh-order Chebyshev Type II highpass filter.

SCHEMATIC FILTER DESIGN

Circuit diagrams of the two prototype filters reported in this article are shown in ***Figure 1***. Figure 1a is a

PHYSICAL ELEMENT DESIGN

Note that by selecting minimum ripple factors, the first and last two elements in each row of Table I are identical. This means that certain elements in the schematics of Figure 1 vanish in the final layout, for example, the capacitor $2/(g_1 - g_2)$ and the inductor $2/(g_5 - g_4)$ in Figure 1a. Others are split into two in favor of layout symmetry; for example, the series inductor having the value $2/g^1$ will be implemented with two series inductors in the physical filter, mirrored, each having a normalized value of $1/g_1$.

A cutoff frequency of 60 GHz is selected for both designs. This requires capacitors ranging from 40 to 120 pF. They are implemented as MIM capacitors with silicon nitride (SiN) dielectrics. The required inductors range from 99 to 199 pH. They are implemented as planar spiral coils having 1.5 turns each in the first metal layer. The fine lithography of the process makes it possible to use trace widths and spacings

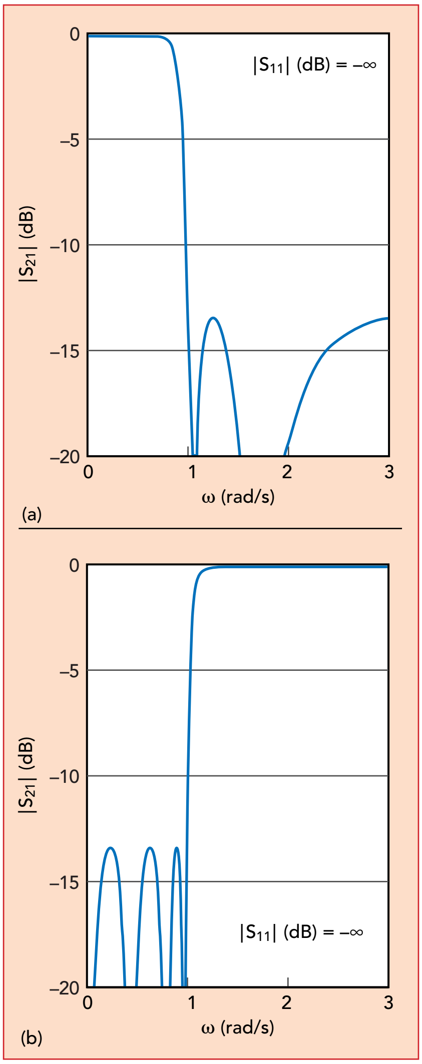

Fig. 2 Ideal, normalized frequency response of fifth-order lowpass (a) and seventh-order highpass (b) reflectionless filters.

TABLE I

CHEBYSHEV PROTOTYPE PARAMETERS FOR LIMITING RIPPLE FACTORS

N	ε	g_1	g_2	g_3	g_4	g_5	g_6	g_7
5	0.2164	1.337	1.337	2.164	1.337	1.337		
7	0.2187	1.377	1.377	2.280	1.498	2.280	1.377	1.377

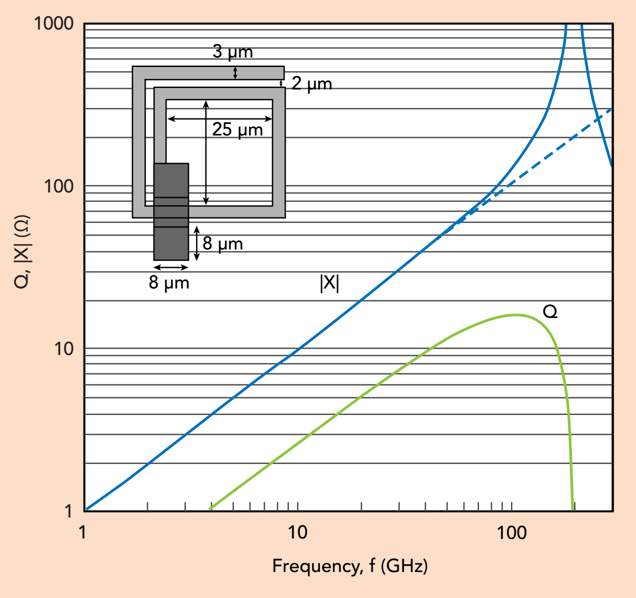

Fig. 3 **Inductor layout (inset), simulated reactance and quality factor (solid lines) and theoretical reactance of an ideal 160 pH inductor (dashed line).**

of 3 and 2 µm, respectively.

The internal node of the coil is brought out using a dielectric bridge (the same SiN dielectric used for the capacitors). This extra parasitic capacitance at the bridge is a compromise between the simplicity of the fabrication process and the self-resonance of the inductor.

A typical inductor layout for these filters is shown in ***Figure 3***, as the inset on a graph showing the simulated reactance and quality factor as a function of frequency. It shows that a linear reactance curve is achieved from the lowest frequencies up to around W-Band, eventually reaching a self-resonance at 200 GHz. The peak Q, modeled at around 100 GHz, is about 16.

THIN FILM FABRICATION PROCESS

The thin film circuits are fabricated on a Corning Fused Silica 7980 quartz substrate. The key process steps are as follows:

- A tantalum nitride (TaN) resist layer with a target sheet resistance of 50 Ω/sq. is deposited across the entire wafer (see ***Figure 4a***). The reflectionless filters are relatively insensitive to resistor value, so a tolerance of +10 is acceptable.
- Next, a TiW/Au seed layer is deposited, then plated up with Au to a thickness of 1.25 µm. This is then etched to form the first metal layer (see ***Figure 4b***).
- After etching the first metal layer, resistors are patterned from the underlying TaN film (see ***Figure 4c***).
- SiN is then deposited and etched (see ***Figure 4d***). The target thickness of the dielectric is 1 µm, yielding an expected capacitance density of 0.062 fF/µm². Note that SiN also covers the resistors, so as not to expose them to the CF_4/O_2 plasma used for patterning the dielectric islands, as this plasma would also etch away the TaN film.
- The second metal layer is then formed once again using a TiW/Au seed layer, plated up this time to a thickness of 2.5 µm and then etched (see ***Figure 4e***).
- After all other processing steps are completed, the wafer is thinned to a final thickness of 125 µm and diced.

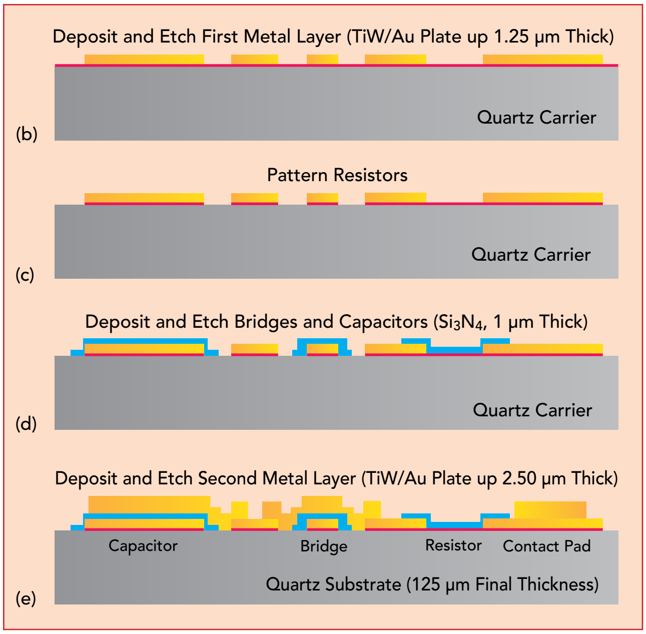

Fig. 4 **Key thin film fabrication process steps: deposition of the TaN resistor film (a), deposition, plating and patterning of the first metal layer (b), resistor patterning (c) deposition (d) and patterning (e).**

An MRC 943 series sputtering system and a TemesCal VES-2550 E-beam evaporator are used for the metal deposition processes. Photolithography imaging is accomplished using positive tone resists and a Canon FPA2000-il 5 X stepper. SiN deposition is done with a Novellus Concept One plasma-enhanced chemical vapor deposition (PECVD) tool. Finally, gold electroplating uses a Tanaka gold sulfite plating system.

The potential for capacitor shorts is considered a risk for this fabrication process. An initial attempt used a much thinner first metalization layer of 0.4 µm to keep the surface as smooth as possible for subsequent SiN deposition. While the capacitor yield was excellent (no shorts were discovered), metal trace ohmic losses were unacceptably high. Having greater confidence in the capacitor process, a second run used a thicker metalization stack described above (see Figure 4).

Microphotographs of the two completed circuits are shown in ***Figure 5***. Scanning electron microscope (SEM) images better reveal the three-dimensional structure of the critical elements and the quality of fabrication; a selection of these scans is shown in ***Figure 6***.

MEASUREMENTS

Both circuits are fabricated on a 100 mm diameter wafer, containing over 14,000 chips (7000 of each design). The chips are wafer probed using a Keysight N5291A-201 vector network analyzer (VNA) capable of measuring two-port scattering parameters from 900 Hz to 120 GHz in a single sweep. The results are plotted in ***Figure 7***.

The measured response curves for both filters (solid lines) are shifted upward in frequency by 5 to 10 percent compared to initial simulations. This is attributed to the SiN capacitor dielectric, initially assumed to have a dielectric constant of εr = 7. For the simulations plotted in Figure 7 (dashed lines), the dielectric constant is decreased to account for this error, but it is still within the acceptable range reported in the literature.[33] This brings the measured and simulated results within good agreement across the entire frequency range. It also partly accounts for the increased reflection coefficients in the stopband of the lowpass filter and the transition band of the highpass filter.

DC resistance measurements are performed at sites across the entire wafer to verify trace conductivity, and to test for shorted or leaking capacitors, which, as discussed previously, are considered a technical risk for this fabrication. One lowpass filter in each of the 82 reticles is probe-tested for DC isolation between one of the port signal pads and ground. This is nominally expected to be an open circuit. However, if either of the first two capacitors, labeled $1/g_2$ in Figure 2a, is shorted or leaky, then a finite resistance will be measured (recall that the grounded capacitor $2/(g_1 - g_2)$ vanishes since $g_1 = g_2$).

The leakage test results are summarized in the wafer map of ***Figure 8*** ("0L" means no measurable leakage is detected). Out of 82 reticles, 13 showed signs of some leakage, all clustered around the outer edge of the wafer. Thus, the global capacitor yield is estimated in ***Equation 3*** to be:

$$Y_c = \sqrt{\frac{69}{82}} \approx 92 \text{ percent} \qquad (3)$$

The square root is used since two capacitors must both be good for the isolation test to pass. Closer to the center, presumably, the yield is much higher (none of the devices tested in the interior, whether at DC or RF, was found to be defective).

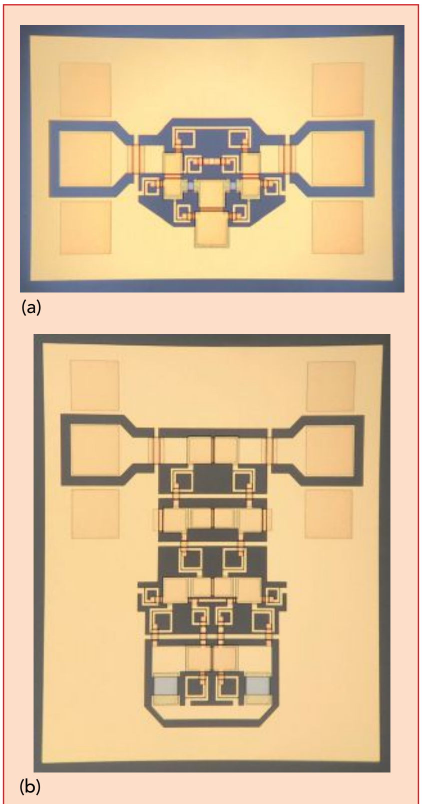

Fig. 5 **Microphotographs of thin film, reflectionless filters: lowpass filter measuring 600 × 400 μm (a) and highpass filter measuring 600 × 700 μm (b). The substrate is 125 μm thick quartz.**

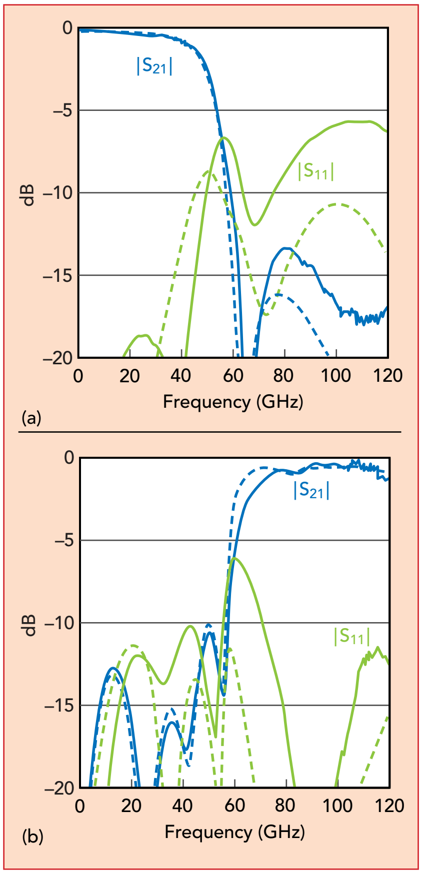

Fig. 7 **Measured (solid lines) and simulated (dashed lines) S-parameters for lowpass (a) and highpass (b) reflectionless filters. The SiN dielectric is adjusted to account for an apparent shift in frequency between measurements and initial simulations.**

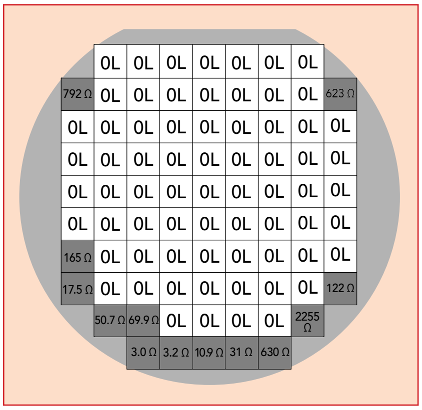

Fig. 8 **DC isolation between the lowpass signal port pad and ground. Out of 82 sites measured, 13 showed evidence of capacitor leakage.**

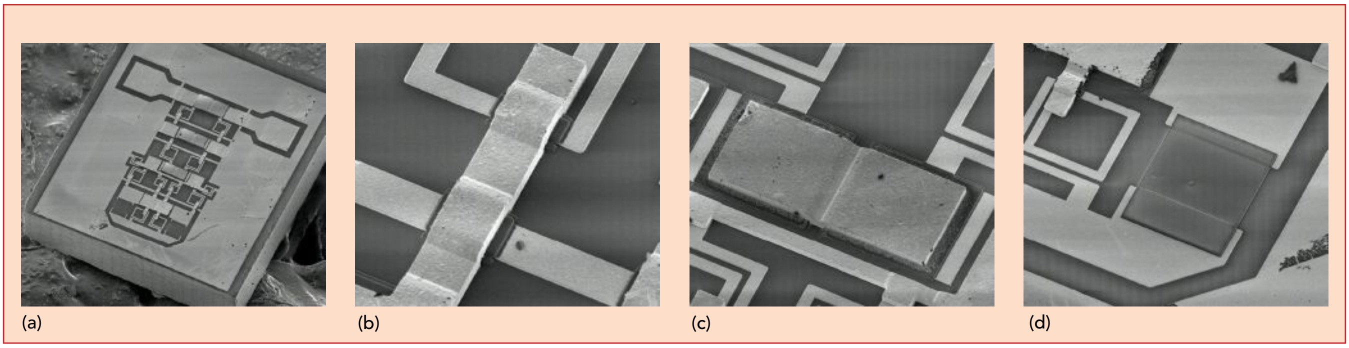

Fig. 6 **SEM images of a fabricated filter: full circuit. (a) closeup of bridges (b), closeup of capacitors (c) and closeup of inductor and thin film resistor (d).**

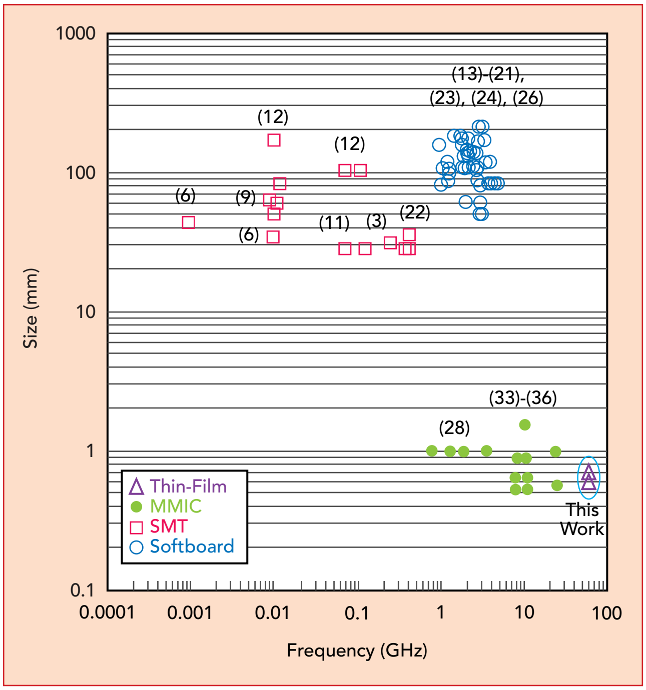

Fig. 9 **Comparison of this work with other approaches in terms of size (largest linear dimension) and cutoff frequency. All cutoff corners for bandpass, bandstop and multiple-band filters are shown. Bond pads are included in the circuit dimensions.**

CONCLUSION

Reflectionless lowpass and highpass filters on quartz in the mmWave band are demonstrated. Each has a cutoff frequency at approximately 60 GHz. The absorptive stopband of the lowpass filter and passband of the highpass filter extend up to 120 GHz, the limit of our measurement equipment. These represent the highest operating frequencies ever reported for reflectionless filters and a landmark achievement for strictly lumped-element-based designs. This performance is made possible by an advanced thin film fabrication process capable of extraordinary lithographic resolution, down to 2 μm, combined with IC elements like MIM capacitors, bridges and thin film resistors. The process shows high yield, suitable for mass production and commercialization.

The advantages of these designs and this fabrication technology are strikingly illustrated in ***Figure 9***, which compares this work to numerous others (included in the references) in terms of compactness (on the vertical axis) versus frequency (on the horizontal axis). Note that both scales are logarithmic, spanning five orders of magnitude in frequency and three orders of magnitude in physical size.

It is interesting to see how well the different approaches to reflectionless filters naturally segregate themselves into clusters on such a plot. Lumped-element designs using surface-mount (SMT) components appear in the upper left as relatively large circuits at low frequency. In contrast, filters on microwave laminates or soft board materials, almost universally implemented using distributed elements such as transmission lines[13-19] or substrate-integrated resonators,[20,21] increase the frequency without any real reduction in size, thus grouping together in the upper right corner.

The smallest and highest-frequency designs have all, until now, been implemented using MMIC fabrication, usually lumped-element on either a GaAs IPD or silicon CMOS wafers. The two filters reported here, using a thin film process on quartz, appear in the extreme bottom right corner of the plot, achieving the highest frequencies in form factors that are among the smallest ever reported. ■

References

1. O. J. Zobel, "Distortion Correction in Electrical Circuits with Constant Resistance Recurrent Networks," *Bell System Technical Journal*, Vol. 7, No. 3, July 1928, pp. 438–534.
2. H. Bode, *Network Analysis and Feedback Amplifier Design*, Van Nostrand, NY, 1945.
3. M. A. Morgan and T. A. Boyd, "Theoretical and Experimental Study of a New Class of Reflectionless Filter," *IEEE Transactions on Microwave Theory and Techniques*, Vol. 59, No. 5, May 2011, pp. 1214–1221.
4. M. A. Morgan, "Reflectionless Filters," U.S. Patent 8 392 495, March 5, 2013.
5. M. A. Morgan, "Reflectionless Filters," *Artech House*, 2017.
6. M. A. Morgan, W. M. Groves and T. A. Boyd, "Reflectionless Filter Topologies Supporting Arbitrary Low-Pass Ladder Prototypes," *IEEE Transactions on Circuits and Systems I*, Vol. 66, No. 2, February 2019, pp. 594–604.
7. M. A. Morgan, "Optimal Response Reflectionless Filters," U.S. Patent 10 263 592, April 16, 2019.
8. M. Morgan, "Deep Rejection Reflectionless Filters," U.S. Patent No. 10 530 321, January 7, 2020.
9. A. Guilabert, M. Morgan and T. A. Boyd, "Reflectionless Filters for Generalized Elliptic Transmission Functions," *IEEE Transactions on Circuits and Systems I*, Vol. 66, No. 12, December 2019, pp. 4606–4618.
10. M. Khalaj-Amirhosseini and A. Khalaj-Amirhosseini, "Reflectionless Filters with Arbitrary Transfer Functions," *Journal of Telecommunication*, Vol. 34, No. 2, October 2016, pp. 1–3.
11. M. Khalaj-Amirhosseini and M. M. Taskhiri, "Twofold Reflectionless Filters of Inverse-Chebyshev Response with Arbitrary Attenuation," *IEEE Transactions on Microwave Theory and Techniques*, Vol. 65, No. 11, November 2017, pp. 4616–4620.
12. J. Lee, B. Lee, S. Nam and J. Lee, "Rigorous Design Method for Symmetric Reflectionless Filters with Arbitrary Prescribed Transmission Response," *IEEE Transactions on Microwave Theory and Techniques*, Vol. 68, No. 6, June 2020, pp. 2300–2307.
13. D. Psychogiou and R. Gomez-Garcia, "Tunable Reflectionless Microstrip Bandpass Filters," *IEEE Radio Wireless Symposium*, January 2018.
14. R. Gomez-Garcia, J. M. Munoz-Ferreras, Wenjie Feng and D. Psychogiou, "Balanced Symmetrical Quasi-Reflectionless Single and Dual-Band Bandpass Filters," *IEEE Microwave and Wireless Components Letters*, Vol. 28, No. 9, September 2018, pp. 798–800.
15. L. Yang, R. Gomez-Garcia, J. M. Munoz-Ferreras, R. Zhang, D. Peroulis and L. Zhu, "Multilayered Reflectionless Wideband Bandpass Filters with Shunt/In-Series Resistively Terminated Microstrip Lines," *IEEE Transactions on Microwave Theory and Techniques*, Vol. 68, No. 3, March 2020, pp. 877–893.
16. R. Gomez-Garcia, L. Yang and J. M. Munoz-Ferreras, "Low-Reflection Signal-Interference Single- and Multi-Passband Filters with Shunted Lossy Stubs," *IEEE Microwave and Wireless Components Letters*, Vol. 30, No. 4, April 2020, pp. 355–358.
17. X. Wu, Y. Li and X. Liu, "Quasi-Reflectionless Microstrip Bandpass Filters with Improved Passband Flatness and Out-of-Band Rejection," *IEEE Access*, Vol. 8, September 2020, pp. 160500–160514.
18. M. Fan, K. Song, L. Yang and R. Gomez-Garcia, "Balanced-Circuit-Based Dual-Band Bandpass Filter with Symmetrical Reflectionless Behavior," *IEEE Radio Wireless Symposium*, January 2021.
19. J. Lee and J. Lee, "Transmission-Line Absorptive Bandpass Filters with Wide Passband: Synthesis and Design," *IEEE Transactions on Microwave Theory and Techniques*, Vol. 69, No. 12, Decem-

ber 2021, pp. 5371–5380.
20. D. Psychogiou and R. Gomez-Garcia, "Quasi-Absorptive Substrate Integrated Bandpass Filters Using Capacitively-Loaded Coaxial Resonators," *IEEE MTT-S International Microwave Symposium*, August 2020.
21. K. Zhao, R. Gomez-Garcia and D. Psychogiou, "Tunable Quasi-Reflectionless Bandpass Filters Using Substrate Integrated Coaxial Resonators," *IEEE Transactions on Circuits and Systems II*, Vol. 69, No. 2, February 2022, pp. 379–383.
22. D. Psychogiou, and R. Gomez-Garcia, "Symmetrical Quasi-Reflectionless SAW-Based Bandpass Filters with Tunable Bandwidth," *IEEE Microwave and Wireless Components Letters*, Vol. 29, No. 7, July 2019, pp. 447–449.
23. R. Gomez-Garcia, J. M. Munoz-Ferreras and D. Psychogiou, "Symmetrical Quasi-Reflectionless BSFs," *IEEE Microwave and Wireless Components Letters*, Vol. 28, No. 4, April 2018, pp. 302–304.
24. R. Gomez-Garcia, J. M. Munoz-Ferreras and D. Psychogiou, "Splittype Input-Reflectionless Multiband Filters," *IEEE Microwave and Wireless Components Letters*, Vol. 28, No. 11, November 2018, pp. 981–983.
25. R. Gomez-Garcia, J. M. Munoz-Ferreras and D. Psychogiou, "Symmetrical Quasi-Absorptive RF Bandpass Filters," *IEEE Transactions on Microwave Theory and Techniques,* Vol. 67, No. 4, April 2019, pp. 1472–1482.
26. R. Gomez-Garcia, J. M. Munoz-Ferreras and D. Psychogiou, "High-Order Input-Reflectionless Bandpass/Bandstop Filters and Multiplexers," *IEEE Transactions on Microwave Theory and Techniques*, Vol. 67, No. 9, September 2019, pp. 3683–3695.
27. R. Gomez-Garcia, D. Psychogiou, J. M. Munoz-Ferreras and L. Yang, "Avoiding RF Isolators: Reflectionless Microwave Bandpass Filtering Components for Advanced RF Front Ends," *IEEE Microwave Magazine*, Vol. 21, No. 12, December 2020, pp. 68–86.
28. M. A. Morgan and T. A. Boyd, "Reflectionless filter structures," *IEEE Transactions on Microwave Theory and Techniques*, Vol. 63, No. 4, April 2015, pp. 1263–1271.
29. "Pairing Mixers With Reflectionless Filters to Improve System Performance," *Mini-Circuits*, Application Note AN-75-007, Rev. OR M153509, October 23, 2015, pp. 1–5, Web: https://www.minicircuits.com/app/AN75-007.pdf.
30. "Advantages of Cascading Reflectionless Filters," *Mini-Circuits*, Application Note AN-75-008, Rev. OR M153778, November 11, 2015, pp. 1–5, Web: https://www.minicircuits.com/app/AN75-008.pdf.
31. R. Setty, B. Kaplan, M. A. Morgan and T. A. Boyd, "Combining MMIC Reflectionless Filters to Create UWB Bandpass Filters," *Microwave Journal*, Vol. 61, No. 3, March 2018, pp. 60–72
32. R. Shrotriya and M. Morgan, "Filtering Without Reflections: Flattening Multiplier Chain Conversion Efficiency & More," White Paper, *Microwave Journal*, Vol. 62, No. 9, September 2019.
33. A. Piccirillo and A. L. Gobbi, "Physical-Electrical Properties of Silicon Nitride Deposited by PECVD on III-V Semiconductors," *Journal of the Electrochemical Society*, Vol. 137, No. 12, December 1990, pp. 3910–3917.
34. D. Simpson and D. Psychogiou, "X-Band Quasi-Reflectionless MMIC Bandpass Filters with Minimum Number of Components," *IEEE Transactions on Electron Devices*, Vol. 68, No. 9, September 2021, pp. 4329–4334.
35. Z. Ge, L. Chen, L. Yang, R. Gomez-Garcia and X. Zhu, "On-Chip Millimeter-Wave Integrated Absorptive Bandstop Filter in (Bi)-CMOS Technology," *IEEE Electron Device Letters*, Vol. 42, No. 1, January 2021, pp. 114–117.
36. K. Zhao and D. Psychogiou, "X-Band MMIC-Based Tunable Quasiabsorptive Bandstop Filter," *IEEE Microwave and Wireless Technology Letters*, Vol. 33, No. 4, April 2023, pp. 391–394.